UNICAMP

KÁTIA REGINA KUHN

“ENCAPSULAÇÃO DE COMPOSTOS BIOATIVOS OBTIDOS A PARTIR DA LINHAÇA”

“ENCAPSULATION OF BIOACTIVE COMPOUNDS OBTAINED FROM FLAXSEED”

CAMPINAS
2013

UNIVERSIDADE ESTADUAL DE CAMPINAS
FACULDADE DE ENGENHARIA DE ALIMENTOS

KÁTIA REGINA KUHN

"ENCAPSULAÇÃO DE COMPOSTOS BIOATIVOS OBTIDOS A PARTIR DA LINHAÇA"

Orientador (a): Profa. Dra. Rosiane Lopes da Cunha

"ENCAPSULATION OF BIOACTIVE COMPOUNDS OBTAINED FROM FLAXSEED"

Tese de doutorado apresentada ao Programa de Pós-Graduação em Engenharia de Alimentos da Faculdade de Engenharia de Alimentos da Universidade Estadual de Campinas para obtenção do título de Doutora em Engenharia de Alimentos.

Doctorate thesis presented to the Food Engineering Postgraduation Programme of the Faculty of Food Engineering of the University of Campinas to obtain the Ph.D. grade in Food Engineering.

ESTE EXEMPLAR CORRESPONDE À VERSÃO FINAL DA TESE DEFENDIDA PELA ALUNA KÁTIA REGINA KUHN E ORIENTADA PELA PROFA. DRA. ROSIANE LOPES DA CUNHA

Assinatura do Orientador

CAMPINAS
2013

Ficha catalográfica
Universidade Estadual de Campinas
Biblioteca da Faculdade de Engenharia de Alimentos
Márcia Regina Garbelini Sevillano - CRB 8/3647

K955e
Kuhn, Kátia Regina, 1984-
Encapsulação de compostos bioativos obtidos a partir da linhaça / Kátia Regina Kuhn. – Campinas, SP : [s.n.], 2013.

Orientador: Rosiane Lopes da Cunha.
Tese (doutorado) – Universidade Estadual de Campinas, Faculdade de Engenharia de Alimentos.

1. Emulsões. 2. Óleo de linhaça. 3. Hidrolisados proteicos. 4. Compostos bioativos. 5. Encapsulação. I. Cunha, Rosiane Lopes da,1967-. II. Universidade Estadual de Campinas. Faculdade de Engenharia de Alimentos. III. Título.

Informações para Biblioteca Digital

Título em inglês: Encapsulation of bioactive compounds obtained from flaxseed
Palavras-chave em inglês:
Emulsions
Flaxseed oil
Protein hydrolysates
Bioactive compounds
Encapsulation
Área de concentração: Engenharia de Alimentos
Titulação: Doutora em Engenharia de Alimentos
Banca examinadora:
Rosiane Lopes da Cunha [Orientador]
Ana Carla Kawazoe Sato
Izabela Dutra Alvim
Miriam Dupas Hubinger
Samantha Cristina de Pinho
Data de defesa: 08-08-2013
Programa de Pós-Graduação: Engenharia de Alimentos

BANCA EXAMINADORA

Profa. Dra. Rosiane Lopes da Cunha
Departamento de Engenharia de Alimentos / FEA / UNICAMP - Orientadora

Dra. Ana Carla Kawazoe Sato
Departamento de Engenharia de Alimentos / FEA / UNICAMP – Membro titular

Dra. Izabela Dutra Alvim
ITAL – Membro titular

Profa. Dra. Miriam Dupas Hubinger
Departamento de Engenharia de Alimentos / FEA / UNICAMP – Membro titular

Profa. Dra. Samantha Cristina de Pinho
Departamento de Engenharia de Alimentos / FZEA / USP – Membro titular

Profa. Dra. Flavia Maria Netto
Departamento de Alimentos e Nutrição / FEA / UNICAMP – Membro suplente

Dra. Renata Valeriano Tonon
EMBRAPA – Membro suplente

Profa. Dra. Vânia Regina Nicoletti Telis
Departamento de Engenharia e Tecnologia de Alimentos / IBILCE / UNESP – Membro suplente

Dedico este trabalho aos meus pais, Erno e Tânia, e a minha irmã, Raquel, que sempre estiveram ao meu lado me apoiando e me incentivando a seguir em frente.

AGRADECIMENTOS

A Deus, por iluminar minhas decisões, guiar meus passos e acima de tudo, pelos obstáculos vencidos e conquistas alcançadas.

À Faculdade de Engenharia de Alimentos, especialmente ao Departamento de Engenharia de Alimentos, e aos professores e funcionários pela oportunidade e estrutura oferecida para a realização deste trabalho.

Ao CNPq, CAPES e FAPESP pela bolsa de doutorado e suporte financeiro.

À Profa. Dra. Rosiane Lopes da Cunha agradeço principalmente pela orientação, confiança, paciência e amizade. Pelo incentivo, apoio, ensinamentos transmitidos e pelos inúmeros conselhos.

À Profa. Dra. Flavia Maria Netto (DEPAN/UNICAMP) pelo auxílio, amizade, confiança e disponibilidade em ajudar sempre que era necessário.

Aos membros da banca examinadora, Profa. Dra. Samantha Cristina de Pinho, Dra. Ana Carla Kawazoe Sato, Dra. Izabela Dutra Alvim, Profa. Dra. Miriam Dupas Hubinger, Profa. Dra. Flavia Maria Netto, Dra. Renata Valeriano Tonon e Profa. Dra. Vânia Regina Nicoletti Telis, pela atenção, correções, sugestões e contribuições para a melhora deste trabalho.

Ao Prof. Dr. Valdemiro Carlos Sgarbieri (DEPAN/UNICAMP), que gentilmente cedeu o isolado protéico de soro de leite bovino. Ao Prof. Dr. Gonçalo Amarante Guimarães Pereira e ao aluno Gleidson Silva Teixeira (LGE/Instituto de Biologia/UNICAMP) pelas análises de Microscopia de Fluorescência. Ao Prof. Dr. Carlos Raimundo Ferreira Grosso e à técnica Yara Fagnani Honório pelas análises iniciais de tamanho de partícula. Ao Prof. Dr. Paulo José do Amaral Sobral (FZEA/USP) e ao técnico Rodrigo Lourenço pelas análises de FTIR.

Aos meus pais, Erno e Tânia, meus grandes amores, que sempre me compreenderam, incentivaram e que mesmo distantes geograficamente, sempre estiveram presentes e nunca mediram esforços pela minha felicidade. Agradeço pela dedicação de vocês, pelos

conselhos sábios, paciência e apoio. Sem vocês, chegar até aqui seria impossível. AMO VOCÊS!!!!

À minha manexxx Kelly, que por dois anos e meio ainda esteve ao meu lado em Campinas e que depois, mesmo distante, continuou me aconselhando, apoiando e incentivando a seguir em frente. Obrigada por tudo ... te amo manex!!!

Ao pessoal do grupo de pesquisa e aos amigos do DEA, obrigada pela amizade, pelos momentos agradáveis de convivência, pelos ensinamentos e por toda a ajuda no desenvolvimento deste trabalho.

À Zil e à Patty, que chegaram no meu último ano de doutorado, mas que foram muito importantes. À vocês, meu muito obrigada pelas inúmeras ajudas no laboratório, pelas risadas, pelos conselhos e pela amizade. Sentirei saudades de vocês!!!

À Fernanda Guimarães Drummond e Silva (DEPAN/UNICAMP) pela amizade e auxílio no desenvolvimento deste trabalho.

À Jana, minha amigona da graduação, que apesar da distância, sempre esteve presente com palavras amigas, incentivo, e que soube compreender a minha ausência em alguns momentos. Às minhas grandes amigas de Santa Cruz, Jú, Manu, Carol, Dani, Elisa, Ana, Patsy, Julia, Vanessa, Lú, que mesmo de longe, também sempre estiveram por perto. Obrigada pela amizade sincera!! Amo todas vocês!!

A todos aqueles que sempre estiveram presentes ao meu lado ou em pensamento, e que de alguma forma contribuíram para a elaboração deste trabalho, meu muito obrigada.

ÍNDICE GERAL

ÍNDICE DE FIGURAS xxi
ÍNDICE DE TABELAS xxvii
LISTA DE ABREVIATURAS E SIGLAS xxix
RESUMO GERAL xxxi
ABSTRACT xxxv
CAPÍTULO 1. INTRODUÇÃO GERAL 1
1.1. INTRODUÇÃO 3
1.2. OBJETIVOS 5
1.3. DESCRIÇÃO DOS CAPÍTULOS 6
1.4. REFERÊNCIAS 8
CAPÍTULO 2. REVISÃO BIBLIOGRÁFICA 15
2.1. SEMENTE DE LINHO (LINHAÇA) 15
  2.1.1. Proteínas da linhaça 16
  2.1.2. Óleo de linhaça 19
2.2. OXIDAÇÃO LIPÍDICA 20
2.3. EMULSÕES EM SISTEMAS ALIMENTÍCIOS 22
  2.3.1. Métodos de emulsificação 27
    2.3.1.1. Homogeneização a alta pressão 27
2.4. MICROENCAPSULAÇÃO: PARTÍCULAS GELIFICADAS 28
2.5. PROCESSOS DE SIMULAÇÃO DA DIGESTÃO *IN VITRO* 30
2.6. REFERÊNCIAS 33
CHAPTER 3. Flaxseed oil – Whey protein isolate emulsions: Effect of high pressure homogenization 47
ABSTRACT 47
3.1. INTRODUCTION 48
3.2. MATERIAL AND METHODS 50
  3.2.1. Material 50
  3.2.2. Preparation of the WPI stock solution 50
  3.2.3. Preparation of the emulsions 50
  3.2.4. Creaming stability 51
  3.2.5. Optical microscopy 52
  3.2.6. Particle size distribution 52

3.2.7. Polyacrylamide gel electrophoresis (SDS-PAGE) 52
3.2.8. Rheological measurements 53
3.2.9. Oxidative stability 54
3.2.10. Statistical analysis 55
3.3. RESULTS AND DISCUSSION 55
3.3.1. Creaming stability of the emulsions 55
3.3.2. Microstructure and droplet size 56
3.3.3. Polyacrylamide gel electrophoresis (SDS-PAGE) 61
3.3.4. Rheology 65
3.3.5. Lipid oxidation 68
3.4. CONCLUSIONS 70
3.5. ACKNOWLEDGEMENTS 71
3.6. REFERENCES 71
CHAPTER 4. Assessing the potential of flaxseed protein as an emulsifier combined with whey protein isolate 79
ABSTRACT 79
4.1. INTRODUCTION 80
4.2. MATERIAL AND METHODS 82
4.2.1. Material 82
4.2.2. Characterization of the WPI and the FPI 83
4.2.2.1. Zeta potential 83
4.2.2.2. Fourier transform infrared spectroscopy (FTIR) 83
4.2.3. Preparation of the WPI and the FPI stock solutions 84
4.2.4. Preparation of the emulsions 84
4.2.5. Characterization of the O/W emulsions 85
4.2.5.1. Interfacial tension 85
4.2.5.2. Creaming stability 85
4.2.5.3. Optical and fluorescence microscopy 86
4.2.5.4. Particle size distribution 87
4.2.5.5. Rheological measurements 87
4.2.5.6. Protein load 88
4.2.6. Statistical analysis 89
4.3. RESULTS AND DISCUSSION 89
4.3.1. Characterization of the biopolymers 89
4.3.2. Characterization of the emulsions 93

4.3.2.1. WPI emulsions 94
4.3.2.2. FPI emulsions.. 97
4.3.2.3. WPI-FPI emulsions 106
4.4. CONCLUSIONS.. 115
4.5. ACKNOWLEDGEMENTS.. 116
4.6. REFERENCES 116
CHAPTER 5. Production of whey protein isolate – gellan microbeads for encapsulation and release of bioactive compounds from flaxseed 125
ABSTRACT 125
5.1. INTRODUCTION.. 126
5.2. MATERIAL AND METHODS... 129
5.2.1. Material 129
5.2.2. Preparation of stock solutions 129
5.2.3. Preparation of the O/W emulsions.. 130
5.2.4. Gelation of the emulsions.. 130
5.2.5. Production of microbeads 131
5.2.6. Evaluation of microbeads.. 132
5.2.6.1. Stability.. 132
5.2.6.2. Rheological properties of microbeads suspensions.................................... 133
5.2.6.3. Simulation of *in vitro* digestion process 133
5.2.7. Characterization of microbeads.. 134
5.2.7.1. Zeta potential 134
5.2.7.2. Particle size distribution 134
5.2.7.3. Optical microscopy.. 135
5.2.7.4. Confocal scanning laser microscopy (CSLM)... 135
5.2.8. Statistical analysis... 136
5.3. RESULTS AND DISCUSSION... 136
5.3.1. Gelation of the O/W emulsions 136
5.3.2. Microbeads.. 137
5.3.2.1. Choosing the ratio gellan/FPH.. 137
5.3.2.2. Evaluation of stability.. 142
5.3.2.3. Rheological properties... 144
5.3.2.4. Confocal microscopy... 147
5.3.2.5. *In vitro* digestion 150
5.4. CONCLUSIONS.. 157

5.5. ACKNOWLEDGEMENTS... 158
5.6. REFERENCES 158
CAPÍTULO 6. CONCLUSÕES GERAIS... 169
7. SUGESTÕES PARA TRABALHOS FUTUROS 171

ÍNDICE DE FIGURAS

CAPÍTULO 2

Figura 2.1. Esquema do mecanismo da oxidação lipídica 21
Figura 2.2. Unidade de tetrassacarídeo que se repete na goma gelana desacilada. Os sítios de ligação dos substituintes gliceril e acetil na gelana altamente acilada ("nativa") estão indicados 25
Figura 2.3. Representação da transição conformacional desordenada-ordenada (1) e da transição sol-gel (2) da gelana 26
Figura 2.4. Diagrama das condições físico-químicas nas diferentes regiões do trato gastrointestinal humano 32

CHAPTER 3

Fig. 3.1. Visual appearance of the O/W emulsions homogenized at 20 and 80 MPa after 3 months of storage. Number of passes: (A) 1, (B) 4 and (C) 7.. 56
Fig. 3.2. Microstructures of the O/W emulsions homogenized at 20 and 80 MPa with 1, 4 and 7 passes through the homogenizer. Scale bar = 10 µm. 57
Fig. 3.3. Effects of homogenization pressure and the number of passes through the homogenizer on the droplet size distribution of the emulsions containing 3% (w/v) WPI and 30% (v/v) flaxseed oil, homogenized at (A) 20 and (B) 80 MPa. Number of passes: 1, 2, 3, 4, 5, 6 and 7. 58
Fig. 3.4. Effects of homogenization pressure and the number of passes through the homogenizer on the temperature of the emulsions containing 3% (w/v) WPI and 30% (v/v) flaxseed oil at the exit of the homogenizer. Homogenization pressure: 20 and 80 MPa..... 61
Fig. 3.5. Polyacrylamide gel electrophoresis (SDS-PAGE) of the O/W emulsions homogenized in an Ultra Turrax (14000 rpm) and at high pressure (20 and 80 MPa) with different numbers of passes through the homogenizer. (A, B) 20 MPa and (C, D) 80 MPa. (A, C) SDS-PAGE under non-reducing conditions, and (B, D) SDS-PAGE under reducing conditions. Columns (1) commercial molecular weight marker, (2) native whey protein solution (non-denatured), (UT) Ultra Turrax, (P_1) 1 pass, (P_2) 2 passes, (P_3) 3 passes, (P_4) 4 passes, (P_5) 5 passes, (P_6) 6 passes and (P_7) 7 passes. The temperatures reached at the exit of the homogenizer after each pass are shown in detail.. 63
Fig. 3.6. Effects of homogenization pressure and the number of passes through the homogenizer on the peroxide value of the emulsions containing 3% (w/v) WPI and 30% (v/v) flaxseed oil, homogenized at (A) 20 and (B) 80 MPa. Number of passes: 1 pass, 4 passes, 7 passes and pure oil. The bars represent the standard deviation amongst replications. 70

CHAPTER 4

Fig. 4.1. pH-dependence of zeta potential for aqueous solutions of WPI, FPI and WPI-FPI. 91
Fig. 4.2. FTIR spectrum of flaxseed protein isolate (FPI).. 92
Fig. 4.3. Interfacial tension (mN/m) between flaxseed oil and protein in the WPI (3% w/v), FPI (0.14, 0.35 or 0.7% (w/v)) and WPI-FPI (3% (w/v) - 0.14% (w/v) or 3% (w/v) - 0.7% (w/v)) systems... 94

Fig. 4.4. Microstructure and particle size distribution of the O/W emulsions containing 3% (w/v) WPI and 30% (v/v) flaxseed oil, homogenized at 20, 40 and 60 MPa, with (A) one or (B) two passes through the homogenizer. Scale bar = 10 μm. 95
Fig. 4.5. Effect of flaxseed protein isolate (FPI) concentration on the creaming index (CI) of the O/W emulsions homogenized at 40 or 60 MPa, with one or two passes through the homogenizer. FPI concentration: 0.14, 0.35 or 0.7% (w/v). 98
Fig. 4.6. Microstructures of the top cream phase of the O/W emulsions containing 0.14, 0.35 or 0.7% (w/v) FPI and 30% (v/v) flaxseed oil. Scale bar = 100 μm. 100
Fig. 4.7. Time-dependence of the top cream phase of the O/W emulsions containing 0.14, 0.35 or 0.7% (w/v) FPI and 30% (v/v) flaxseed oil. S_1 (open symbols): data without prior shearing and S_2 (closed symbols): data at steady state. FPI concentration: 0.14, 0.35 or 0.7% (w/v). 103
Fig. 4.8. Visual appearance and separation percentage (BCP = bottom cream phase and BSP = bottom serum phase) of the O/W emulsions containing 3% (w/v) WPI, (A, B) 0.14 or (C, D) 0.7% (w/v) FPI and 30% (v/v) flaxseed oil, homogenized at 40 MPa, with (A, C) one or (B, D) two passes through the homogenizer. 107
Fig. 4.9. Particle size distribution of the O/W emulsions containing 3% (w/v) WPI, (A) 0.14 or (B) 0.7% (w/v) FPI and 30% (v/v) flaxseed oil, homogenized at 40 or 60 MPa, with one or two passes through the homogenizer. Phase of the emulsion: Top (black color) and bottom (gray color) phase. 108
Fig. 4.10. Microstructures of the top (TP) and bottom (BP) phases of the O/W emulsions containing 3% (w/v) WPI, 0.14 or 0.7% (w/v) FPI and 30% (v/v) flaxseed oil. Scale bar = 25 μm. 111

CHAPTER 5

Fig. 5.1. A) Schematic representation of the production of microbeads by extrusion and B) atomizer nozzle. H = distance between the atomizer nozzle and the salt solution, d_l = diameter of the feed nozzle exit (1 mm) and d_g = diameter of air nozzle exit (3.08 mm). 132
Fig. 5.2. Visual appearance of the particles composed by 15% (v/v) flaxseed oil, 1.5% (w/v) WPI and 0.1, 0.3 or 0.5% (w/v) gellan, gelled in 0.56, 0.74, 0.93 or 1.11% (w/v) $CaCl_2$. Scale bar = 0.5 cm. 137
Fig. 5.3. Particle size distribution, mean particle diameter (d_{32}) and span of microbeads containing 15% (v/v) flaxseed oil, 1.5% (w/v) WPI, (A) 0, (B) 0.25 or (C) 0.5% (w/v) FPH and 0.1, 0.3 or 0.5% (w/v) gellan. 139
Fig. 5.4. Microstructure of microbeads composed by 15% (v/v) flaxseed oil, 1.5% (w/v) WPI, 0 – 0.5% (w/v) FPH and 0.1 – 0.5% (w/v) gellan. Scale bar = 100 μm. 141
Fig. 5.5. Mean particle diameter (d_{32}) of microbeads containing 15% (v/v) flaxseed oil, 1.5% (w/v) WPI and 0.3% (w/v) gellan, dispersed in distilled water and in $CaCl_2$ solutions: 0.56, 1.11 and 2.22% (w/v). 143
Fig. 5.6. Microstructure of microbeads composed by 15% (v/v) flaxseed oil, 1.5% (w/v) WPI and 0.3% (w/v) gellan in different media. Scale bar = 100 μm. 144
Fig. 5.7. Apparent viscosity of microbeads suspensions composed by 15% (v/v) flaxseed oil, 1.5% (w/v) WPI, (A) 0 or (B) 0.25% (w/v) FPH and 0.3% (w/v) gellan in $CaCl_2$ solution (0.56% w/v). Volume fraction of microbeads: 10, 30, 50, 70 and 90% (w/v)..... 145
Fig. 5.8. CSLM micrographs of microbeads composed by 15% (v/v) flaxseed oil, 1.5% (w/v) WPI, 0 or 0.25% (w/v) FPH and 0.1% or 0.3% (w/v) gellan. Scale bar = 20 μm. .. 149

Fig. 5.9. Zeta potential (mV) of microbeads composed by 15% (v/v) flaxseed oil, 1.5% (w/v) WPI, (A) 0 or (B) 0.25% (w/v) FPH and 0.3% (w/v) gellan, before digestion and of microbeads in gastric and intestinal media during digestion. 150

Fig. 5.10. Microstructure of microbeads composed by 15% (v/v) flaxseed oil, 1.5% (w/v) WPI, 0 or 0.25% (w/v) FPH and 0.3% (w/v) gellan, before and during the gastric and intestinal steps. Scale bar = 100 μm. 153

Fig. 5.11. Particle size distribution, mean particle diameter (d_{32}) and span of microbeads composed by 15% (v/v) flaxseed oil, 1.5% (w/v) WPI, (black color) 0 or (gray color) 0.25% (w/v) FPH and 0.3% (w/v) gellan, before and during the (A) gastric and (B) intestinal steps. Time of gastric step: 0, 15, 30, 45 and 60 min and of intestinal step: 15, 30, 45, 60, 75, 90, 105 and 120 min. 155

ÍNDICE DE TABELAS

CHAPTER 3

Table 3.1. Mean droplet diameter (μm) and span of the O/W emulsions stabilized by WPI. 60
Table 3.2. Rheological parameters obtained from the power law model and the apparent viscosity at 100 s^{-1} (η_{100}) for the O/W emulsions stabilized by WPI. 67

CHAPTER 4

Table 4.1. Composition of the O/W emulsions evaluated..........85
Table 4.2. Mean droplet diameter (d_{32}) and span of the WPI emulsions (3% w/v)........... 96
Table 4.3. Rheological parameters obtained from the Newtonian and the power law model and the apparent viscosity at 3 s^{-1} (η_3) for the O/W emulsions stabilized by FPI (0.14, 0.35 or 0.7% w/v). 102
Table 4.4. Area between the curves corresponding to the first (S_1) and last cycle (S_2) of shear (thixotropy, Pa/s) of the emulsions stabilized by FPI (0.14, 0.35 or 0.7% w/v)...... 104
Table 4.5. Protein concentration of the top (TP) and bottom (BP) phases and protein load (PL) of the O/W emulsions containing different FPI concentrations (0.14, 0.35 or 0.7% w/v). 105
Table 4.6. Mean droplet diameter (d_{32}) and span of the O/W emulsions stabilized by WPI (3% w/v) and FPI (0.14 or 0.7% w/v).......... 109
Table 4.7. Rheological parameters obtained from the Newtonian and the power law model and the apparent viscosity at 3 s^{-1} (η_3) for the O/W emulsions stabilized by WPI (3% w/v) and FPI (0.14 or 0.7% w/v). 113
Table 4.8. Surface protein concentration (SPC) (mg/m^2) of the O/W emulsions stabilized by WPI (3% w/v) and FPI (0.14 or 0.7% w/v). 114

CHAPTER 5

Table 5.1. Rheological parameters obtained from the power law model and the apparent viscosity at 50 s^{-1} (η_{50}) for the microbeads suspensions composed by 15% (v/v) flaxseed oil, 1.5% (w/v) WPI, 0 or 0.25% (w/v) FPH and 0.3% (w/v) gellan in $CaCl_2$ solution (0.56% w/v). 147

LISTA DE ABREVIATURAS E SIGLAS

α-La	α-lactalbumin
BCP	Bottom cream phase
β-Lg	β-lactoglobulin
BP	Bottom phase
BSA	Bovine serum albumin
BSP	Bottom serum phase
CI	Creaming index
CSLM	Confocal scanning laser microscopy
DMSO	Dimethyl sulfoxide
FITC	Fluorescein-5-isothiocyanate
FPC	Flaxseed protein concentrate
FPH	Flaxseed protein hydrolysate
FPI	Flaxseed protein isolate
FTIR	Fourier transform infrared spectroscopy
GI	Gastrointestinal
IPL	Isolado protéico da linhaça
IPS	Isolado protéico de soro de leite
O/A	Óleo em água
O/W	Oil-in-water
PL	Protein load
PV	Peroxide value
SDS-PAGE	Sodium dodecyl sulfate polyacrylamide gel electrophoresis
SPC	Surface protein concentration
TP	Top phase
W/O	Water-in-oil
WPI	Whey protein isolate

Tese de doutorado

AUTORA: Kátia Regina Kuhn

TÍTULO: Encapsulação de compostos bioativos obtidos a partir da linhaça

ORIENTADORA: Profa. Dra. Rosiane Lopes da Cunha

Departamento de Engenharia de Alimentos – FEA – UNICAMP

RESUMO GERAL

A encapsulação de compostos bioativos vem sendo utilizada como uma alternativa para minimizar a degradação destes ingredientes durante o processamento, armazenamento e/ou processo digestivo, permitindo o aumento da vida de prateleira dos alimentos e a liberação controlada destes compostos. Nesse sentido, o objetivo geral deste trabalho foi produzir microgéis a partir da extrusão de emulsões O/A contendo isolado protéico de soro de leite (IPS) e gelana em uma solução gelificante de cloreto de cálcio visando a encapsulação e liberação controlada de óleo e hidrolisado protéico da linhaça. Na primeira parte deste estudo, a influência das condições de homogeneização (pressão e número de passagens) no preparo de emulsões estabilizadas por IPS foi avaliada com o intuito de obter sistemas mais estáveis e com menor oxidação lipídica. Todos os sistemas foram estáveis à cremeação e um aumento da pressão de homogeneização para 800 bar e do número de passagens para até 3 vezes, diminuiu o tamanho médio de gota das emulsões. Condições extremas de homogeneização levaram à formação de agregados protéicos de alta massa molecular (>200 kDa), favorecendo o aumento na viscosidade das emulsões. Com o aumento da pressão, uma distribuição de tamanho de gotas bimodal, indicando que coalescência pode ter ocorrido, e um aumento na formação de produtos primários da oxidação foram observados. Na segunda etapa do trabalho, avaliou-se o potencial do isolado protéico da linhaça (IPL) como agente emulsificante em sistemas puros e mistos com proteínas do soro de leite preparados sob alta pressão de homogeneização. As emulsões estabilizadas por IPL ou IPS-IPL mostraram-se cineticamente instáveis e o aumento da concentração de IPL e das condições de homogeneização melhoraram a estabilidade dos sistemas puros, o que foi atribuído à sua maior viscosidade. No entanto, a maior estabilidade foi obtida com a adição de IPS nas emulsões contendo menor concentração de IPL (0,14% m/v) e utilizando condições mais drásticas de homogeneização. Por último, microgéis de IPS e gelana foram

produzidos a partir da gelificação iônica de emulsões visando a encapsulação de compostos bioativos da linhaça. Os microgéis foram avaliados quanto à estabilidade, resistência e liberação destes compostos bioativos através da simulação *in vitro* do processo digestivo. Os resultados mostraram que óleo e hidrolisado protéico da linhaça foram encapsulados e que os microgéis resistiram às condições gástricas, mas foram desintegrados no meio intestinal. Além disso, a adição de hidrolisado diminuiu o tamanho das partículas e parece ter auxiliado na encapsulação do óleo de linhaça. Sendo assim, os microgéis produzidos poderiam ser utilizados para a proteção e liberação controlada dos compostos bioativos encapsulados.

Palavras chave: Emulsões O/A, proteínas do soro, óleo de linhaça, hidrolisado protéico da linhaça, microgéis, digestão *in vitro*

Ph. D. Thesis

AUTHOR: Kátia Regina Kuhn

TITLE: Encapsulation of bioactive compounds obtained from flaxseed

SUPERVISOR: Profa. Dra. Rosiane Lopes da Cunha

Department of Food Engineering – FEA – UNICAMP

ABSTRACT

The encapsulation of bioactive compounds has been used as an alternative to minimize degradation of these ingredients during processing, storage and/or digestive process, allowing increased shelf life of foods and the controlled release of these compounds. In this way, the general purpose of this work was to produce microbeads from extrusion of the O/W emulsions containing whey protein isolate (WPI) and gellan into a gelling solution of calcium chloride aiming the encapsulation and controlled release of oil and protein hydrolysate from flaxseed. In the first part of this study, the influence of homogenization conditions (pressure and number of passes) in the preparation of emulsions stabilized by WPI was assessed in order to obtain more stable systems and decreased lipid oxidation. All the systems were stable to creaming and an increase of homogenization pressure to 80 MPa and the number of passes up to 3 times, decreased the mean droplet size of the emulsions. Extreme homogenization conditions led to the formation of high molecular weight protein aggregates (>200 kDa), favoring the increase in viscosity of the emulsions. Increasing pressure, a bimodal droplets size distribution, indicating droplets coalescence, and an increase in the formation of primary oxidation products were observed. In the second step of the work, the potential of flaxseed protein isolate (FPI) as an emulsifying agent was evaluated in pure systems and mixed with whey proteins prepared under high pressure homogenization. The emulsions stabilized by FPI or WPI-FPI were kinetically unstable and the increase of FPI concentration and homogenization conditions improved the stability of pure systems, which was attributed to its higher viscosity. However, the greatest stability was achieved with the WPI addition in the emulsions containing the lowest FPI concentration (0.14% w/v) and using more drastic homogenization conditions. Finally, WPI-gellan microgels were produced by ionic gelation of the emulsions aiming the encapsulation of bioactive compounds from flaxseed. Microgels were evaluated in relation

to stability, resistance and release of these bioactive compounds by simulating *in vitro* digestion process. The results showed that oil and protein hydrolysate from flaxseed were encapsulated and that microbeads resisted to gastric conditions, but were disintegrated in intestinal medium. Furthermore, the hydrolysate addition decreased the particle size and seems to have contributed for the flaxseed oil encapsulation. Thus, microbeads produced could be used for protection and controlled release of the encapsulated bioactive compounds.

Keywords: O/W emulsions, whey proteins, flaxseed oil, flaxseed protein hydrolysate, microbeads, *in vitro* digestion

CAPÍTULO 1

Introdução Geral

1.1. INTRODUÇÃO

A incorporação e encapsulação de compostos bioativos, tais como vitaminas, probióticos, peptídeos, lipídeos, antioxidantes, entre outros, possibilita a proteção às condições de processo, estocagem e/ou no sistema digestivo destes ingredientes funcionais (CHEN et al., 2006). Emulsões óleo-água (O/A) apresentam elevado potencial para a encapsulação de compostos bioativos, principalmente por apresentarem regiões polares e apolares, baixo custo de produção e relativa facilidade de preparo (McCLEMENTS et al., 2007). No entanto, emulsões são sistemas termodinamicamente instáveis que tendem a se desestabilizar com o tempo, sendo o uso de forças mecânicas intensas e/ou a adição de um emulsificante/estabilizante, necessários para aumentar essa estabilidade por um determinado período de tempo (McCLEMENTS et al., 2007). Além disso, a gelificação da fase contínua de emulsões estabilizadas por biopolímeros pode aumentar a sua estabilidade (McCLEMENTS et al., 2007). Para isso, o método de extrusão seguido por gelificação ionotrópica pode ser utilizado, resultando na formação de microgéis (BUREY et al., 2008; PERRECHIL et al., 2012), que podem incorporar e proteger compostos bioativos, inclusive compostos termolábeis (AZEREDO, 2005), além de poderem ser adicionados em meios com elevada atividade de água (BUREY et al., 2008).

Atualmente, a linhaça está recebendo atenção como um alimento funcional devido aos benefícios à saúde relacionados principalmente ao seu óleo, lignanas e polissacarídeos solúveis, enquanto que as informações sobre os benefícios das suas proteínas são ainda limitadas (MARAMBE et al., 2008). O óleo de linhaça é muito rico em ácidos graxos insaturados, sendo reconhecido como uma das maiores fontes vegetais de ômega 3 (ácido α-linolênico) na natureza (TONON et al., 2011), o qual tem um efeito positivo na redução do risco de doenças cardiovasculares (TONON et al., 2011; ZHAO et al., 2007). No entanto, estes óleos podem oxidar facilmente, devido a seu alto grau de insaturação (TONON et al., 2011), sendo sua oxidação o principal fator de deterioração da qualidade de muitos alimentos naturais ou processados (McCLEMENTS & DECKER, 2000; SUN & GUNASEKARAN, 2009). Hidrolisados protéicos da linhaça vêm sendo estudados com relação a suas atividades biológicas, tais como propriedades antioxidantes, anti-hipertensivas e antiinflamatórias (MARAMBE et al., 2008; UDENIGWE et al., 2009a,b). No entanto, apesar destas propriedades e do perfil de aminoácidos de boa qualidade nutricional, que é comparado ao das proteínas da soja (RABETAFIKA et al., 2011; UDENIGWE et al., 2009a,b; WANG et al., 2009), as proteínas da linhaça ainda não têm sido amplamente exploradas na nutrição humana (MARAMBE et al., 2008; UDENIGWE et al., 2009b), o que poderia estar relacionado com a dificuldade de isolar a proteína, que tem baixo rendimento de extração devido à presença de gomas (OOMAH & MAZZA, 1993; SMITH et al., 1946; UDENIGWE et al., 2009b).

Para a obtenção de benefícios à saúde, é também necessário garantir a estabilidade dos compostos bioativos no sistema gastrointestinal e facilitar a sua liberação em local adequado para que os mesmos possam ser absorvidos pelo organismo (CHAMPAGNE & FUSTIER, 2007). A liberação controlada pode melhorar a efetividade de compostos encapsulados, ampliar a sua faixa de aplicação e garantir dosagem ótima (GOUIN, 2004). Sendo assim, a encapsulação destes compostos pode ser interessante na tentativa de evitar a perda de sua funcionalidade e biodisponibilidade, possibilitando a sua liberação no local desejado.

Existem na literatura trabalhos envolvendo a encapsulação de óleo de linhaça, visando retardar, inibir ou apenas minimizar a sua oxidação (CARNEIRO et al., 2013; LIU et al., 2010; PARTANEN et al., 2008). São encontrados também estudos que avaliam o efeito da adição de aminoácidos e peptídeos de soja e de gelatina com atividade antioxidante a sistemas de encapsulação de ácidos graxos poliinsaturados ω-3 com o intuito de melhorar a sua estabilidade oxidativa (PARK et al., 2005a,b). No entanto, não são encontrados estudos relacionados à adição de hidrolisados protéicos da linhaça a sistemas de encapsulação do óleo de mesma fonte, visando evitar a sua oxidação e ainda obter benefícios à saúde em função das propriedades funcionais dos mesmos.

1.2. OBJETIVOS

O objetivo geral deste trabalho foi encapsular hidrolisados protéicos bioativos, obtidos da farinha de linhaça, juntamente com o óleo de linhaça, rico em ômega 3, através da gelificação iônica de emulsões óleo-água (O/A), visando sua proteção e liberação controlada.

Os objetivos específicos deste trabalho foram:

A) Estudar a influência das condições de processo, pressão de homogeneização (200–1000 bar) e número de passagens pelo homogeneizador (1–7), sobre a estabilidade e oxidação lipídica do óleo de linhaça das emulsões O/A estabilizadas por proteínas do soro de leite, visando definir uma melhor condição para o preparo destes sistemas;

B) Avaliar o potencial das proteínas da linhaça como agente emulsificante através do estudo de emulsões O/A contendo apenas proteínas do soro, proteínas da linhaça ou uma mistura de proteínas do soro – proteínas da linhaça, preparadas sob alta pressão de homogeneização (200, 400 ou 600 bar), com uma ou duas passagens pelo homogeneizador;

C) Produzir microgéis através da extrusão de emulsões O/A contendo proteínas do soro e gelana utilizando o cloreto de cálcio ($CaCl_2$) como agente gelificante. Estes microgéis foram utilizados para encapsular óleo e hidrolisado protéico da linhaça, sendo avaliada a sua estabilidade e resistência às condições de cisalhamento, assim como a liberação controlada dos compostos bioativos encapsulados através da simulação *in vitro* do processo digestivo.

1.3. DESCRIÇÃO DOS CAPÍTULOS

A apresentação deste trabalho foi organizada em 5 capítulos como descrito a seguir:

Capítulo 1: *Introdução Geral*

Capítulo 2: *Revisão Bibliográfica*

Neste capítulo são abordados aspectos teóricos dos sistemas estudados, bem como uma revisão bibliográfica relatando a literatura recente e mais relevante sobre o tema deste trabalho.

Capítulo 3: *Flaxseed oil – Whey protein isolate emulsions: Effect of high pressure homogenization*

Neste capítulo foi realizado um estudo da influência das condições de homogeneização (pressão e número de passagens) sobre a estabilidade e oxidação lipídica das emulsões óleo de linhaça – proteínas do soro. A partir deste estudo, foram identificados os fatores responsáveis pela alteração nas características das emulsões e uma condição para o seu preparo foi definida, visando maior estabilidade e menor oxidação lipídica. Os diferentes sistemas foram avaliados quanto à estabilidade à cremeação, microscopia, diâmetro médio das gotas, propriedades reológicas, estabilidade oxidativa e distribuição de massa molecular, esta última avaliada através da eletroforese em gel de poliacrilamida.

Capítulo 4: *Assessing the potential of flaxseed protein as an emulsifier combined with whey protein isolate*

Nesta etapa, o poder emulsificante do isolado protéico da linhaça (IPL) foi avaliado em sistemas puros e mistos com proteínas do soro (IPS). Primeiramente, foram preparadas emulsões de IPS em três diferentes pressões de homogeneização (200, 400 ou 600 bar), utilizando uma ou duas passagens pelo homogeneizador. Estas condições foram definidas com base nos resultados encontrados no Capítulo 3, visando avaliar a influência de pressões intermediárias e de um menor número de passagens pelo homogeneizador sobre o tamanho de gotas das emulsões formadas. A partir deste estudo, foram escolhidas as pressões de homogeneização de 400 e 600 bar, com uma ou duas passagens pelo homogeneizador, para o preparo das emulsões estabilizadas por IPL ou por IPS-IPL, visando a obtenção de sistemas com maior estabilidade cinética.

Para a caracterização dos sistemas, foram utilizadas as técnicas de potencial zeta, FTIR e método da gota pendente e/ou ascendente. A determinação das propriedades das emulsões e das condições necessárias para a formação de sistemas menos instáveis foi feita a partir da avaliação da estabilidade à cremeação, diâmetro médio das gotas, microscopia, reologia e carga protéica.

Capítulo 5: *Production of whey protein isolate – gellan microbeads for encapsulation and release of bioactive compounds from flaxseed*

Neste capítulo foi realizado um estudo da produção de microgéis a partir da gelificação de emulsões O/A em pH ~ 7,0 utilizando a técnica de extrusão em uma solução de $CaCl_2$ para a encapsulação de compostos bioativos da linhaça. As condições de homogeneização (600 bar, duas passagens) utilizadas no preparo destas emulsões foram definidas com base nos resultados obtidos no Capítulo 4. Nesta etapa, foram avaliadas a concentração de sal mínima necessária para a gelificação, bem como as concentrações de gelana e de hidrolisado protéico da linhaça a serem utilizadas. Os microgéis produzidos foram caracterizados quanto à morfologia, tamanho e potencial zeta, além de serem avaliados quanto à estabilidade e comportamento reológico de suas suspensões e resistência frente às condições gastrointestinais.

Capítulo 6: *Conclusões Gerais*

Neste capítulo são relatadas as principais conclusões sobre os resultados obtidos.

1.4. REFERÊNCIAS

AZEREDO, H. M. C. Encapsulação: Aplicação à tecnologia de alimentos. **Alimentos e Nutrição**, v. 16, n. 1, p. 89-97, 2005.

BUREY, P.; BHANDARI, B. R.; HOWES, T.; GIDLEY, M. J. Hydrocolloid gel particles: Formation, characterization, and application. **Critical Reviews in Food Science and Nutrition**, v. 48, n. 5, p. 361-377, 2008.

CARNEIRO, H. C. F.; TONON, R. V.; GROSSO, C. R. F.; HUBINGER, M. D. Encapsulation efficiency and oxidative stability of flaxseed oil microencapsulated by spray drying using different combinations of wall materials. **Journal of Food Engineering**, v. 115, n. 4, p. 443-451, 2013.

CHAMPAGNE, C. P.; FUSTIER, P. Microencapsulation for the improved delivery of bioactive compounds into foods. **Current Opinion in Biotechnology**, v. 18, n. 2, p. 184-190, 2007.

CHEN, L.; REMONDETTO, G. E.; SUBIRADE, M. Food protein-based materials as nutraceutical delivery systems. **Trends in Food Science and Technology**, v. 17, n. 5, p. 272-283, 2006.

GOUIN, S. Microencapsulation: industrial appraisal of existing technologies and trends. **Trends in Food Science & Technology**, v. 15, n. 7-8, p. 330-347, 2004.

LIU, S.; LOW, N. H.; NICKERSON, M. T. Entrapment of flaxseed oil within gelatin-gum arabic capsules. **Journal of the American Oil Chemists' Society**, v. 87, n. 7, p. 809-815, 2010.

MARAMBE, P. W. M. L. H. K.; SHAND, P. J.; WANASUNDARA, J. P. D. An in-vitro investigation of selected biological activities of hydrolysed flaxseed (*Linum usitatissimum* L.) proteins. **Journal of the American Oil Chemists' Society**, v. 85, n. 12, p. 1155-1164, 2008.

McCLEMENTS, D. J.; DECKER, E. A. Lipid oxidation in oil-in-water emulsions: Impact of molecular environment on chemical reactions in heterogeneous food systems. **Journal of Food Science**, v. 65, n. 8, p. 1270-1282, 2000.

McCLEMENTS, D. J.; DECKER, E. A.; WEISS, J. Emulsion-based delivery systems for lipophilic bioactive components. **Journal of Food Science**, v. 72, n. 8, p. R109-R124, 2007.

OOMAH, B. D.; MAZZA, G. Flaxseed proteins – a review. **Food Chemistry**, v. 48, n. 2, p. 109-114, 1993.

PERRECHIL, F. A.; VILELA, J. A. P.; GUERREIRO, L. M. R.; CUNHA, R. L. Development of Na-CN—κ-carrageenan microbeads for the encapsulation of lipophilic compounds. **Food Biophysics**, v. 7, n. 3, p. 264-275, 2012.

PARK, E. Y.; MURAKAMI, H.; MATSUMURA, Y. Effects of the addition of amino acids and peptides on lipid oxidation in a powdery model system. **Journal of Agricultural and Food Chemistry**, v. 53, n. 21, p. 8334-8341, 2005a.

PARK, E. Y.; MURAKAMI, H.; MORI, T.; MATSUMURA, Y. Effects of protein and peptide addition on lipid oxidation in powder model system. **Journal of Agricultural and Food Chemistry**, v. 53, n. 1, p. 137-144, 2005b.

PARTANEN, R.; RAULA, J.; SEPPÄNEN, R.; BUCHERT, J.; KAUPPINEN, E.; FORSSELL, P. Effect of relative humidity on oxidation of flaxseed oil in spray dried whey protein emulsions. **Journal of Agricultural and Food Chemistry**, v. 56, n. 14, p. 5717-5722, 2008.

RABETAFIKA, H. N.; REMOORTEL, V. V.; DANTHINE, S.; PAQUOT, M.; BLECKER, C. Flaxseed proteins: food uses and health benefits. **International Journal of Food Science and Technology**, v. 46, n. 2, p. 221-228, 2011.

SMITH, A. K.; JOHNSEN, V. L.; BECKEL, A. C. Linseed proteins: Alkali dispersion and acid precipitation. **Industrial and Engineering Chemistry**, v. 38, n. 3, p. 353-356, 1946.

SUN, C.; GUNASEKARAN, S. Effects of protein concentration and oil-phase volume fraction on the stability and rheology of menhaden oil-in-water emulsions stabilized by whey protein isolate with xanthan gum. **Food Hydrocolloids**, v. 23, n. 1, p. 165-174, 2009.

TONON, R. V.; GROSSO, C. R. F.; HUBINGER, M. D. Influence of emulsion composition and inlet air temperature on the microencapsulation of flaxseed oil by spray drying. **Food Research International**, v. 44, n. 1, p. 282-289, 2011.

UDENIGWE, C. C.; LIN, Y.-S.; HOU, W.-C.; ALUKO, R. E. Kinetics of the inhibition of renin and angiotensin I-converting enzyme by flaxseed protein hydrolysate fractions. **Journal of Functional Foods**, v. 1, n. 2, p. 199-207, 2009a.

UDENIGWE, C. C.; LU, Y.-L.; HAN, C.-H.; HOU, W.-C.; ALUKO, R. E. Flaxseed protein-derived peptide fractions: Antioxidant properties and inhibition of lipopolysaccharide-induced nitric oxide production in murine macrophages. **Food Chemistry**, p. 116, n. 1, p. 277-284, 2009b.

WANG, B.; WANG, L.-J.; LI, D.; BHANDARI, B.; WU, W.-F.; SHI, J.; CHEN, X. D.; MAO, Z.-H. Effects of potato starch addition and cooling rate on rheological characteristics of flaxseed protein concentrate. **Journal of Food Engineering**, v. 91, n. 3, p. 392-401, 2009.

ZHAO, G.; ETHERTON, T. D.; MARTIN, K. R.; GILLIES, P. J.; WEST, S. G.; KRIS-ETHERTON, P. M. Dietary α-linolenic acid inhibits proinflammatory cytokine production by peripheral blood mononuclear cells in hypercholesterolemic subjects. **The American Journal of Clinical Nutrition**, v. 85, n. 2, p. 385-391, 2007.

CAPÍTULO 2

Revisão Bibliográfica

2. REVISÃO BIBLIOGRÁFICA

2.1. SEMENTE DE LINHO (LINHAÇA)

O linho (*Linum usitatissimum* L.) é um dos cultivos mais antigos conhecidos pelo homem, principalmente pelo uso de seu óleo e fibras (CHEN et al., 2006; CUI, 2001; MAZZA & BILIADERIS, 1989; WANASUNDARA & SHAHIDI, 1997). A sua semente é oval, tem dimensões aproximadas de 2,5 mm X 5 mm X 1 mm e peso médio de 3-13 mg por semente (WANASUNDARA & SHAHIDI, 1997). A semente de linho (linhaça) contém aproximadamente 35% de lipídeos, 30% de proteínas e 35% de fibras, dos quais 7-10% são fibras solúveis, cuja composição varia em função do cultivar, condições ambientais e localização geográfica (GOH et al., 2006).

O crescente interesse na linhaça como fonte alimentícia é devido às inúmeras pesquisas que comprovam que ela pode fornecer uma variedade de benefícios à saúde (HALL et al., 2006), como redução dos riscos de doenças cardiovasculares e câncer, atividade antiviral e bactericida, atividade antiinflamatória, efeito laxativo, efeito hipoglicêmico e prevenção de sintomas da menopausa e osteoporose (BABU & WIESENFELD, 2003). Os componentes que estão relacionados a estes benefícios incluem as lignanas (na sua forma predominante Secoisolariciresinol Diglicosídeo (SDG)), o ácido α-linolênico (ALA) e os polissacarídeos (gomas ou fibras) (HALL et al., 2006). O interesse no ALA e nas lignanas como ingredientes alimentícios tem aberto oportunidades para a utilização da linhaça em alimentos (HALL et al., 2006). Porém, o mesmo nível de interesse não tem sido observado para outros componentes da linhaça, como as proteínas (HALL et al., 2006).

2.1.1. Proteínas da linhaça

O conteúdo de proteína na linhaça varia entre 10 e 31% (HALL et al., 2006; OOMAH & MAZZA, 1993), de acordo com o cultivar, a localização geográfica e o tipo de processamento da semente (HALL et al., 2006).

Diferentes métodos podem ser utilizados para o isolamento de proteínas da linhaça (OOMAH & MAZZA, 1993). Os primeiros processos, que são clássicos, envolviam extração com solução salina e precipitação da proteína por remoção do sal através de diálise (OOMAH & MAZZA, 1993; OSBORNE, 1892). Porém, devido à falta de praticidade deste método, outros foram sendo utilizados ao longo dos anos com o intuito de melhorar o rendimento de extração da proteína (DEV et al., 1986; SMITH et al., 1946; SOSULSKI & BAKAL, 1969). Um dos fatores que podem influenciar o rendimento é a presença de mucilagem na casca das sementes (OOMAH & MAZZA, 1993; SMITH et al., 1946; UDENIGWE et al., 2009a). Por isso, existem alguns trabalhos que estudam a possibilidade de melhorar o rendimento do isolado protéico da linhaça utilizando diferentes métodos de remoção da mucilagem (UDENIGWE et al., 2009a). Entre alguns destes métodos, estão o descascamento da semente (SMITH et al., 1946), a utilização de solução salina (MARAMBE et al., 2008) e a hidrólise enzimática das fibras (UDENIGWE et al., 2009a,b) antes da separação da proteína. Segundo Smith et al. (1946), a casca das sementes contém também pigmentos de coloração escura, os quais, se não eliminados, são extraídos com a proteína e dão a ela uma cor escura indesejável.

Estudos revelam que as proteínas da linhaça consistem em duas principais frações, uma de alta massa molecular do tipo globulina (11S-12S) solúvel em solução salina e outra de menor massa molecular do tipo albumina (1,6S-2S) solúvel em água (CHUNG et al., 2005; MADHUSUDHAN & SINGH, 1985a,b; MARCONE et al., 1998; YOULE &

HUANG, 1981). Quanto à composição de aminoácidos, as proteínas da linhaça possuem altos níveis de arginina, leucina, ácido aspártico e ácido glutâmico, enquanto a metionina e cistina estão em menor concentração (HALL et al., 2006; OOMAH & MAZZA, 1993).

O perfil de aminoácidos da proteína da linhaça é bastante similar ao da proteína da soja, a qual é vista como uma das proteínas vegetais mais nutritivas (OOMAH & MAZZA, 1993; RABETAFIKA et al., 2011; UDENIGWE et al., 2009b). No entanto, a proteína da linhaça é mais efetiva na diminuição do colesterol e triglicerídeos do plasma sangüíneo se comparada com a proteína da soja e a caseína (BHATHENA et al., 2002). Estudo realizado por Xu et al. (2008) também mostrou que o extrato de proteína da linhaça apresenta atividade antifúngica contra uma ampla variedade de fungos alimentícios.

Hidrolisados de proteína, especialmente aqueles que contêm peptídeos de cadeia curta, são ingredientes interessantes para a formulação de alimentos funcionais e produtos nutracêuticos (OMONI & ALUKO, 2006). Tem sido aceito que de 30-50% do nitrogênio da dieta é absorvido no corpo na forma de pequenos peptídeos, os quais podem exercer diferentes funções fisiológicas (MARAMBE et al., 2008). Sendo assim, atenção tem sido dada para estudar e entender a habilidade das proteínas alimentícias em gerar peptídeos bioativos, pois estes estão inativos quando presentes na seqüência de proteínas, mas podem ser liberados durante a digestão gastrointestinal ou no processamento de alimentos (MARAMBE et al., 2008). Após sua liberação, os peptídeos exercem várias funções fisiológicas baseadas na seqüência e composição de aminoácidos (MARAMBE et al., 2008).

Recentemente foram publicados alguns trabalhos relacionados aos efeitos benéficos promovidos pelos hidrolisados biologicamente ativos extraídos da linhaça. Marambe et al. (2008) reportaram que o hidrolisado protéico da linhaça não fracionado apresentou atividade anti-hipertensiva, e também propriedades antioxidantes. Udenigwe et al. (2009a,b) também encontraram resultados favoráveis em relação à atividade anti-hipertensiva, antioxidante e antiinflamatória para frações de peptídeos catiônicos e de baixa massa molecular da linhaça obtidos a partir de hidrólise utilizando diferentes proteases.

Além das propriedades funcionais nutricionais, as proteínas da linhaça também possuem propriedades tecnológicas interessantes. Em geral, o isolado protéico da linhaça exibe maior capacidade de absorção de água e de óleo e melhorada atividade emulsificante e estabilizante se comparado com o isolado protéico da soja (DEV & QUENSEL, 1986). As proteínas da linhaça parecem ser estruturalmente mais lipofílicas do que as proteínas da soja, e as propriedades hidrofílicas (ou polaridade) do isolado protéico da linhaça são influenciadas pela presença de mucilagem na extração da proteína (OOMAH & MAZZA, 1993).

No entanto, além de conter consideráveis quantidades de mucilagem (pentosanas), as proteínas da linhaça também possuem compostos anti-nutricionais, tais como o ácido fítico, que influenciam as propriedades funcionais destes ingredientes (KRAUSE et al., 2002). Sendo assim, Krause et al. (2002) decidiram avaliar a extração de proteína da linhaça por micelização e comparar com a precipitação isoelétrica, com o intuito de obter um isolado com reduzido conteúdo de ácido fítico e pentosanas. O conteúdo de pentosanas e ácido fítico encontrado no isolado preparado por precipitação isoelétrica foi de 2,3% e 0,6%, respectivamente, enquanto que para o isolado obtido por micelização foi encontrado muito baixo conteúdo de pentosanas (0,6%) e praticamente nulo de ácido fítico (KRAUSE et al., 2002). Em relação às propriedades tecnológicas, a proteína obtida por precipitação isoelétrica apresentou menor solubilidade (entre 40-50%), maior capacidade de retenção de água e menor atividade emulsificante (KRAUSE et al., 2002).

2.1.2. Óleo de linhaça

O óleo de linhaça bruto, o mais íntegro nas suas propriedades terapêuticas e nutricionais, é obtido pelo processo de esmagamento e prensagem mecânica a frio das sementes de linho (TRUCOM, 2006). A extração deve ser realizada a frio, ou seja, a 45 °C no máximo (ideal a 40 °C), pois a temperatura é uma variável que pode acelerar a oxidação do óleo, alterando também sua qualidade e tempo de validade (TRUCOM, 2006). O óleo de linhaça possui 73% de ácidos graxos poliinsaturados (~57% de ácido alfa-linolênico (ω-3) e ~16% de ácido linoléico (ω-6)), cerca de 18% de ácidos monoinsaturados e somente 9% de ácidos graxos saturados, sendo considerado o alimento de origem vegetal mais rico em ômega 3 (TRUCOM, 2006; VAISEY-GENSER & MORRIS, 2003).

Os ácidos graxos poliinsaturados ômega 3 são essenciais para o crescimento e desenvolvimento normal do corpo e possuem um papel importante na prevenção e tratamento de doenças cardíacas coronárias, hipertensão, obesidade, diabetes do tipo 2, artrite, outras desordens inflamatórias e auto-imunes, e câncer (SIMOPOULOS, 1999; SUN & GUNASEKARAN, 2009). Sendo assim, a percepção dos benefícios dos ácidos graxos essenciais, especialmente o ω-3, tem estimulado o consumo de alimentos com alto teor deste composto ao longo dos últimos anos e, por isso, existe um crescente interesse em incorporar estes lipídeos bioativos em novas formulações (HIGGINS et al., 1999; KOLANOWSKI et al., 1999; WALLACE et al., 2000). No entanto, ainda existem inúmeros desafios de produção, transporte, e armazenamento de alimentos fortificados com ω-3, pois este é extremamente susceptível à deterioração oxidativa (KOLANOWSKI et al., 1999).

2.2. OXIDAÇÃO LIPÍDICA

A tendência dos lipídeos de sofrerem oxidação é uma das principais causas de deterioração da qualidade de muitos alimentos naturais ou processados, levando a alterações no sabor, aroma, textura, vida de prateleira, aparência e perfil nutricional, além de diminuir a aceitabilidade destes alimentos (McCLEMENTS & DECKER, 2000; PENG et al., 2010). A oxidação lipídica é indesejável na maioria dos alimentos, pois leva ao desenvolvimento de sabores e odores indesejáveis (McCLEMENTS & DECKER, 2000; RAMALHO & JORGE, 2006), além de provocar outras alterações que irão afetar não só a qualidade nutricional, devido à degradação de vitaminas lipossolúveis e de ácidos graxos essenciais, mas também a integridade e segurança dos alimentos, através da formação de produtos de reação potencialmente tóxicos (RAMALHO & JORGE, 2006).

Lipídeos são suscetíveis a processos oxidativos na presença de alguns catalisadores, tais como luz, calor, enzimas, metais e microrganismos (SHAHIDI & ZHONG, 2005). A autoxidação é o processo mais comum que leva à deterioração oxidativa e está associada à reação do oxigênio atmosférico com ácidos graxos insaturados e ocorre em três etapas (Figura 2.1) (RAMALHO & JORGE, 2006; SHAHIDI & ZHONG, 2005). A etapa 1 é a Iniciação, em que ocorre a formação dos radicais livres devido à retirada de um hidrogênio do carbono alílico na molécula do ácido graxo, em condições favorecidas por luz e calor. A etapa 2 é a Propagação, em que os radicais livres (que são prontamente susceptíveis ao ataque do oxigênio atmosférico), são convertidos em outros radicais, aparecendo os produtos primários de oxidação (peróxidos e hidroperóxidos), cuja estrutura depende da natureza dos ácidos graxos presentes. Os radicais livres formados atuam como propagadores da reação, resultando em um processo auto-catalítico. A etapa 3 é o Término, no qual dois radicais combinam-se, com a formação de produtos estáveis (produtos secundários de oxidação) obtidos por cisão e rearranjo dos peróxidos (epóxidos, compostos voláteis e não voláteis) (RAMALHO & JORGE, 2006).

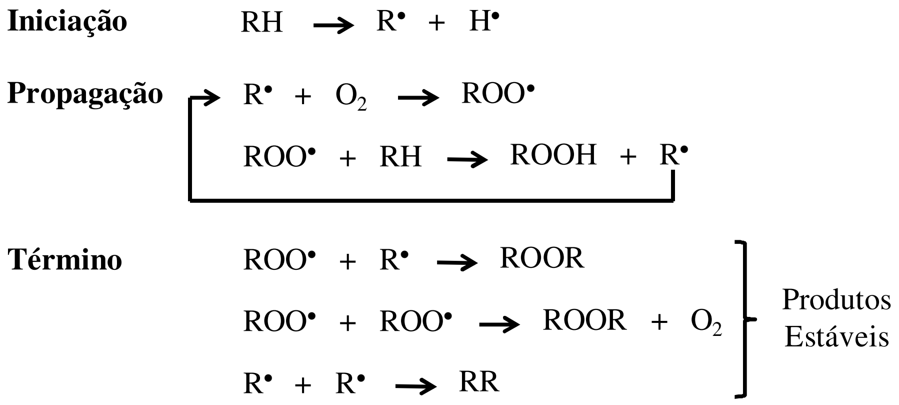

Iniciação $RH \rightarrow R^{\bullet} + H^{\bullet}$

Propagação $R^{\bullet} + O_2 \rightarrow ROO^{\bullet}$

$ROO^{\bullet} + RH \rightarrow ROOH + R^{\bullet}$

Término $ROO^{\bullet} + R^{\bullet} \rightarrow ROOR$

$ROO^{\bullet} + ROO^{\bullet} \rightarrow ROOR + O_2$

$R^{\bullet} + R^{\bullet} \rightarrow RR$

onde: RH – Ácido graxo insaturado; $R^{\bullet}$ – Radical livre;
$ROO^{\bullet}$ – Radical peróxido e ROOH – Hidroperóxido.

Figura 2.1. Esquema do mecanismo da oxidação lipídica (Fonte: RAMALHO & JORGE, 2006).

A susceptibilidade dos lipídeos à oxidação é uma das principais causas de deterioração da qualidade de emulsões alimentícias (COUPLAND & McCLEMENTS, 1996; McCLEMENTS & DECKER, 2000). A oxidação de lipídeos emulsionados é mecanicamente diferente da que ocorre com os óleos a granel, devido às propriedades da interface das gotas da emulsão e da habilidade dos pró-oxidantes, antioxidantes e substratos oxidáveis em se dividir entre as fases óleo, interface e água (RICHARDS et al., 2002). As propriedades da interface das gotas influenciam na oxidação lipídica devido à sua capacidade de atrair/repelir pró-oxidantes e antioxidantes, formando uma barreira física que altera as interações entre os lipídeos e os pró-oxidantes solúveis em água (RICHARDS et al., 2002).

Existem muitos fatores que podem influenciar na taxa de oxidação lipídica de emulsões O/A, tais como: a composição de ácidos graxos; o pH da fase aquosa e a composição iônica; o tipo e concentração de antioxidantes e pró-oxidantes; a concentração de oxigênio; as características das gotas lipídicas, como distribuição de tamanho, concentração e estado físico; e as propriedades interfaciais das gotas da emulsão, como espessura, carga, reologia, e permeabilidade (WARAHO et al., 2011).

2.3. EMULSÕES EM SISTEMAS ALIMENTÍCIOS

Uma emulsão pode ser simplesmente definida como um sistema composto de dois líquidos imiscíveis, no qual um dos líquidos está disperso (fase dispersa ou interna) no outro (fase contínua ou externa) como pequenas gotas esféricas (JAFARI et al., 2008). As emulsões óleo em água (O/A), que são as mais comuns em alimentos, consistem em sistemas onde as gotas de óleo estão dispersas em uma fase contínua aquosa como, por exemplo, leite, maionese, sorvete, sopas e molhos (McCLEMENTS & DECKER, 2000; WARAHO et al., 2011).

Emulsões são sistemas termodinamicamente instáveis devido à energia livre positiva necessária para aumentar a área entre as fases aquosa e oleosa, bem como às diferentes densidades das fases (McCLEMENTS, 2005; McCLEMENTS & DECKER, 2000). Particularmente para emulsões O/A, existem diversos mecanismos de desestabilização, sendo os principais a cremeação, sedimentação, floculação e coalescência das gotas (DICKINSON, 1992).

No entanto, emulsões cineticamente estáveis por um período de tempo suficientemente longo podem ser produzidas pela adição de ingredientes conhecidos como estabilizantes, tais como emulsificantes e/ou espessantes (McCLEMENTS et al., 2007). Emulsificantes são moléculas com atividade superficial que adsorvem na superfície das gotas formadas durante o processo de homogeneização. Uma vez presentes na superfície da gota, elas atuam de duas maneiras: reduzindo a tensão interfacial e formando uma camada protetora que impede a agregação das gotas (GUZEY & McCLEMENTS, 2006; McCLEMENTS, 2005; McCLEMENTS et al., 2007). Já os espessantes modificam propriedades da fase aquosa da emulsão, promovendo o aumento da viscosidade ou então a gelificação desta fase, o que retarda ou evita o movimento das gotas (DICKINSON, 2003; McCLEMENTS et al., 2007).

Muitas proteínas podem ser utilizadas como agentes emulsificantes devido à sua habilidade em facilitar a formação da emulsão, melhorar sua estabilidade e induzir propriedades físico-químicas desejáveis (McCLEMENTS, 2004). Alguns parâmetros que afetam diretamente a estabilidade de emulsões com adição de proteína são: temperatura, pH, força iônica, concentração e carga da proteína, razão proteína/óleo, tamanho de gota e fração volumétrica de óleo (KHALLOUFI et al., 2009).

Proteínas do soro de leite são largamente utilizadas em produtos alimentícios devido a seu alto valor nutricional e excelentes propriedades tecnológicas, como a habilidade de formar emulsões (MORR & HA, 1993), visto que possuem grupos hidrofílicos e hidrofóbicos, os quais possibilitam apresentar excelente atividade superficial e propriedades de estabilização de emulsões (PATEL & CHEN, 2008). Além disso, tem sido reportado que o isolado protéico de soro possui atividade antioxidante (HU et al., 2003; SUN & GUNASEKARAN, 2009; TONG et al., 2000), o que poderia ser extremamente benéfico aos sistemas contendo componentes sensíveis à oxidação na fase dispersa (SUN & GUNASEKARAN, 2009).

As principais frações protéicas do soro incluem a β-lactoglobulina (β-Lg, 60%), a α-lactoalbumina (α-La, 22%), a albumina bovina sérica (BSA, 5,5%) e as imunoglobulinas

(Ig, 9,1%), cujos valores de ponto isoelétrico correspondem à 5,2, 4,8-5,1, 4,8-5,1, e 5,5-6,8, respectivamente (BRYANT & McCLEMENTS, 1998). As propriedades funcionais das proteínas do soro dependem não só da sua composição, mas também do seu grau de desnaturação (BRYANT & McCLEMENTS, 1998). Em sua forma nativa, as proteínas do soro têm uma estrutura compacta e rígida estabilizada por interações intramoleculares, como interações hidrofóbicas, eletrostáticas, pontes de hidrogênio e dissulfídicas (KIOKAS et al., 2007). Porém, o aquecimento a altas temperaturas induz à desnaturação, resultando em um desdobramento das moléculas de proteína e exposição dos seus sítios reativos (KIOKAS et al., 2007). Uma pequena modificação das proteínas do soro por desnaturação induzida pelo aquecimento poderia levar à melhoria ou extensão das propriedades funcionais e então aumentar suas aplicações nos alimentos (KIOKAS et al., 2007).

Polissacarídeos são freqüentemente empregados como agentes espessantes em emulsões óleo-água, conferindo propriedades de textura desejáveis e estabilizando as gotas contra a cremeação (McCLEMENTS & DECKER, 2000). A goma gelana é um polissacarídeo aniônico extracelular produzido pela bactéria *Sphyngomonas elodea* e tem potencial para ser utilizada em uma ampla variedade de produtos alimentícios, atuando como agente gelificante, texturizante, estabilizante e formador de filme (SWORN et al., 1995), sendo a sua propriedade gelificante importante para a produção de microgéis.

Na sua forma acilada, como biossintetizada, a gelana produz géis fracos devido à presença de grupos gliceril (Figura 2.2) que causam impedimento estérico para a formação da rede tridimensional (VILELA, 2012). No entanto, um tratamento térmico em pH alcalino resulta na gelana desacilada (MORITAKA et al., 1995), que constitui sua forma comercial e possui elevado poder gelificante (PICONE, 2008). Na sua forma desacilada, ela é composta por unidades de tetrassacarídeos que se repetem, sendo eles: 1,3-β-D-glicose, 1,4-β-D-ácido glicurônico, 1,4-β-D-glicose e 1,4-α-L-ramnose, com um grupo carboxílico lateral em cada unidade (Figura 2.2) (JANSSON et al., 1983; MIYOSHI et al., 1995; O'NEILL et al., 1983). A gelana possui um valor de pKa próximo ao pH 3,5, o qual é dado pelo seu monômero, ácido glicurônico (PICONE & CUNHA, 2010).

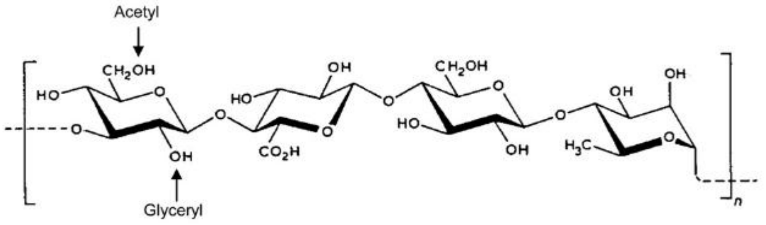

Figura 2.2. Unidade de tetrassacarídeo que se repete na goma gelana desacilada. Os sítios de ligação dos substituintes gliceril e acetil na gelana altamente acilada ("nativa") estão indicados (Fonte: MORRIS et al., 2012).

O mecanismo de gelificação da gelana é dividido em duas etapas. Na primeira ocorre a formação de duplas-hélices ordenadas (transição conformacional), e em seguida, ocorre a interação entre as hélices (transição sol – gel) (Figura 2.3) (MILAS et al., 1990; PICONE & CUNHA, 2011; RODRÍGUEZ-HERNÁNDEZ et al., 2003; SOSA-HERRERA et al., 2008; VILELA, 2012; YAMAMOTO, 2006). A temperatura de transição conformacional varia entre 30 e 50 °C, dependendo da concentração de polímero e da composição da solução (NICKERSON et al., 2003; PICONE, 2008; VILELA, 2012; YAMAMOTO, 2006).

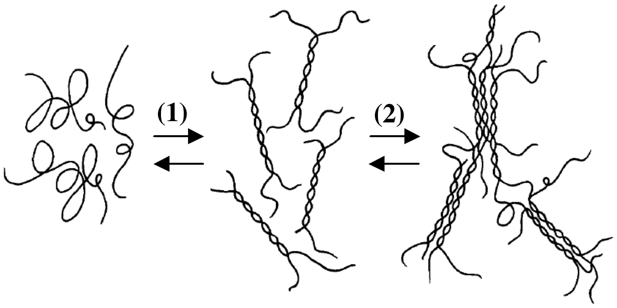

Figura 2.3. Representação da transição conformacional desordenada-ordenada (1) e da transição sol-gel (2) da gelana (Fonte: MIYOSHI et al., 1995).

O processo de gelificação pode ser induzido pela adição de sais, por alterações de pH, tratamento térmico ou aumento da concentração do polímero (PICONE, 2008) e, por isso, vai depender da força iônica, tipo de cátion, pH, temperatura e concentração utilizados (RODRÍGUEZ-HERNÁNDEZ et al., 2003; SANDERSON,1990; SOSA-HERRERA et al. 2008; VILELA et al., 2011; YAMAMOTO & CUNHA, 2007). Tem sido reportado que a gelana é capaz de formar géis em baixas concentrações (0,05% m/m), porém as concentrações normalmente utilizadas variam a partir de 0,2-0,4% (m/m) (RODRÍGUEZ-HERNÁNDEZ et al., 2003). Estas baixas concentrações juntamente com as propriedades multifuncionais da goma, permitem obter uma ampla variedade de texturas e utilizá-la em combinação com outros hidrocolóides para melhorar a estabilidade, formação da estrutura e liberação de sabor em sistemas alimentícios (RODRÍGUEZ-HERNÁNDEZ et al., 2003).

Além dos ingredientes utilizados na formulação das emulsões, a estabilidade destes sistemas também depende do método de emulsificação utilizado, o que vai influenciar diretamente o tamanho das gotas formadas (PERRECHIL, 2012).

2.3.1. Métodos de emulsificação

O processo de emulsificação inclui duas etapas, onde primeiramente uma alta tensão de cisalhamento leva à deformação da gota, aumentando sua área superficial específica até o seu rompimento e em seguida, a nova interface é estabilizada por um emulsificante (PERRIER-CORNET et al., 2005). Existem diferentes sistemas disponíveis para a formação de emulsões, sendo os misturadores do tipo rotor-estator e os homogeneizadores a altas pressões os mais comuns (PERRIER-CORNET et al., 2005). Estes processos influenciam diretamente a adsorção da proteína na interface, diâmetro de gota e estabilidade dos sistemas, produzindo emulsões com diferentes propriedades físico-químicas e organolépticas (PERRIER-CORNET et al., 2005; SANTANA, 2009).

2.3.1.1. Homogeneização a alta pressão

A homogeneização a alta pressão é uma tecnologia que visa a redução do tamanho de gotas de macro-emulsões pré-formadas, por exemplo, por misturadores do tipo rotor-estator (McCLEMENTS, 2005; SANTANA, 2009). A maioria das emulsões alimentícias possui diâmetro de gotas que varia entre 0,1 e 100 μm (McCLEMENTS et al., 2007). No entanto, o uso de homogeneização a alta pressão permite produzir emulsões com gotas dispersas de diâmetros menores que 500 nm, sendo então denominadas de nano-emulsões (WEISS et al., 2006). Em geral, emulsões com reduzido tamanho de gota da fase dispersa, possuem maior estabilidade e textura mais fina (McCLEMENTS, 2005).

Durante a homogeneização a alta pressão, o fluido é forçado através de um pequeno orifício sob pressão elevada, onde acelera a uma alta velocidade em uma distância curta, resultando em um alto gradiente de pressão entre a entrada e a saída da válvula, que gera forças cisalhantes intensas com a abertura da válvula (CORTÉS-MUÑOZ et al., 2009). Devido aos efeitos do cisalhamento e da conversão de energia cinética em calor, o fluido pode aquecer, porém isto pode ser controlado através de dispositivos de refrigeração (CORTÉS-MUÑOZ et al., 2009). A turbulência é o mecanismo predominante neste processo, sendo responsável pela ruptura da fase dispersa em pequenas gotas, porém o cisalhamento laminar e a cavitação também desempenham um papel importante (FLOURY et al., 2000). Um dos problemas que podem ocorrer nestes processos de homogeneização empregando alta energia é a ocorrência do fenômeno conhecido como "over-processing", que leva a um aumento no tamanho das partículas em função da recoalescência das novas gotas formadas (JAFARI et al., 2008). Este fenômeno pode ser explicado pela maior colisão entre as gotas (coalescência), menores tempos de residência, menor taxa de adsorção do emulsificante e concentração de emulsificante insuficiente para cobrir completamente as novas gotas (JAFARI et al., 2007).

2.4. MICROENCAPSULAÇÃO: PARTÍCULAS GELIFICADAS

A microencapsulação é o aprisionamento de pequenas quantidades de ingredientes, como compostos bioativos, que tem como objetivos reduzir a reatividade do material encapsulado nas condições ambientais, tais como, luz, oxigênio, umidade e temperatura, facilitar o seu manuseio, evitar a evaporação de compostos voláteis, mascarar sabores indesejáveis e controlar a liberação do composto encapsulado (SHAHIDI & HAN, 1993). Dependendo da estrutura das cápsulas, assim como da interação entre o núcleo e a parede, a liberação dos compostos encapsulados pode se dar através da ruptura da parede da cápsula pela ação de forças mecânicas, da difusão do composto encapsulado pela membrana, que deve ser semi-permeável, ou pela dissolução da parede quando submetida a condições apropriadas (SHAHIDI & HAN, 1993).

Microgéis derivados de biopolímeros (biomicrogéis) são usados como agentes encapsulantes e possuem uma ampla faixa de aplicações devido a sua baixa toxicidade, biocompatibilidade e habilidade de desintegração sob a ação de estímulos biológicos, tais como mudanças no pH ou interações com enzimas e proteínas (ZHANG et al., 2007). Para a sua preparação, dois processos são empregados: a emulsificação das fases oleosa com a aquosa do biopolímero e a gelificação das gotas resultantes pela reticulação química ou física (ZHANG et al., 2007).

Dentre os métodos físicos que podem ser utilizados para a produção de microgéis a partir de emulsões O/A está a extrusão, que é uma técnica comumente utilizada devido a sua relativa simplicidade (PERRECHIL et al., 2012). Neste caso, a emulsão O/A é inicialmente produzida pela emulsificação da solução de biopolímero com o óleo e alimentada em uma seringa ou bico aspersor (extrusor). Após, a emulsão é extrusada dentro de uma solução promotora de gelificação (salina ou com pH diferente), sob agitação, de modo que resulte na formação dos microgéis (PERRECHIL, 2012). O tamanho das gotas, e conseqüentemente dos microgéis, vai depender do diâmetro da agulha da seringa ou do bico utilizado, da vazão da solução e da sua viscosidade (BUREY et al., 2008) e da distância entre o bico e a solução gelificante (PERRECHIL et al., 2012).

A grande vantagem dos microgéis é que eles apresentam a mesma estabilidade e resistência que as matrizes de gel (PERRECHIL, 2012), porém podem ser incorporados a diversos tipos de alimentos, inclusive aqueles com alta atividade de água (BUREY et al., 2008), sem que haja grandes alterações nas características de textura destes alimentos e na estrutura e propriedades dos microgéis (PERRECHIL, 2012).

2.5. PROCESSOS DE SIMULAÇÃO DA DIGESTÃO *IN VITRO*

Modelos de digestão simulada *in vitro* são amplamente utilizados para estudar alterações estruturais, digestibilidade, biodisponibilidade e liberação de componentes alimentícios em condições simuladas das condições gastrointestinais (HUR et al., 2011). No entanto, seus resultados são muitas vezes diferentes dos encontrados utilizando modelos *in vivo* devido às dificuldades para simular com precisão os eventos físico-químicos e fisiológicos altamente complexos que ocorrem no trato digestivo humano e animal (HUR et al., 2011). Apesar disso, esforços têm sido dedicados para o desenvolvimento de procedimentos *in vitro*, uma vez que os métodos *in vivo* são demorados e caros (BOISEN & EGGUM, 1991; HUR et al., 2011). Entre as vantagens dos testes *in vitro* está o menor custo e tempo, segurança, relativa reprodutibilidade e o fato de não haver restrição ética, o que muitas vezes pode limitar os experimentos com seres humanos (KONG & SINGH, 2008; PARADA & AGUILERA, 2007).

Existem dois tipos de modelos *in vitro* do trato gastrointestinal (GI): o estático e o dinâmico (KONG & SINGH, 2008). Os modelos estáticos não simulam os processos físicos que ocorrem ao longo do trato GI, tais como cisalhamento e mistura (PARADA & AGUILERA, 2007), simulando apenas a composição e as condições dos meios, como a presença de enzimas, força iônica, pH, tempo e temperatura (GARRETT et al., 1999). Já nos modelos dinâmicos, há uma tentativa de simulação das condições fisiológicas, entre elas os processos mecânicos que ocorrem durante o processo digestivo (KONG & SINGH, 2008).

Na digestão, os alimentos passam por uma grande redução de seu tamanho para a liberação dos nutrientes, os quais passarão para a corrente sanguínea e então serão absorvidos pelas células do corpo (KONG & SINGH, 2008). As forças mecânicas e reações químicas são as responsáveis pela quebra do alimento ingerido em pequenas partículas, e a cinética da digestão vai depender das características físicas e químicas dos alimentos e da sua interação com as substâncias envolvidas no processo (KONG & SINGH, 2008).

O processo de digestão (Figura 2.4) se inicia na boca, etapa que tem como principal função ingerir os alimentos e convertê-los em uma forma apropriada para a deglutição (McCLEMENTS & LI, 2010). Nesta etapa, a mastigação é responsável pela redução no tamanho das partículas, aumentando a sua área superficial, pela hidratação e lubrificação dos alimentos através da sua mistura com a saliva e pela redução da viscosidade dos alimentos ricos em amido pela ação rápida da amilase salivar (HOEBLER et al., 2002; KONG & SINGH, 2008). Tais fatos resultam na formação de um bolo alimentar que será transportado pelo canal do esôfago até o estômago (KONG & SINGH, 2008). O pH da saliva humana é geralmente em torno de 5,5-6,1 durante o jejum e ao redor de 7-8 após a ingestão de alimentos (McCLEMENTS & LI, 2010). A mastigação tem uma influência significativa sobre o processo digestivo, e se realizada de forma inadequada, pode levar à má digestão (KONG & SINGH, 2008).

No estômago, o bolo alimentar é misturado com os sucos digestivos ácidos contendo enzimas gástricas, minerais, substâncias com atividade de superfície, e outros componentes biológicos, e é submetido à agitação mecânica devido à motilidade estomacal (McCLEMENTS & LI, 2010). O pH do estômago humano é em torno de 1-3, sob condições de jejum, mas muda consideravelmente após a entrada do bolo alimentar (McCLEMENTS & LI, 2010).

Após entrar no duodeno, tubo que liga o estômago ao intestino delgado, o quimo é misturado com bicarbonato de sódio, sais biliares, fosfolipídios e enzimas secretadas pelo fígado, pâncreas e vesícula biliar (McCLEMENTS & LI, 2010). Nessa etapa o pH da mistura passa de altamente ácido (pH 1-3) para neutro (pH 5,8-6,5), em que as enzimas pancreáticas são mais eficientes (McCLEMENTS & LI, 2010). Os processos de absorção dos nutrientes normalmente ocorrem no intestino delgado (KONG & SINGH, 2008; McCLEMENTS & LI, 2010) e o que não é absorvido segue para o intestino grosso, o qual pode ser dividido em quatro principais regiões que diferem em suas funções fisiológicas: ceco, cólon, reto e canal anal (McCLEMENTS & LI, 2010). As principais funções do cólon são a absorção de água e eletrólitos, a fermentação de polissacarídeos e proteínas, a re-absorção de sais biliares e a formação, armazenamento e eliminação da matéria fecal (McCLEMENTS & LI, 2010).

No caso das emulsões, aproximadamente 10-30% da hidrólise lipídica ocorre no estômago, sendo a maior parte dos lipídeos digerida no intestino delgado (MUN et al., 2007). Porém, a presença de substâncias com atividade superficial no duodeno, como os sais biliares, enzimas, proteínas e fosfolipídios, pode alterar a composição interfacial destes lipídeos e então, influenciar sobre a sua taxa de hidrólise (MUN et al., 2007).

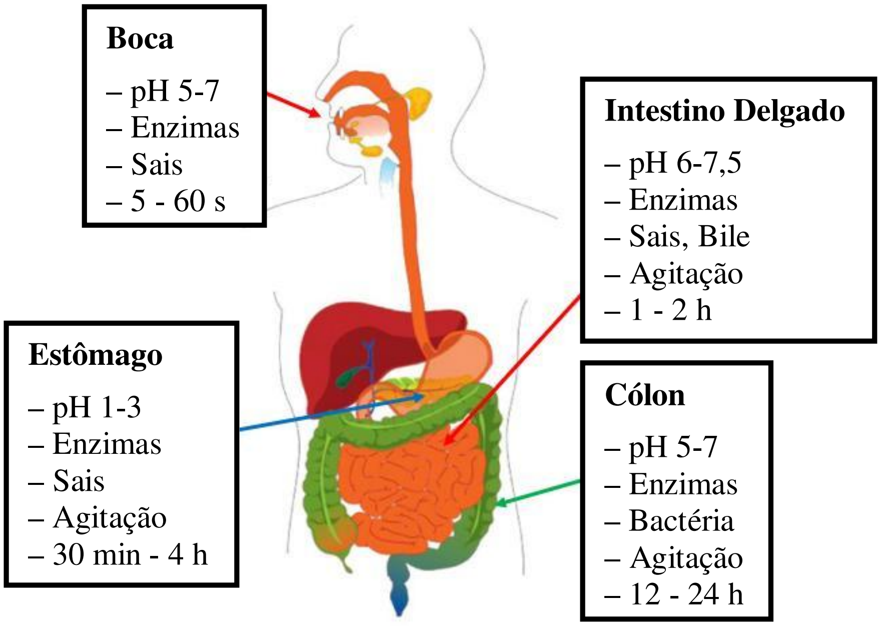
Boca
– pH 5-7
– Enzimas
– Sais
– 5 - 60 s
Intestino Delgado
– pH 6-7,5
– Enzimas
– Sais, Bile
– Agitação
– 1 - 2 h
Estômago
– pH 1-3
– Enzimas
– Sais
– Agitação
– 30 min - 4 h
Cólon
– pH 5-7
– Enzimas
– Bactéria
– Agitação
– 12 - 24 h

Figura 2.4. Diagrama das condições físico-químicas nas diferentes regiões do trato gastrointestinal humano (Fonte: McCLEMENTS & LI, 2010).

2.6. REFERÊNCIAS

BABU, U. S.; WIESENFELD, P. W. Nutritional and hematological effects of flaxseed. In: THOMPSON, L. U.; CUNNANE, S. C. (Eds.). **Flaxseed in human nutrition**. Champaign, IL: AOCS Press, 2003. Chap. 7, p. 150-173.

BHATHENA, S. J.; ALI, A. A.; MOHAMED, A. I.; HANSEN, C. T.; VELASQUEZ, M. T. Differential effects of dietary flaxseed protein and soy protein on plasma triglyceride and uric acid levels in animal models. **Journal of Nutritional Biochemistry**, v. 13, n. 11, p. 684-689, 2002.

BOISEN, S.; EGGUM, B. O. Critical evaluation of in vitro methods for estimating digestibility in simple-stomach animals. **Nutrition Research Reviews**, v. 4, n. 1, p. 141-162, 1991.

BRYANT, C. M.; McCLEMENTS, D. J. Molecular basis of protein functionality with special consideration of cold-set gels derived from heat-denatured whey. **Trends in Food Science & Technology**, v. 9, n. 4, p. 143-151, 1998.

BUREY, P.; BHANDARI, B. R.; HOWES, T.; GIDLEY, M. J. Hydrocolloid gel particles: Formation, characterization, and application. **Critical Reviews in Food Science and Nutrition**, v. 48, n. 5, p. 361-377, 2008.

CHEN, H.-H.; XU, S.-Y.; WANG, Z. Gelation properties of flaxseed gum. **Journal of Food Engineering**, v. 77, n. 2, p. 295-303, 2006.

CHUNG, M. W. Y.; LEI, B.; LI-CHAN, E. C. Y. Isolation and structural characterization of the major protein fraction from NorMan flaxseed (*Linum usitatissimum L.*). **Food Chemistry**, v. 90, n. 1-2, p. 271–279, 2005.

CORTÉS-MUÑOZ, M.; CHEVALIER-LUCIA, D.; DUMAY, E. Characteristics of submicron emulsions prepared by ultra-high pressure homogenisation: Effect of chilled or frozen storage. **Food Hydrocolloids**, v. 23, n. 3, p. 640-654, 2009.

COUPLAND, J. N.; McCLEMENTS, D. J. Lipid oxidation in food emulsions. **Trends in Food Science and Technology**, v. 7, n. 3, p. 83-91, 1996.

CUI, S. W. Flaxseed Gum. In: CUI, S. W. (Ed.). **Polysaccharide gums from agricultural products: Processing, structures and functionality**. Lancaster, Penn., USA: Technomic Publishing Co., 2001. Chap. 2, p. 59-101.

DEV, D. K.; QUENSEL, E. Functional and microstructural characteristics of linseed (*Linum usitatissimum* L.) flour and a protein isolate. **LWT - Food Science and Technology**, v. 19, n. 4, p. 331-337, 1986.

DEV, D. K.; QUENSEL, E.; HANSEN, R. Nitrogen extractability and buffer capacity of deffated linseed (*Linum usitatissimum* L.) flour. **Journal of the Science of Food and Agriculture**, v. 37, n. 2, p. 199-205, 1986.

DICKINSON, E. **An Introduction to Food Colloids**. Oxford, UK: University Press, 1992.

DICKINSON, E. Hydrocolloids at interfaces and the influence on the properties of dispersed systems. **Food Hydrocolloids**, v. 17, n. 1, p. 25-39, 2003.

FLOURY, J.; DESRUMAUX, A.; LARDIÈRES, J. Effect of high-pressure homogenization on droplet size distributions and rheological properties of model oil-in-water emulsions. **Innovative Food Science & Emerging Technologies**, v. 1, n. 2, p. 127-134, 2000.

GARRETT, D. A.; FAILLA, M. L.; SARAMA, R. J. Development of an in vitro digestion method to assess carotenoid bioavailability from meals. **Journal of Agricultural and Food Chemistry**, v. 47, n. 10, p. 4301-4309, 1999.

GOH, K. K. T.; PINDER, D. N.; HALL, C. E.; HEMAR, Y. Rheological and light scattering properties of flaxseed polysaccharide aqueous solutions. **Biomacromolecules**, v. 7, n. 11, p. 3098-3103, 2006.

GUZEY, D.; McCLEMENTS, D. J. Formation, stability and properties of multilayer emulsions for application in the food industry. **Advances in Colloid and Interface Science**, v. 128-130, p. 227-248, 2006.

HALL, C., III.; TULBEK, M. C.; XU, Y. Flaxseed. **Advances in Food and Nutrition Research**, v. 51, p. 1-97, 2006.

HIGGINS, S.; CARROLL, Y. L.; O'BRIEN, N. M.; MORRISSEY, P. A. Use of microencapsulated fish oil as a means of increasing *n*-3 polyunsaturated fatty acid intake. **Journal of Human Nutrition and Dietetics**, v. 12, n. 4, p. 265-271, 1999.

HOEBLER, C.; LECANNU, G.; BELLEVILLE, C.; DEVAUX, M.-F.; POPINEAU, Y.; BARRY, J.-L. Development of an *in vitro* system simulating bucco-gastric digestion to assess the physical and chemical changes of food. **International Journal of Food Sciences and Nutrition**, v. 53, n. 5, p. 389-402, 2002.

HU, M.; McCLEMENTS, D. J.; DECKER, E. A. Impact of whey protein emulsifiers on the oxidative stability of salmon oil-in-water emulsions. **Journal of Agricultural and Food Chemistry**, v. 51, n. 5, p. 1435-1439, 2003.

HUR, S. J.; LIM, B. O.; DECKER, E. A.; McCLEMENTS, D. J. *In vitro* human digestion models for food applications. **Food Chemistry**, v. 125, n. 1, p. 1-12, 2011.

JAFARI, S. M.; ASSADPOOR, E.; HE, Y.; BHANDARI, B. Re-coalescence of emulsion droplets during high-energy emulsification. **Food Hydrocolloids**, v. 22, n. 7, p. 1191-1202, 2008.

JAFARI, S. M.; HE, Y.; BHANDARI, B. Effectiveness of encapsulating biopolymers to produce sub-micron emulsions by high energy emulsification techniques. **Food Research International**, v. 40, n. 7, p. 862-873, 2007.

JANSSON, P.-E.; LINDBERG, B.; SANDFORD, P. A. Structural studies of gellan gum, an extracellular polysaccharide elaborated by *Pseudomonas elodea*. **Carbohydrate Research**, v. 124, n. 1, p. 135-139, 1983.

KHALLOUFI, S.; CORREDIG, M.; GOFF, H. D.; ALEXANDER, M. Flaxseed gums and their adsorption on whey protein-stabilized oil-in-water emulsions. **Food Hydrocolloids**, v. 23, n. 3, p. 611-618, 2009.

KIOKAS, S.; DIMAKOU, C.; OREOPOULOU, V. Effect of heat treatment and droplet size on the oxidative stability of whey protein emulsions. **Food Chemistry**, v. 105, n. 1, p. 94-100, 2007.

KOLANOWSKI, W.; SWIDERSKI, F.; BERGER, S. Possibilities of fish oil application for food products enrichment with ω-3 PUFA. **International Journal of Food Sciences and Nutrition**, v. 50, n. 1, p. 39-49, 1999.

KONG, F.; SINGH, R. P. Disintegration of solid foods in human stomach. **Journal of Food Science**, v. 73, n. 5, p. R67-R80, 2008.

KRAUSE, J.-P.; SCHULTZ, M.; DUDEK, S. Effect of extraction conditions on composition, surface activity and rheological properties of protein isolates from flaxseed (*Linum usitativissimum* L). **Journal of the Science of Food and Agriculture**, v. 82, n. 9, p. 970-976, 2002.

MADHUSUDHAN, K. T.; SINGH, N. Isolation and characterization of a small molecular weight protein of linseed meal. **Phytochemistry**, v. 24, n. 11, p. 2507-2509, 1985a.

MADHUSUDHAN, K. T.; SINGH, N. Isolation and characterization of the major fraction (12 S) of linseed proteins. **Journal of Agricultural and Food Chemistry**, v. 33, n. 4, p. 673-677, 1985b.

MARAMBE, P. W. M. L. H. K.; SHAND, P. J.; WANASUNDARA, J. P. D. An in-vitro investigation of selected biological activities of hydrolysed flaxseed (*Linum usitatissimum* L.) proteins. **Journal of the American Oil Chemists' Society**, v. 85, n. 12, p. 1155-1164, 2008.

MARCONE, M. F.; KAKUDA, Y.; YADA, R. Y. Salt-soluble seed globulins of various dicotyledonous and monocotyledonous plants - I. Isolation/purification and characterization. **Food Chemistry**, v. 62, n. 1, p. 27-47, 1998.

MAZZA, G.; BILIADERIS, C. G. Functional properties of flax seed mucilage. **Journal of Food Science**, v. 54, n. 5, p. 1302-1305, 1989.

McCLEMENTS, D. J. Protein-stabilized emulsions. **Current Opinion in Colloid & Interface Science**, v. 9, n. 5, p. 305-313, 2004.

McCLEMENTS, D. J. **Food emulsions: Principles, practice, and techniques**. 2nd ed. Boca Raton, FL: CRC Press, 2005.

McCLEMENTS, D. J.; DECKER, E. A. Lipid oxidation in oil-in-water emulsions: Impact of molecular environment on chemical reactions in heterogeneous food systems. **Journal of Food Science**, v. 65, n. 8, p. 1270-1282, 2000.

McCLEMENTS, D. J.; DECKER, E. A.; WEISS, J. Emulsion-based delivery systems for lipophilic bioactive components. **Journal of Food Science**, v. 72, n. 8, p. R109-R124, 2007.

McCLEMENTS, D. J.; LI, Y. Review of *in vitro* digestion models for rapid screening of emulsion-based systems. **Food & Function**, v. 1, n. 1, p. 32-59, 2010.

MILAS, M.; SHI, X.; RINAUDO, M. On the physicochemical properties of gellan gum. **Biopolymers**, v. 30, n. 3-4, p. 451-464, 1990.

MIYOSHI, E.; TAKAYA, T.; NISHINARI, K. Effects of salts on the gel-sol transition of gellan gum by differential scanning calorimetry and thermal scanning rheology. **Thermochimica Acta**, v. 267, p. 269-287, 1995.

MORITAKA, H.; NISHINARI, K.; TAKI, M.; FUKUBA, H. Effects of pH, potassium chloride, and sodium chloride on the thermal and rheological properties of gellan gum gels. **Journal of Agricultural and Food Chemistry**, v. 43, n. 6, p. 1685-1689, 1995.

MORR, C. V.; HA, E. Y. W. Whey protein concentrates and isolates: Processing and functional properties. **Critical Reviews in Food Science and Nutrition**, v. 33, n. 6, p. 431-476, 1993.

MORRIS, E. R.; NISHINARI, K.; RINAUDO, M. Gelation of gellan - A review. **Food Hydrocolloids**, v. 28, n. 2, p. 373-411, 2012.

MUN, S.; DECKER, E. A.; McCLEMENTS, D. J. Influence of emulsifier type on *in vitro* digestibility of lipid droplets by pancreatic lipase. **Food Reasearch International**, v. 40, n. 6, p. 770-781, 2007.

NICKERSON, M. T.; PAULSON, A. T.; SPEERS, R. A. Rheological properties of gellan solutions: effect of calcium ions and temperature on pre-gel formation. **Food Hydrocolloids**, v. 17, n. 5, p. 577-583, 2003.

OMONI, A. O.; ALUKO, R. E. Mechanism of the inhibition of calmodulin-dependent neuronal nitric oxide synthase by flaxseed protein hydrolysates. **Journal of the American Oil Chemists' Society**, v. 83, n. 4, p. 335-340, 2006.

O'NEILL, M. A.; SELVENDRAN, R. R.; MORRIS, V. J. Structure of the acidic extracellular gelling polysaccharide produced by *Pseudomonas elodea*. **Carbohydrate Research**, v. 124, n. 1, p. 123-133, 1983.

OOMAH, B. D.; MAZZA, G. Flaxseed proteins – a review. **Food Chemistry**, v. 48, n. 2, p. 109-114, 1993.

OSBORNE, T. B. Proteins of the flaxseed. **Journal of the American Chemical Society**, v. 14, p. 629-661, 1892.

PARADA, J.; AGUILERA, J. M. Food microstructure affects the bioavailability of several nutrients. **Journal of Food Science**, v. 72, n. 2, p. R21-R32, 2007.

PATEL, K. C.; CHEN, X. D. Sensitivity analysis of the reaction engineering approach to modeling spray drying of whey proteins concentrate. **Drying Technology**, v. 26, n. 11, p. 1334-1343, 2008.

PENG, X.; KONG, B.; XIA, X.; LIU, Q. Reducing and radical-scavenging activities of whey protein hydrolysates prepared with Alcalase. **International Dairy Journal**, v. 20, n. 5, p. 360-365, 2010.

PERRECHIL, F. A. **Produção de microgéis para encapsulação de compostos hidrofóbicos**. Campinas, 2012. 167p. Tese (Doutor em Engenharia de Alimentos). Faculdade de Engenharia de Alimentos, Universidade Estadual de Campinas, Campinas, 2012.

PERRECHIL, F. A.; VILELA, J. A. P.; GUERREIRO, L. M. R.; CUNHA, R. L. Development of Na-CN—κ-carrageenan microbeads for the encapsulation of lipophilic compounds. **Food Biophysics**, v. 7, n. 3, p. 264-275, 2012.

PERRIER-CORNET, J. M.; MARIE, P.; GERVAIS, P. Comparison of emulsification efficiency of protein-stabilized oil-in-water emulsions using jet, high pressure and colloid mill homogenization. **Journal of Food Engineering**, v. 66, n. 2, p. 211-217, 2005.

PICONE, C. S. F. **Influência da conformação da gelana sobre a gelificação das proteínas do soro**. Campinas, 2008. 141p. Dissertação (Mestre em Engenharia de Alimentos). Faculdade de Engenharia de Alimentos, Universidade Estadual de Campinas, Campinas, 2008.

PICONE, C. S. F.; CUNHA, R. L. Interactions between milk proteins and gellan gum in acidified gels. **Food Hydrocolloids**, v. 24, n. 5, p. 502-511, 2010.

PICONE, C. S. F.; CUNHA, R. L. Influence of pH on formation and properties of gellan gels. **Carbohydrate Polymers**, v. 84, n. 1, p. 662-668, 2011.

RABETAFIKA, H. N.; REMOORTEL, V. V.; DANTHINE, S.; PAQUOT, M.; BLECKER, C. Flaxseed proteins: food uses and health benefits. **International Journal of Food Science and Technology**, v. 46, n. 2, p. 221-228, 2011.

RAMALHO, V. C.; JORGE, N. Antioxidantes utilizados em óleos, gorduras e alimentos gordurosos. **Química Nova**, v. 29, n. 4, p. 755-760, 2006.

RICHARDS, M. P.; CHAIYASIT, W.; McCLEMENTS, D. J.; DECKER, E. A. Ability of surfactant micelles to alter the partitioning of phenolic antioxidants in oil-in-water emulsions. **Journal of Agricultural and Food Chemistry**, v. 50, n. 5, p. 1254-1259, 2002.

RODRÍGUEZ-HERNÁNDEZ, A. I.; DURAND, S.; GARNIER, C.; TECANTE, A.; DOUBLIER, J. L. Rheology-structure properties of gellan systems: evidence of network formation at low gellan concentrations. **Food Hydrocolloids**, v. 17, n. 5, p. 621-628, 2003.

SANDERSON, G. R. Gellan gum. In: HARRIS, P. (Ed.). **Food gels**. New York: Elsevier Applied Science Publishers, 1990. p. 201-232.

SANTANA, R. C. **Emulsões estabilizadas por colágeno: efeito da hidrólise térmica e do processo de homogeneização**. Campinas, 2009. 111p. Dissertação (Mestre em Engenharia de Alimentos). Faculdade de Engenharia de Alimentos, Universidade Estadual de Campinas, Campinas, 2009.

SHAHIDI, F.; HAN, X.-Q. Encapsulation of food ingredients. **Critical Reviews in Food Science and Nutrition**, v. 33, n. 6, p. 501-547, 1993.

SHAHIDI, F.; ZHONG, Y. Lipid oxidation: Measurement methods. In: SHAHIDI, F. (Ed.). **Bailey's Industrial Oil and Fat Products**. Hoboken, NJ: John Wiley & Sons, Inc., 2005. Chap. 8, p. 357-385.

SIMOPOULOS, A. P. Essential fatty acids in health and chronic disease. **The American Journal of Clinical Nutrition**, v. 70, n. 3, p. 560S-569S, 1999.

SMITH, A. K.; JOHNSEN, V. L.; BECKEL, A. C. Linseed proteins: alkali dispersion and acid precipitation. **Industrial and Engineering Chemistry**, v. 38, n. 3, p. 353-356, 1946.

SOSA-HERRERA, M. G.; BERLI, C. L. A.; MARTÍNEZ-PADILLA, L. P. Physicochemical and rheological properties of oil-in-water emulsions prepared with sodium caseinate/gellan gum mixtures. **Food Hydrocolloids**, v. 22, n. 5, p. 934-942, 2008.

SOSULSKI, F. W.; BAKAL, A. Isolated proteins from rapessed, flax, and sunflower meals. **Canadian Institute of Food Science and Technology Journal**, v. 2, n. 1, p. 28-32, 1969.

SUN, C.; GUNASEKARAN, S. Effects of protein concentration and oil-phase volume fraction on the stability and rheology of menhaden oil-in-water emulsions stabilized by whey protein isolate with xanthan gum. **Food Hydrocolloids**, v. 23, n. 1, p. 165-174, 2009.

SWORN, G.; SANDERSON, G. R.; GIBSON, W. Gellan gum fluid gels. **Food Hydrocolloids**, v. 9, n. 4, p. 265-271, 1995.

TONG, L. M.; SASAKI, S.; McCLEMENTS, D. J.; DECKER, E. A. Antioxidant activity of whey in a salmon oil emulsion. **Journal of Food Science**, v. 65, n. 8, p. 1325-1329, 2000.

TRUCOM, C. **A importância da linhaça na saúde**. São Paulo, SP: Alaúde Editorial, 2006.

UDENIGWE, C. C.; LU, Y.-L.; HAN, C.-H.; HOU, W.-C.; ALUKO, R. E. Flaxseed protein-derived peptide fractions: antioxidant properties and inhibition of lipopolysaccharide-induced nitric oxide production in murine macrophages. **Food Chemistry**, v. 116, n. 1, p. 277-284, 2009a.

UDENIGWE, C. C.; LIN, Y.-S.; HOU, W.-C.; ALUKO, R. E. Kinetics of the inhibition of rennin and angiotensin I-converting enzyme by flaxseed protein hydrolysate fractions. **Journal of Functional Foods**, v. 1, n. 2, p. 199-207, 2009b.

VAISEY-GENSER, M.; MORRIS, D. H. Introduction: history of the cultivation and uses of flaxseed. In: MUIR, A. D.; WESTCOTT, N. D. (Eds.). **Flax: The genus *Linum***. New York, USA: Taylor & Francis, 2003. Chap. 1, p. 1-21.

VILELA, J. A. P. **Propriedades de microgéis de gelana-quitosana obtidos a partir de extrusão**. Campinas, 2012. 103p. Dissertação (Mestre em Engenharia de Alimentos).

Faculdade de Engenharia de Alimentos, Universidade Estadual de Campinas, Campinas, 2012.

VILELA, J. A. P.; CAVALLIERI, A. L. F.; CUNHA, R. L. The influence of gelation rate on the physical properties/structure of salt-induced gels of soy protein isolate-gellan gum. **Food Hydrocolloids**, v. 25, n. 7, p. 1710-1718, 2011.

WALLACE, J. M. W.; McCABE, A. J.; ROBSON, P. J.; KEOGH, M. K.; MURRAY, C. A.; KELLY, P. M.; MÁRQUEZ-RUIZ, G.; McGLYNN, H.; GILMORE, W. S.; STRAIN, J. J. Bioavailability of n–3 polyunsaturated fatty acids (PUFA) in foods enriched with microencapsulated fish oil. **Annals of Nutrition & Metabolism**, v. 44, n. 4, p. 157-162, 2000.

WANASUNDARA, P. K. J. P. D.; SHAHIDI, F. Removal of flaxseed mucilage by chemical and enzymatic treatments. **Food Chemistry**, v. 59, n. 1, p. 47-55, 1997.

WARAHO, T., McCLEMENTS, D. J.; DECKER, E. A. Mechanisms of lipid oxidation in food dispersions. **Trends in Food Science and Technology**, v. 22, n. 1, p. 3-13, 2011.

WEISS, J.; TAKHISTOV, P.; McCLEMENTS, D. J. Functional materials in food nanotechnology. **Journal of Food Science**, v. 71, n. 9, p. R107-R116, 2006.

XU, Y.; HALL, C., III.; WOLF-HALL, C. Antifungical activity stability of flaxseed protein extracts using response surface methodology. **Journal of Food Science**, v. 73, n. 1, p. M9-M14, 2008.

YAMAMOTO, F. **Reologia e microestrutura de géis ácidos de gelana**. Campinas, 2006. 126p. Dissertação (Mestre em Engenharia de Alimentos). Faculdade de Engenharia de Alimentos, Universidade Estadual de Campinas, Campinas, 2006.

YAMAMOTO, F.; CUNHA, R. L. Acid gelation of gellan: Effect of final pH and heat treatment conditions. **Carbohydrate Polymers**, v. 68, n. 3, p. 517-527, 2007.

YOULE, R. J.; HUANG, A. H. C. Occurrence of low molecular weight and high cysteine containing albumin storage proteins in oilseeds of diverse species. **American Journal of Botany**, v. 68, n. 1, p. 44-48, 1981.

ZHANG, H.; TUMARKIN, E.; SULLAN, R. M. A.; WALKER, G. C.; KUMACHEVA, E. Exploring microfluidic routes to microgels of biological polymers. **Macromolecular Rapid Communications**, v. 28, n. 5, p. 527-538, 2007.

CHAPTER 3

Flaxseed oil – Whey protein isolate emulsions: Effect of high pressure homogenization

Kuhn, K. R.; Cunha, R. L.

Journal of Food Engineering,
v. 111, n. 2, p. 449-457, 2012

CHAPTER 3. Flaxseed oil – Whey protein isolate emulsions: Effect of high pressure homogenization

K.R. Kuhn, R.L. Cunha∗

Department of Food Engineering, Faculty of Food Engineering, University of Campinas (UNICAMP), 13083-862 – Campinas, SP, Brazil

∗Corresponding author: Tel: +55 19 3521 4047; fax: +55 19 3521 4027

E-mail address: rosiane@fea.unicamp.br

ABSTRACT

The effect of high-pressure homogenization (20–100 MPa) and the number of homogenization cycles (1–7) on the stability of flaxseed oil–whey protein isolate emulsions was evaluated. All the emulsions were stable to creaming for at least 9 d of storage. An increase in homogenization pressure from 20 to 80 MPa and number of passes through the homogenizer up to 3, decreased the mean droplet size of the O/W emulsions despite the higher polydispersity. Emulsions homogenized at lower pressures (20 MPa) showed a monomodal distribution of the particles, whereas, an increase in pressure to 80 MPa led to a bimodal distribution, indicating droplets coalescence. High-pressure homogenization (80 MPa) and an increase in the number of homogenization cycles, led to the formation of high molecular weight aggregates (>200 kDa), which favored an increase in viscosity of the emulsions. The increase in homogenization pressure also increased the formation of primary oxidation products, which could be explained by the increase in temperature and in the surface area of the droplets.

Keywords: Emulsion; Whey protein; Flaxseed oil; High-pressure homogenization; Microstructure; Lipid oxidation.

3.1. INTRODUCTION

An emulsion can be simply defined as ‘‘a system comprised of two immiscible liquids, one of which is dispersed as droplets (the dispersed or internal phase) in the other (the continuous or external phase)’’ (Jafari et al., 2008). Emulsions are thermodynamically unfavorable systems that tend to break down over time, due to a variety of physicochemical mechanisms. However, it is possible to form emulsions that are kinetically stable for a reasonable period of time, by using intense mechanical forces and/or including substances known as stabilizers, for example, emulsifiers (McClements et al., 2007).

High-pressure homogenizers are the most frequently used to produce food emulsions, providing fine emulsions with good texture properties and greater stability (Desrumaux and Marcand, 2002). In this process, the combination of intense shear, cavitation and turbulent flow conditions leads to disruption of the fat droplets (McClements, 2005). The decrease in average size of the fat droplets reduces the creaming velocity (Stokes law) and increases the stability of the emulsion (Desrumaux and Marcand, 2002). On the other hand, emulsifiers are surface-active molecules that adsorb to the surface of freshly formed droplets during homogenization. Once adsorbed onto the droplet surface, they act in two ways: lowering interfacial tension and forming a protective layer that prevents the droplets from aggregating (Guzey and McClements, 2006; McClements et al., 2007; Walstra, 2003).

Proteins are ingredients widely used in food emulsions as emulsifiers/stabilizers due to their amphiphilic character. The ability of proteins to generate repulsive interactions (e.g., steric and electrostatic) between oil droplets, and at the same time form an interfacial membrane that is resistant to rupture, plays an important role in stabilizing the droplets against flocculation and coalescence during long-term storage (McClements, 2004). Whey proteins are often used in food emulsion systems because of their ability to stabilize oil-in-water (O/W) emulsions (Dalgleish, 1996; Dickinson, 2001; Kerstens et al., 2006; Ye, 2010). Whey proteins adsorbed at an oil/water interface interact with neighboring molecules adsorbed on the same droplet, or on different droplets via a combination of non-covalent bonds or covalent disulfide bonding, increasing stability to coalescence (McClements et al., 1993). Moreover, whey protein isolate (WPI) has been reported to possess antioxidant activity (Hu et al., 2003; Sun and Gunasekaran, 2009; Tong et al., 2000), which could be extremely beneficial to systems containing labile oxidative components as the dispersed phase (Sun and Gunasekaran, 2009).

Flaxseed oil is very rich in unsaturated fatty acids, being recognized as one of the greatest sources of Omega-3 in nature, thus having a positive effect on human health, being increasingly recognized for their role in reducing the risk of cardiovascular diseases (Zhao et al., 2007). However, during processing, distribution and handling, these oils can easily oxidize, due to their high degree of unsaturation (Tonon et al., 2011). Oxidation leads to the formation of unpleasant tastes and odors, and consequently to a reduction in product shelf life, besides promoting the generation of free radicals, which may have negative physiological effects on the organism (Tonon et al., 2011).

Thus, the objective of the present research was to study the best conditions to prepare O/W emulsions stabilized by whey proteins, aiming at greater stability and decreased oxidation of the flaxseed oil in these systems during the storage period. The effect of high-pressure homogenization (20–100 MPa) and the number of homogenization cycles (1–7) on the creaming stability, droplet size, rheology, oxidative stability and molecular weight distribution of the emulsions was evaluated, the latter being evaluated by polyacrylamide gel electrophoresis.

3.2. MATERIAL AND METHODS

3.2.1. Material

The whey protein isolate (WPI) was obtained from New Zealand Milk Products (ALACEN 895, New Zealand) and the flaxseed oil purchased from Cisbra (Panambi, RS, Brazil), showing the following fatty acid composition: 6.2% C16:0, 5.3% C18:0, 20.1% C18:1, 13.7% C18:2 and 52.3% C18:3. The protein concentration, determined by the Kjeldahl procedure (AOAC, 1997), lipid (Bligh and Dyer, 1959), moisture (AOAC, 1997) and ash (AOAC, 1997) contents (w/w wet basis) of WPI were 87.66 ± 0.91% (N x 6.38), 0.36 ± 0.02%, 4.54 ± 0.11% and 1.36 ± 0.07%, respectively. All other reagents were of analytical grade.

3.2.2. Preparation of the WPI stock solution

The WPI stock solution (5% w/v) was prepared by dissolution of the powder in deionized water (pH 6.7) with magnetic stirring for 90 min at room temperature (25 °C). The pH of the solution was then adjusted to 7.0 ± 0.2 using 2.0 M NaOH. The solution was kept overnight at 10 °C to allow complete protein dissolution.

3.2.3. Preparation of the emulsions

Oil-in-water (O/W) emulsions were prepared at 25 °C by homogenizing the oil in the aqueous phase using two sequential homogenization methods. The first method involved mixing the solutions in an Ultra Turrax model T18 homogenizer (IKA, Germany) for 4 min at 14,000 rpm. The second method involved subjecting the previously prepared macroemulsion to a high-pressure homogenization process using a Panda 2K NS1001L double stage homogenizer (Niro Soavi, Italy). The pressure in the first stage was from 20, 40, 60, 80 or 100 MPa and in the second stage it was fixed at 5 MPa. The number of passes through the homogenizer (1, 2, 3, 4, 5, 6 or 7) at each pressure, totaling 35 emulsions produced, was also evaluated. The WPI and flaxseed oil contents were fixed at 3% (w/v) and 30% (v/v), respectively. Sodium azide (0.02% w/v) was added to the emulsions to prevent microbial growth and the pH was adjusted to 7.0 using 2.0 M NaOH.

3.2.4. Creaming stability

Immediately after preparation, 10 mL of each emulsion were poured into a cylindrical glass tube (internal diameter = 11 mm, height = 94 mm), sealed with a plastic cap and stored at 25 °C for a period of 9 d. The emulsion stability was measured by the change in height of the bottom serum phase (H) with storage time. The creaming index (CI) was determined according to Eq. (3.1).

$$CI\ (\%) = (H/H_0) \times 100 \tag{3.1}$$

where H_0 represents the initial height of the emulsion. To facilitate visualization of the phase separation, Sudam III (reddish dye) was added to the flaxseed oil. The analyzes were carried out in duplicate. Emulsions homogenized at 20 and 80 MPa were also stored in glass bottles (~60 mL of emulsion, internal diameter = 45 mm, height = 70 mm), at 25 °C, and evaluated for 3 months.

3.2.5. Optical microscopy

The microstructure of the emulsions was evaluated after 1 d of storage. The samples were poured onto microscopes slides, covered with glass cover slips and observed using a Carl Zeiss Model Axio Scope.A1 optical microscope (Zeiss, Germany) with the x100 objective lens.

3.2.6. Particle size distribution

A Mastersizer 2000 (Malvern Instruments Ltd., UK) was used to determine the particle size distribution of the emulsions. About 0.1 mL of the emulsion was added to 150 mL distilled water (0.06% v/v) while stirring in the dispersion unit. The mean diameter of the oil droplets was expressed as the volume mean diameter (d_{43}) and the dispersion index (span) was also reported, according to Eqs. (3.2) and (3.3), respectively. The emulsions were analyzed 1 d after their preparation and each sample was measured in triplicate.

$$d_{43} = \sum n_i d_i^4 \Big/ \sum n_i d_i^3 \tag{3.2}$$

$$Span = \left(\mathrm{d}_{90} - d_{10}\right) / d_{50} \tag{3.3}$$

where n_i was the number of particles with diameter di, and d_{10}, d_{50} and d_{90} were diameters at 10%, 50% and 90% cumulative volume, respectively.

3.2.7. Polyacrylamide gel electrophoresis (SDS-PAGE)

Molecular weight distribution of proteins resulting from the high-pressure homogenization of the O/W emulsions was evaluated by polyacrylamide gel electrophoresis (SDS-PAGE) under reducing and non-reducing conditions, according to Laemmli (1970). Under dissociating non-reducing conditions, occurs the rupture of protein aggregates stabilized by electrostatic and hydrophobic interactions. While that, under dissociating reducing conditions, occurs the rupture of disulfide interactions formed between free sulfhydryl groups of proteins. A vertical slab Mini-Protean electrophoresis system (Bio-Rad Laboratories, Hercules, CA, USA) was used and the resolving and stacking gels contained 15% and 5% of acrylamide, respectively. The whole emulsions, without phase separation, were diluted in deionized water (2 mg protein/mL) and the resulting solution was diluted in a sample buffer (1:1) to obtain dissociating non-reducing conditions (50 mM Tris–HCl (pH 6.8), plus 2% SDS (w/v), 10% glycerol (v/v) and 0.1% (w/v) bromophenol blue) and dissociating reducing conditions (50 mM Tris–HCl (pH 6.8), plus 2% SDS (w/v), 10% glycerol (v/v), 0.1% (w/v) bromophenol blue and 5% (v/v) β-mercaptoethanol). Under dissociating conditions, the samples were heat treated at 70 °C for 5 min and 10 μL aliquots then loaded into the polyacrylamide wells in the stacking gel. The gels were run at 100 V with a running buffer (pH 8.3) containing 25 mM Tris–HCl, 250 mM glycine and 0.1% (w/v) SDS. The gels were then stained with 0.25% (w/v) Coomassie Brilliant Blue in ethanol:acetic acid:water (45:10:45 v/v), and diffusion-destained by repeated washing in an ethanol:acetic acid:water solution (10:5:85 v/v). A native whey protein solution (non-denatured) was used as reference, and a commercial molecular weight marker (Pre-Stained Invitrogen^{TM} Bench Marker Protein Ladder, Bioagency International, Jacksonville, USA) was used for the control of molecular weight.

3.2.8. Rheological measurements

A Physica MCR301 modular compact rheometer (Anton Paar, Germany) with stainless steel plate geometry (75 mm) and a 0.7 mm gap was used for the measurements.

The emulsions were evaluated after 1 d of storage and the measurements made in triplicate at 25 °C. Flow curves were obtained using an up-down-up steps program with the shear rate varying between 0 and 300 s^{-1}. The model for shear-thinning fluids (Power Law model) (Eq. (3.4)) was used to fit the flow curves.

$$\sigma = k \,.\left(\dot{\gamma}\right)^{n} \tag{3.4}$$

where σ is the shear stress (Pa), $\dot{\gamma}$ is the shear rate (s^{-1}), k is the consistency index ($Pa.s^{n}$) and n is the flow behavior index (dimensionless).

3.2.9. Oxidative stability

The peroxide value (PV) of the WPI-stabilized emulsions was evaluated during the 30 d of storage at room temperature. The emulsions were placed in sealed bottles and covered with aluminum foil to avoid exposure to light. A control sample containing only flaxseed oil was also analyzed. The peroxide value (PV) was determined spectrophotometrically according to the IDF standard method with some modifications (Shantha and Decker, 1994). Initially the oil was extracted from the emulsions by adding 0.3 mL emulsion to 1.5 mL of isooctane/isopropanol (3:2, v/v), in triplicate. The mixtures were then vortexed three times for 10 s each, and left to stand for 30 min. After standing, 0.2 mL of the clear upper solvent layer was collected and mixed with 2.8 mL of chloroform/methanol (7:3, v/v) and vortexed again (4 s). Ammonium thiocyanate solution (15 µL) was then added, and the samples mixed on the vortex mixer for a further 4 s. Finally 15 µL iron (II) solution was added, the samples vortexed once again for 4 s, and after 5 min incubation at room temperature, the absorbance of the samples was determined at 500 nm against a blank containing all the reagents except the sample, using an UNICO SpectroQuest™ 2800 UV/VIS Spectrophotometer (United Products & Instruments Inc., New Jersey, USA). The entire procedure was carried out in subdued light and completed within 3 min. The hydroperoxide concentration was determined using a Fe^{+3} standard curve with an iron concentration varying from 1 to 20 μg, as described by Shantha and Decker (1994). The peroxide value, expressed as milliequivalents of peroxide per kilogram of oil, was calculated using Eq. (3.5).

$$Peroxide\,Value\,(PV) = \frac{(A_s - A_b)\; x\; m}{55.84\; x\; m_0\; x\; 2} \tag{3.5}$$

where A_s = absorbance of the sample, A_b = absorbance of the blank, m = slope of the calibration curve, m_0 = mass (g) of the oil, 55.84 = atomic weight of iron. The result was divided by a factor of 2 to express the peroxide value as milliequivalents of peroxide instead of milliequivalents of oxygen.

3.2.10. Statistical analysis

The results were evaluated by an analysis of variance (ANOVA), and significant differences ($p<0.05$) between the treatments were evaluated by the Tukey procedure. The statistical analyzes were carried out using the software STATISTICA 6.0 (Statisoft Inc., Tulsa, USA).

3.3. RESULTS AND DISCUSSION

3.3.1. Creaming stability of the emulsions

All the emulsions homogenized by high-pressure (20–100 MPa), irrespective of the number of passes through the homogenizer (1–7 passes), showed good stability, with no signs of phase separation into a top cream phase and a bottom serum phase up to 9 d of storage in cylindrical glass tubes (10 mL of emulsion, internal diameter = 11 mm, height = 94 mm).

In order to reduce the wall effects, stability tests of the emulsions homogenized at 20 and 80 MPa with 1, 4 and 7 passes through the homogenizer, were carried out at 25 °C in glass bottles (~60 mL of emulsion, internal diameter = 45 mm, height = 70 mm) for 3 months, since it has been well established that the confining walls can exert an extra retardation effect on a spherical particle settling in a liquid (Chhabra et al., 2003). However, under these conditions, the emulsions still showed no phase separation, even after 3 months of storage (Fig. 3.1).

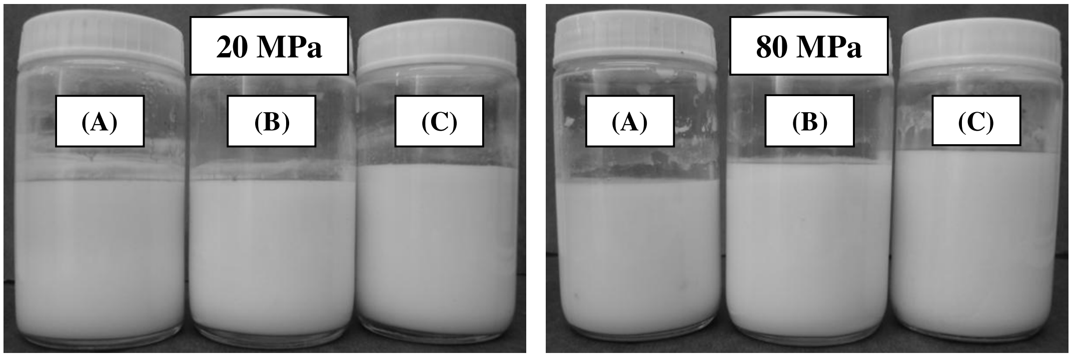

Fig. 3.1. Visual appearance of the O/W emulsions homogenized at 20 and 80 MPa after 3 months of storage. Number of passes: (A) 1, (B) 4 and (C) 7.

3.3.2. Microstructure and droplet size

The influence of different pressures and number of passes through the homogenizer on the structure of the emulsions was evaluated by optical microscopy. The microscopic images of the emulsions showed that increasing the homogenization pressure and the number of passes, decreased the droplet size, in agreement with another studies (Qian and McClements, 2011; Santana et al., 2011). However, at high pressures, an increase in the number of passes seems to promote coalescence of the emulsion droplets, as can be observed in Fig. 3.2.

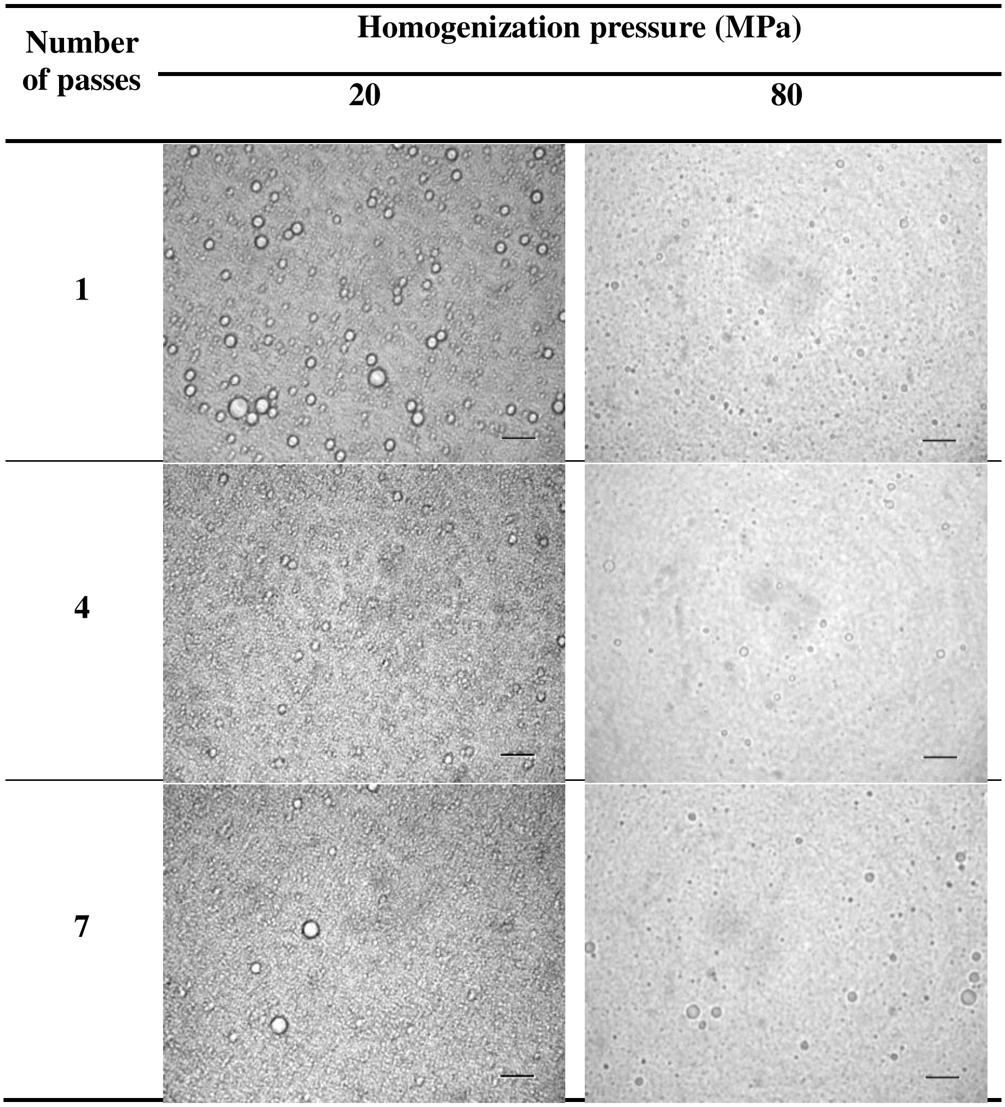

Fig. 3.2. Microstructures of the O/W emulsions homogenized at 20 and 80 MPa with 1, 4 and 7 passes through the homogenizer. Scale bar = 10 µm.

Fig. 3.3 shows the changes in particle size distribution with the number of passes through the homogenizer, for the emulsions homogenized at 20 and 80 MPa (Fig. 3.3A and B, respectively). It can be seen that at lower homogenization pressures (20 MPa), the width of the distribution of particle size decreased appreciably with increasing number of passes, making the oil droplets smaller and more mono-dispersed. However, when the pressure was increased to 80 MPa, the distribution of the emulsion particles became bimodal, indicating that droplet–droplet aggregation (coalescence) may have occurred.

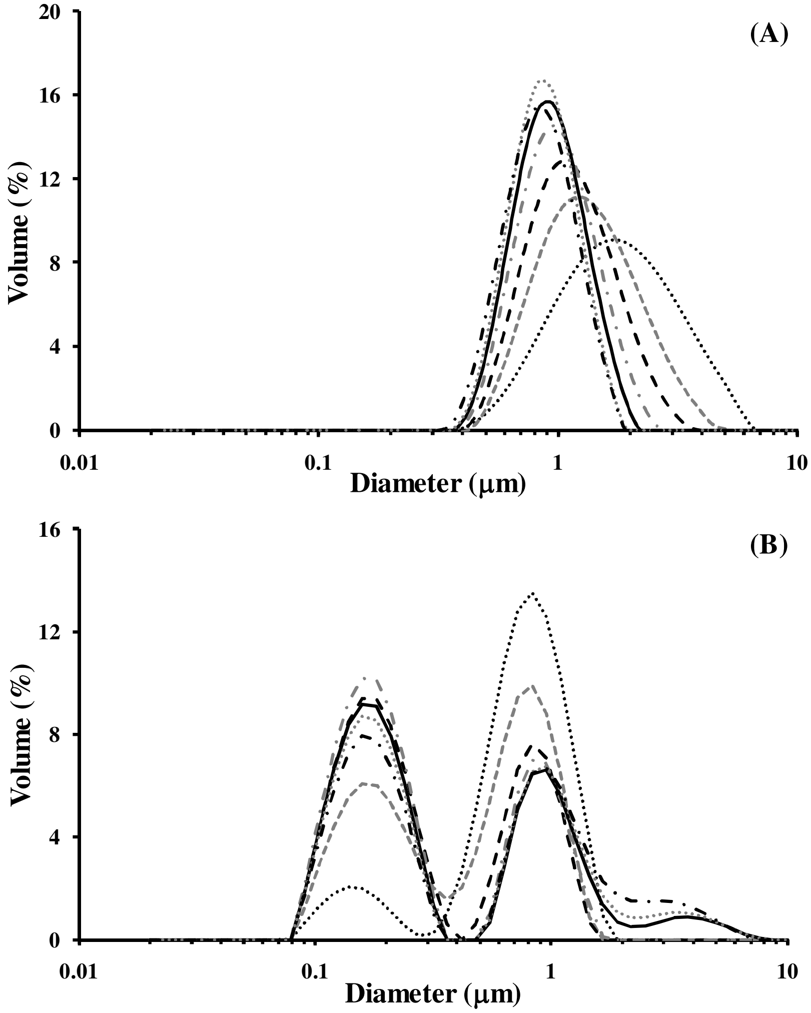

Fig. 3.3. Effects of homogenization pressure and the number of passes through the homogenizer on the droplet size distribution of the emulsions containing 3% (w/v) WPI and 30% (v/v) flaxseed oil, homogenized at (A) 20 and (B) 80 MPa. Number of passes: (·····) 1, (- - ·) 2, (– –) 3, (– ·) 4, (——) 5, (·····) 6 and (– ·) 7.

The evaluation of the mean droplet diameter and the span, or dispersion index, of the emulsions homogenized at 20 and 80 MPa (Table 3.1) showed that a significant reduction ($p<0.05$) in the d_{43} values was obtained at 20 MPa with up to 7 passes through the homogenizer, as confirmed in Fig. 3.3A. At higher homogenization pressures (80 MPa), with up to 3 passes, the smallest droplet size (d_{43}) was obtained. However, it can be seen that the d_{43} values showed a significant increase as from 5 passes through the homogenizer, indicating droplet re-coalescence, which can also be observed from the higher values for span. Despite producing very small particles, they may immediately re-coalescence, causing low emulsification efficiency under severe homogenization conditions. This might be related to lower adsorption rate of the WPI onto the droplets interface, which would have the following consequences: some of the new droplets may not be covered within a very short period of time during the deformation and disruption of the droplets in the homogenizer valve, or part of the new interfaces may be incompletely covered (Jafari et al., 2007). At the same time, the rate (frequency) of droplet collisions would be very high, particularly at the higher energy densities (pressures). Thus, this combination of more energy input, higher volume flow rate and shorter residence times could lead to more intense re-coalescence and a bigger emulsion droplet size, creating a bimodal distribution (Jafari et al., 2007).

Table 3.1. Mean droplet diameter (μm) and span of the O/W emulsions stabilized by WPI.

Number of passes	Homogenization pressure (MPa)			
	20		80	
	d_{43} (μm)	Span	d_{43} (μm)	Span
1	2.17 ± 0.00^{aA}	1.62 ± 0.02	0.83 ± 0.01^{aB}	1.33 ± 0.01
2	1.55 ± 0.03^{bA}	1.33 ± 0.01	0.59 ± 0.00^{bB}	1.65 ± 0.01
3	1.32 ± 0.01^{cA}	1.14 ± 0.00	0.47 ± 0.00^{cB}	3.83 ± 0.02
4	1.14 ± 0.01^{dA}	0.97 ± 0.03	0.46 ± 0.00^{cB}	4.27 ± 0.01
5	1.03 ± 0.00^{eA}	0.88 ± 0.01	0.72 ± 0.00^{dB}	5.24 ± 0.02
6	0.97 ± 0.00^{fA}	0.82 ± 0.02	0.79 ± 0.00^{eB}	5.59 ± 0.03
7	0.93 ± 0.02^{gA}	0.89 ± 0.05	0.90 ± 0.00^{fB}	5.91 ± 0.04

Different letters indicate significant differences ($p<0.05$). Small letters: differences in the same column. Capital letters: differences in the same line for the different homogenization pressures.

High-pressure homogenization and an increase in the number of passes through the homogenizer are related to a greater dissipation of mechanical energy in the form of heat, which leads to an increased temperature of the emulsions. Thus, the temperature of the O/W emulsions was measured at the exit from the homogenizer after each pass, at the pressures of 20 and 80 MPa, and the results are shown in Fig. 3.4. According to the results, it can be seen that an increase in pressure and in the number of passes through the homogenizer, led to an increase in temperature of the emulsions, as also observed by Sandra and Dalgleish (2005) and Santana et al. (2011). According to Hayes and Kelly (2003), the increase in temperature is due to adiabatic heating, in addition to high turbulence, shear and cavitation forces during high-pressure homogenization. At 80 MPa, after 4 passes through the homogenizer, the temperature of denaturation (62 °C) of the second most abundant fraction of the whey proteins, α-lactalbumin (α-La) (22%), was reached, and after 6 passes, the temperature of denaturation (64 °C) of the least abundant fraction, bovine serum albumin (BSA) (5.5%), was reached (Bryant and McClements, 1998). Thus, the increase in droplet size (d_{43}) with the number of passes through the homogenizer at high pressure (Table 3.1) and temperature (Fig. 3.4), could also result in protein unfolding, exposure and interaction between hydrophobic groups via the formation of covalent bonds, thereby resulting in a decrease in the emulsifying capacity and promoting droplet coalescence.

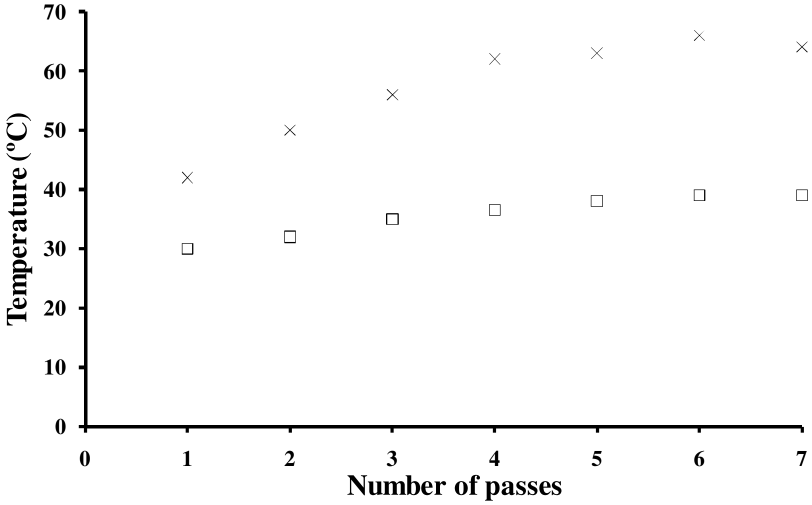

Fig. 3.4. Effects of homogenization pressure and the number of passes through the homogenizer on the temperature of the emulsions containing 3% (w/v) WPI and 30% (v/v) flaxseed oil at the exit of the homogenizer. Homogenization pressure: (□) 20 and (X) 80 MPa.

3.3.3. Polyacrylamide gel electrophoresis (SDS-PAGE)

Polyacrylamide gel electrophoresis (SDS-PAGE) was carried out to determine if the high-pressure homogenization process and the number of passes through the homogenizer could have caused protein aggregation due to the increase in temperature observed in the emulsions (Fig. 3.4). Emulsions homogenized at 20 MPa and diluted to obtain non-reducing and reducing conditions, are shown in Fig. 3.5A and B, respectively, and emulsions homogenized at 80 MPa and diluted to obtain non-reducing and reducing conditions, are shown in Fig. 3.5C and D, respectively. Fig. 3.5A and C show the temperatures reached at the exit of the homogenizer after each pass at pressures of 20 and 80 MPa, respectively.

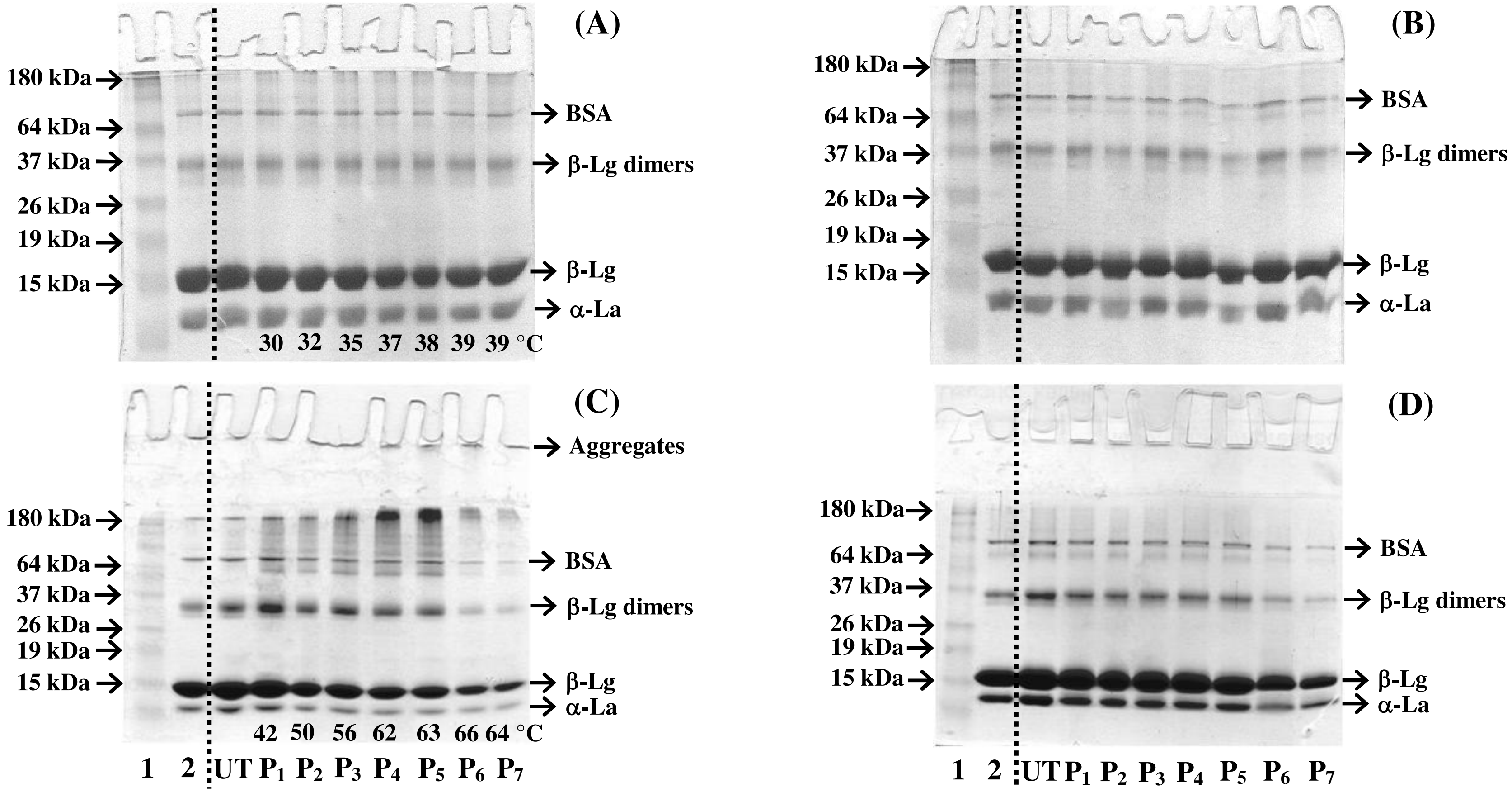
(A)
180 kDa
64 kDa
37 kDa
26 kDa
19 kDa
15 kDa
BSA
β-Lg dimers
β-Lg
α-La
30 32 35 37 38 39 39 °C
(B)
180 kDa
64 kDa
37 kDa
26 kDa
19 kDa
15 kDa
BSA
β-Lg dimers
β-Lg
α-La
(C)
Aggregates
180 kDa
64 kDa
37 kDa
26 kDa
19 kDa
15 kDa
BSA
β-Lg dimers
β-Lg
α-La
42 50 56 62 63 66 64 °C
1 2 UT P1 P2 P3 P4 P5 P6 P7
(D)
180 kDa
64 kDa
37 kDa
26 kDa
19 kDa
15 kDa
BSA
β-Lg dimers
β-Lg
α-La
1 2 UT P1 P2 P3 P4 P5 P6 P7

Fig. 3.5. Polyacrylamide gel electrophoresis (SDS-PAGE) of the O/W emulsions homogenized in an Ultra Turrax (14000 rpm) and at high pressure (20 and 80 MPa) with different numbers of passes through the homogenizer. (A, B) 20 MPa and (C, D) 80 MPa. (A, C) SDS-PAGE under non-reducing conditions, and (B, D) SDS-PAGE under reducing conditions. Columns (1) commercial molecular weight marker, (2) native whey protein solution (non-denatured), (UT) Ultra Turrax, (P_1) 1 pass, (P_2) 2 passes, (P_3) 3 passes, (P_4) 4 passes, (P_5) 5 passes, (P_6) 6 passes and (P_7) 7 passes. The temperatures reached at the exit of the homogenizer after each pass are shown in detail.

Two major bands were visualized under the different homogenization conditions (pressure and number of passes) in the molecular weight region around 15 and 19 kDa, corresponding to the fractions of α-lactalbumin (α-La) and β-lactoglobulin (β-Lg), respectively. Furthermore, minor bands were observed in the molecular weight regions between 26–37 kDa and around 64 kDa, related to the fractions of β-Lg dimers and bovine serum albumin (BSA), respectively.

According to Fig. 3.5A and B, there was no formation of high molecular weight protein aggregates in the emulsions homogenized at 20 MPa, which could be explained by the lower pressure and lower temperatures reached after each pass through the homogenizer. However, when the pressure was increased to 80 MPa, it can be seen that, with only 1 pass through the homogenizer, there was already some formation of aggregates with molecular weight above 64 kDa, and this has been intensified after 4 and 5 passes (Fig. 3.5C). Therefore one must say that, despite not having reached the denaturation temperature of the whey protein fractions after a smaller number of passes, pressure promoted the formation of high molecular weight aggregates. The effects of high hydrostatic pressure on proteins are primarily related to the rupture of non-covalent interactions (hydrophobic and electrostatic), leading to disruption of the quaternary and tertiary structure of the globular proteins, with relatively little influence on their secondary structure (Bouaouina et al., 2006). This aggregation process was intensified by the increase in temperature after 4 and 5 passes through the homogenizer. Partial globular whey proteins unfolding can result in more compact adsorbed layers, exposing reactive sulphydryl groups (Singh and Sarkar, 2011). Thus sulfhydryl-disulfide interchange reactions could be formed between protein molecules adsorbed at the interface, leading to an increase in the surface viscoelasticity of the protein film surrounding the droplet, which could explain the stability of these emulsions against coalescence (Dickinson et al., 1990; Dickinson and Matsumura, 1991; McClements et al., 1993).

Under non-reducing conditions (Fig. 3.5C), the formation of high molecular weight protein aggregates was also visualized in the stacking gel, which could correspond to a molecular weight exceeding 200 kDa (Copeland, 1990). However, in the presence of β-mercaptoethanol, a rather sharp decrease in these aggregates bands occurred (Fig. 3.5D), indicating that they were stabilized by disulfide bonds. Thus, the aggregation process could also be evaluated by the decrease in the whey protein fractions, mainly after 6 and 7 passes, simultaneously with the formation of high molecular weight aggregates in the stacking gel after a higher number of passes through the homogenizer (4–7). The gradual disappearance of low molecular weight proteins from the electrophoretic profiles is also linked to the aggregation process with increasing pressure (from 400 MPa) in emulsions stabilized by 11S soy protein. Such behavior was observed for both adsorbed and non-adsorbed proteins, indicating that regardless of the location of the proteins (aqueous phase or interface), the use of high pressure induced the aggregation of this globular protein (Puppo et al., 2011).

3.3.4. Rheology

The flow curves data for WPI-stabilized emulsions, homogenized at high pressure with different numbers of passes through the homogenizer, were fitted to the power law model equation well (Table 3.2) for all the emulsions ($R^2 > 0.993$). The values for apparent viscosity at a shear rate of 100 s^{-1} are also shown in Table 3.2. This parameter was evaluated at this shear rate since it is typical of food processes, such as flow through a pipe, stirring or mastication (McClements, 2005). The O/W emulsions showed low pseudoplasticity, since the flow behavior index (*n*) of all the emulsions was in the range from 0.78 to 0.95. According to Table 3.2, in general, one can observe that the consistency index (*k*) increased with the number of passes through the homogenizer, whereas the values for the flow behavior index (*n*) decreased, suggesting an increase in viscosity and in the pseudoplasticity of the O/W emulsions, respectively. An increase in homogenization pressure and in the number of passes led to an increase in viscosity of the emulsions, which can be seen from the values for apparent viscosity at 100 s^{-1} (η_{100}), and could be associated with a higher protein aggregation and mean droplet size.

Table 3.2. Rheological parameters obtained from the power law model and the apparent viscosity at 100 s^{-1} (η_{100}) for the O/W emulsions stabilized by WPI.

Number of passes	Homogenization pressure (MPa)														
	20			40			60			80			100		
	n	*k* (Pa.s^n)	η_{100} (mPa.s)	*n*	*k* (Pa.s^n)	η_{100} (mPa.s)	*n*	*k* (Pa.s^n)	η_{100} (mPa.s)	*n*	*k* (Pa.s^n)	η_{100} (mPa.s)	*n*	*k* (Pa.s^n)	η_{100} (mPa.s)
1	0.94^{aA}	0.004^{aA}	3.1^{aA}	0.91^{aA}	0.004^{aA}	3.0^{aA}	0.90^{aA}	0.004^{aA}	3.0^{aA}	0.94^{aA}	0.006^{aA}	4.5^{aB}	0.95^{aA}	0.005^{aA}	4.5^{aB}
2	0.85^{bA}	0.007^{abAB}	3.8^{bA}	0.91^{aB}	0.005^{acA}	3.6^{bA}	0.89^{aAB}	0.006^{abAB}	4.0^{bB}	0.92^{aB}	0.006^{aAB}	4.2^{aC}	0.90^{aAB}	0.007^{abB}	5.0^{bD}
3	0.92^{abA}	0.005^{abA}	3.8^{bA}	0.89^{abA}	0.006^{abcAB}	3.9^{bcA}	0.91^{aA}	0.006^{abAB}	4.1^{bcB}	0.92^{aA}	0.006^{aAB}	4.7^{aC}	0.92^{aA}	0.007^{abB}	5.1^{bcD}
4	0.92^{abA}	0.005^{abA}	3.7^{bA}	0.88^{abA}	0.007^{bcA}	4.1^{cdB}	0.92^{aA}	0.006^{abA}	4.3^{cB}	0.78^{bB}	0.015^{bB}	5.5^{bcC}	0.91^{aA}	0.008^{abC}	5.3^{cC}
5	0.88^{abA}	0.006^{abA}	3.8^{bA}	0.90^{abA}	0.006^{abcA}	4.1^{cdA}	0.88^{aA}	0.008^{bA}	4.8^{dB}	0.89^{abA}	0.009^{abA}	5.2^{cB}	0.95^{aA}	0.007^{abA}	5.9^{dC}
6	0.87^{abAB}	0.007^{abA}	3.9^{bA}	0.89^{abAB}	0.007^{bcA}	4.2^{deA}	0.92^{aAB}	0.006^{abA}	4.8^{dB}	0.82^{abA}	0.014^{abB}	5.9^{bdC}	0.93^{aB}	0.009^{bAB}	7.0^{eD}
7	0.87^{abA}	0.008^{bAB}	4.1^{bA}	0.85^{bA}	0.008^{bAB}	4.4^{eAB}	0.91^{aA}	0.007^{bA}	4.9^{dB}	0.88^{abA}	0.010^{abAB}	6.0^{dC}	0.90^{aA}	0.013^{cB}	9.0^{fD}

Different letters indicate significant differences ($p<0.05$). Small letters: differences in the same column. Capital letters: differences in the same line.

3.3.5. Lipid oxidation

The progress of lipid oxidation was monitored by measuring the formation of primary reaction products (lipid hydroperoxides) in the O/W emulsions homogenized at high pressure (Fig. 3.6). The emulsions homogenized at 20 MPa showed lower or statistically similar peroxide values to the pure oil, except after 30 d of storage (7 passes) (Fig. 3.6A). The presence of an emulsifier (protein) prevents the binding of some pro-oxidant impurities (such as transition metals), protecting against oil oxidation (Fomuso et al., 2002; McClements and Decker, 2000). However, the peroxide value only increased from 0.420 to 0.714 meq/kg oil for the pure oil after 30 d of storage. When the pressure was increased to 80 MPa, there was an increase in the formation of primary oxidation products in the emulsions in relation to the pure oil (Fig. 3.6B) and the emulsions homogenized at 20 MPa (Fig. 3.6A), which may have been a consequence of the increase in temperature observed in these emulsions (Fig. 3.4) (Shahidi and Zhong, 2005). Moreover, the decrease in droplet size (d_{43}) with increase in pressure (Table 3.1) may also have influenced the increase in oxidation, since the surface area of the droplets increased. According to McClements and Decker (2000), lipid oxidation can be accelerated by reactions that take place at the surface of the emulsion droplets. Therefore the rate of lipid oxidation should increase as the droplet size decreases, since smaller droplets expose a larger surface area per unit volume to the pro-oxidants at the interface (Lee et al., 2011; McClements and Decker, 2000; Osborn and Akoh, 2004). The emulsions homogenized at 80 MPa showed an increase in peroxide value from 0 to 1.777 meq/kg oil after 1 pass through the homogenizer, from 0 to 0.847 meq/kg oil after 4 passes, and from 0.026 to 2.957 meq/kg oil after 7 passes. Furthermore, it seems that the primary oxidation products continued to increase after 30 d, whereas in the pure oil they only increased from 0.401 to 0.647 meq/kg oil (Fig. 3.6B). The increase observed in the oxidation of the emulsions and pure oil can be considered small, since the WPI probably acted as an antioxidant in the emulsions. Moreover, the low temperature used in the assays (25 °C) may have prevented greater oxidation, since, according to Pu and Sathivel (2011), flaxseed oil at 30 °C exhibited minimal lipid oxidation with time, but showed higher peroxide values with increase in temperature (30–60 °C).

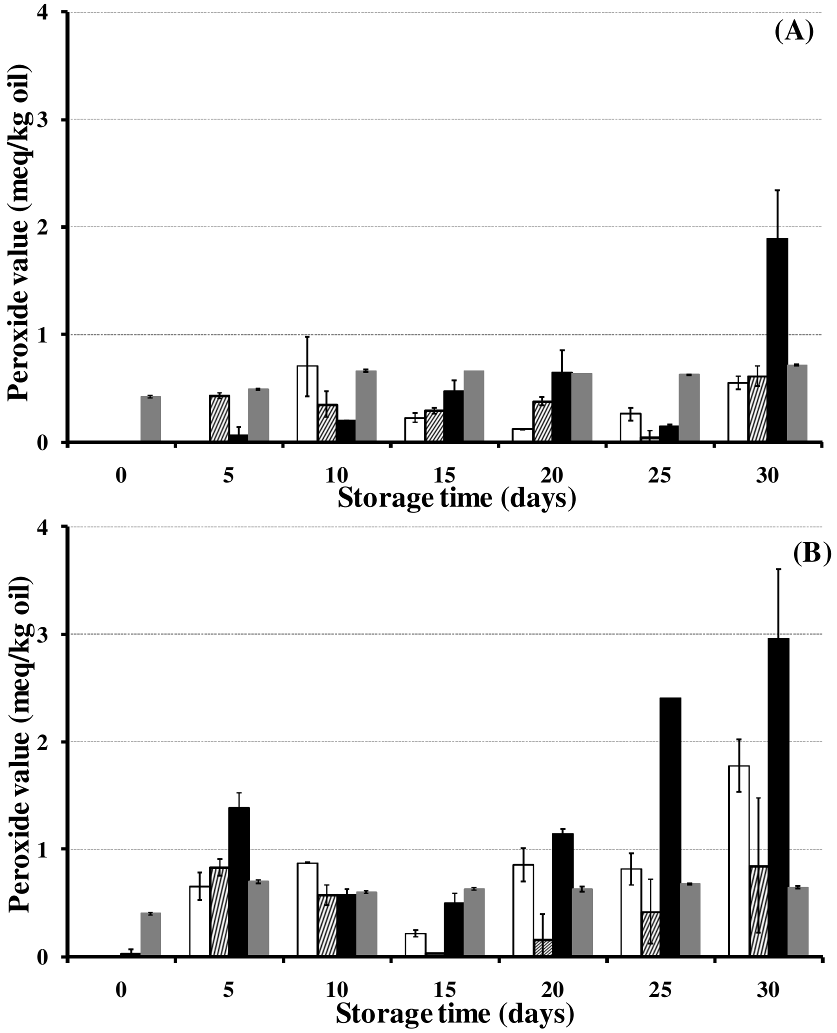

Fig. 3.6. Effects of homogenization pressure and the number of passes through the homogenizer on the peroxide value of the emulsions containing 3% (w/v) WPI and 30% (v/v) flaxseed oil, homogenized at (A) 20 and (B) 80 MPa. Number of passes: (□) 1 pass, (▨) 4 passes, (■) 7 passes and (▒) pure oil. The bars represent the standard deviation amongst replications.

3.4. CONCLUSIONS

The results of this study revealed that emulsions stabilized by whey proteins showed good stability, with no sign of phase separation, when homogenized at high-pressure (20–100 MPa) with different numbers of homogenization cycles (1–7). An increase in homogenization pressure from 20 to 80 MPa, and in the number of passes up to 3, resulted in a smaller mean droplet size of the O/W emulsions. However, higher pressures and a greater number of passes led to droplets coalescence and the formation of high molecular weight protein aggregates due to shear and the increase in temperature, which reduced its emulsifying capacity. In addition, there was an increase in viscosity of the O/W emulsions and the formation of primary oxidation products, the latter being explained by the increase in temperature and decrease in droplet size (increase in surface area) of the emulsions at the higher pressure. Therefore, when aiming for greater stability and a reduction in oxidation of the flaxseed oil in the O/W emulsions, the best process conditions would be the use of a homogenization pressure of 20 MPa and up to 5 passes through the homogenizer.

3.5. ACKNOWLEDGEMENTS

The authors would like to acknowledge the financial support of CNPq (140287/2009-4) and Fapesp (2007/58017-5), the donation of whey protein isolate by Professor Valdemiro Carlos Sgarbieri (DEPAN/UNICAMP) and to the Professor Carlos Raimundo Ferreira Grosso (DEPAN/UNICAMP) by the particle size distribution analysis.

3.6. REFERENCES

AOAC, 1997. Official Methods of Analysis of Association of Official Analytical Chemists (AOAC) International. Association of Official Analytical Chemists, Gaithersburg, USA.

Bligh, E.G., Dyer, W.J., 1959. A rapid method of total lipid extraction and purification. Canadian Journal of Biochemistry 37 (8), 911-917.

Bouaouina, H., Desrumaux, A., Loisel, C., Legrand, J., 2006. Functional properties of whey proteins as affected by dynamic high-pressure treatment. International Dairy Journal 16 (4), 275-284.

Bryant, C.M., McClements, D.J., 1998. Molecular basis of protein functionality with special consideration of cold-set gels derived from heat-denatured whey. Trends in Food Science & Technology 9 (4), 143-151.

Chhabra, R.P., Agarwal, S., Chaudhary, K., 2003. A note on wall effect on the terminal falling velocity of a sphere in quiescent Newtonian media in cylindrical tubes. Powder Technology 129 (1-3), 53-58.

Copeland, R.A., 1990. Eletrophoretic and chromatographic methods for assessing protein purity. In: Copeland, R.A. (Ed.), Methods for Protein Analysis: a Practical Guide to Laboratory Protocols. Chapman & Hall, New York, USA, pp. 59-98.

Dalgleish, D.G., 1996. Conformations and structures of milk proteins adsorbed to oil-water interfaces. Food Research International 29 (5-6), 541-547.

Desrumaux, A., Marcand, J., 2002. Formation of sunflower oil emulsions stabilized by whey proteins with high-pressure homogenization (up to 350 MPa): Effect of pressure on emulsion characteristics. International Journal of Food Science and Technology 37 (3), 263-269.

Dickinson, E., 2001. Milk protein interfacial layers and the relationship to emulsion stability and rheology. Colloids and Surface B: Biointerfaces 20 (3), 197-210.

Dickinson, E., Matsumura, Y., 1991. Time-dependent polymerization of β-lactoglobulin through disulphide bonds at the oil-water interface in emulsions. International Journal of Biological Macromolecules 13 (1), 26-30.

Dickinson, E., Rolfe, S.E., Dalgleish, D.G., 1990. Surface shear viscometry as a probe of protein-protein interactions in mixed milk protein films adsorbed at the oil-water interface. International Journal of Biological Macromolecules 12 (3), 189-194.

Fomuso, L.B., Corredig, M., Akoh, C.C., 2002. Effect of emulsifier on oxidation properties of fish oil-based structured lipid emulsions. Journal of Agricultural and Food Chemistry 50 (10), 2957-2961.

Guzey, D., McClements, D.J., 2006. Formation, stability and properties of multilayer emulsions for application in the food industry. Advances in Colloid and Interface Science 128-130 (21), 227-248.

Hayes, M.G., Kelly, A.L., 2003. High pressure homogenisation of raw whole bovine milk (a) effects on fat globule size and other properties. Journal of Dairy Research 70 (3), 297-305.

Hu, M., McClements, D.J., Decker, E.A., 2003. Impact of whey protein emulsifiers on the oxidative stability of salmon oil-in-water emulsions. Journal of Agricultural and Food Chemistry 51 (5), 1435-1439.

Jafari, S.M., He, Y., Bhandari, B., 2007. Effectiveness of encapsulating biopolymers to produce sub-micron emulsions by high energy emulsification techniques. Food Research International 40 (7), 862-873.

Jafari, S.M., Assadpoor, E., He, Y., Bhandari, B., 2008. Re-coalescence of emulsion droplets during high-energy emulsification. Food Hydrocolloids 22 (7), 1191-1202.

Kerstens, S., Murray, B.S., Dickinson, E., 2006. Microstructure of β-lactoglobulin-stabilized emulsions containing non-ionic surfactant and excess free protein: Influence of heating. Journal of Colloid and Interface Science 296 (1), 332-341.

Laemmli, U.K., 1970. Cleavage of structural proteins during the assembly of the head of bacteriophage T4. Nature 227 (5259), 680-685.

Lee, S.J., Choi, S.J., Li, Y., Decker, E.A., McClements, D.J., 2011. Protein-stabilized nanoemulsions and emulsions: Comparison of physicochemical stability, lipid oxidation, and lipase digestibility. Journal of Agricultural and Food Chemistry 59 (1), 415-427.

McClements, D.J., 2004. Protein-stabilized emulsions. Current Opinion in Colloid & Interface Science 9 (5), 305-313.

McClements, D.J., 2005. Food emulsions: Principles, Practices and Techniques. CRC Press, Boca Raton, FL.

McClements, D.J., Decker, E.A., 2000. Lipid oxidation in oil-in-water emulsions: Impact of molecular environment on chemical reactions in heterogeneous food systems. Journal of Food Science 65 (8), 1270-1282.

McClements, D.J., Decker, E.A., Weiss, J., 2007. Emulsion-based delivery systems for lipophilic bioactive components. Journal of Food Science 72 (8), R109-R124.

McClements, D.J., Monahan, F.J., Kinsella, J.E., 1993. Disulfide bond formation affects stability of whey protein isolate emulsions. Journal of Food Science 58 (5), 1036-1039.

Osborn, H.T., Akoh, C.C., 2004. Effect of emulsifier type, droplet size, and oil concentration on lipid oxidation in structured lipid-based oil-in-water emulsions. Food Chemistry 84 (3), 451-456.

Pu, J., Sathivel, S., 2011. Kinetics of lipid oxidation and degradation of flaxseed oil containing crawfish (*Procambarus clarkii*) astaxanthin. Journal of the American Oil Chemists' Society 88 (5), 595-601.

Puppo, M. C., Beaumal, V., Speroni, F., de Lamballerie, M., Añón, M. C., Anton, M., 2011. β-Conglycinin and glycinin soybean protein emulsions treated by combined temperature–high-pressure treatment. Food Hydrocolloids 25 (3), 389-397.

Qian, C., McClements, D.J., 2011. Formation of nanoemulsions stabilized by model food-grade emulsifiers using high-pressure homogenization: Factors affecting particle size. Food Hydrocolloids 25 (5), 1000-1008.

Sandra, S., Dalgleish, D.G., 2005. Effects of ultra-high-pressure homogenization and heating on structural properties of casein micelles in reconstituted skim milk powder. International Dairy Journal 15 (11), 1095-1104.

Santana, R.C., Perrechil, F.A., Sato, A.C.K., Cunha, R.L., 2011. Emulsifying properties of collagen fibers: Effect of pH, protein concentration and homogenization pressure. Food Hydrocolloids 25 (4), 604-612.

Shahidi, F., Zhong, Y., 2005. Lipid Oxidation: Measurement Methods. In: Shahidi, F. (Ed.), Bailey's Industrial Oil and Fat Products. John Wiley & Sons, Inc, pp. 357-385.

Shantha, N.C., Decker, E.A., 1994. Rapid, sensitive, iron-based spectrophotometric methods for determination of peroxide values of food lipids. Journal of AOAC International 77 (2), 421-424.

Singh, H., Sarkar, A., 2011. Behaviour of protein-stabilised emulsions under various physiological conditions. Advances in Colloid and Interface Science 165 (1), 47-57.

Sun, C., Gunasekaran, S., 2009. Effects of protein concentration and oil-phase volume fraction on the stability and rheology of menhaden oil-in-water emulsions stabilized by whey protein isolate with xanthan gum. Food Hydrocolloids 23 (1), 165-174.

Tong, L.M., Sasaki, S., McClements, D.J., Decker, E.A., 2000. Antioxidant activity of whey in a salmon oil emulsion. Journal of Food Science 65 (8), 1325-1329.

Tonon, R.V., Grosso, C.R.F., Hubinger, M.D., 2011. Influence of emulsion composition and inlet air temperature on the microencapsulation of flaxseed oil by spray drying. Food Research International 44 (1), 282-289.

Walstra, P., 2003. Physical chemistry of foods. Marcel Decker, New York, NY.

Ye, A., 2010. Surface protein composition and concentration of whey protein isolate-stabilized oil-in-water emulsions: Effect of heat treatment. Colloids and Surfaces B: Biointerfaces 78 (1), 24-29.

Zhao, G., Etherton, T.D., Martin, K.R., Gillies, P.J., West, S.G., Kris-Etherton, P.M., 2007. Dietary α-linolenic acid inhibits proinflammatory cytokine production by peripheral blood mononuclear cells in hypercholesterolemic subjects. The American Journal of Clinical Nutrition 85 (2), 385-391.

CHAPTER 4

Assessing the potential of flaxseed protein as an emulsifier combined with whey protein isolate

Kuhn, K. R.; Silva, F. G. D.; Netto, F. M.;
Cunha, R. L.

To be submitted to Food Research International

CHAPTER 4. Assessing the potential of flaxseed protein as an emulsifier combined with whey protein isolate

Kátia Regina Kuhn[a], Fernanda Guimarães Drummond e Silva[b], Flavia Maria Netto[b], Rosiane Lopes da Cunha[a,]*

[a]Department of Food Engineering, Faculty of Food Engineering, University of Campinas (UNICAMP), 13083-862 – Campinas, SP, Brazil

[b]Department of Food and Nutrition, Faculty of Food Engineering, University of Campinas (UNICAMP), 13083-862 – Campinas, SP, Brazil

*Corresponding author: Tel.: +55 19 3521 4047; fax: +55 19 3521 4027

E-mail address: rosiane@fea.unicamp.br

ABSTRACT

The potential use of flaxseed protein isolate (FPI) as an emulsifying agent was studied in combination with whey protein isolate (WPI) or alone without the presence of other emulsifier. All the FPI and WPI-FPI emulsions were kinetically unstable, while WPI emulsions were stable for at least 11 days of storage. The increase of FPI concentration led to a higher stability of the FPI emulsions, due to increased viscosity at higher concentration (0.7% w/v). However, WPI-FPI emulsions showed a smaller droplet size and were more unstable at this FPI concentration, maybe due to the presence of flaxseed gum in the protein. An emulsion in destabilization process was observed at lower concentration (0.14% w/v) in the FPI systems, while at higher concentrations there was gelation and an excess protein, which was confirmed by the saturation of the droplets interface. In the mixed systems (0.14 or 0.7% (w/v) FPI) excess protein was also verified. However, the increase of FPI concentration led to a greater surface protein content, except at higher homogenization pressure and protein concentration (0.7% (w/v), 60 MPa, two passes), which showed a reduction due to the higher surface area. The rheological behavior of the bottom phase of the WPI-FPI emulsions was also influenced by the FPI concentration. A shear thinning behavior was observed at 0.14% (w/v) FPI and a Newtonian behavior was found at 0.7% (w/v) FPI. On the other hand, FPI emulsions were not influenced by the protein concentration and exhibited a shear thinning and thixotropic behavior. Increasing homogenization conditions (pressure and number of passes), the stability of the FPI systems increased, mainly at higher concentration (0.7% w/v). Meanwhile, in the mixed systems, the stability of the emulsions containing 0.7% (w/v) FPI decreased even more, but was improved for the emulsions with 0.14% (w/v) FPI. A higher viscosity and pseudoplasticity was observed for the top cream phase of the WPI-FPI emulsions in more drastic process conditions, while the top phase of the FPI emulsions showed lower pseudoplasticity with increasing number of passes. WPI stable emulsions showed a smaller droplet size at higher pressure and number of passes, and the reduction in the mean droplet diameter of the WPI-FPI unstable emulsions was mainly influenced by the increase in the number of passes through the homogenizer.

Keywords: O/W emulsions; High-pressure homogenization; Whey protein; Flaxseed protein isolate; Stability; Rheology.

4.1. INTRODUCTION

Many food products are partially or fully composed by emulsions, as for example, mayonnaise, ice cream, milk, butter, cheese, soups, beverages, and the most common form of emulsions in foods is oil-in-water (O/W) (McClements, 2005; Waraho, McClements, &

Decker, 2011). Traditionally, the high-pressure homogenization of the oil and aqueous phases in the presence of one or more emulsifiers is used to produce O/W emulsions (Guzey & McClements, 2006). Proteins are used as emulsifiers because of their amphiphilic character, which facilitates the emulsion formation, improves its stability and produces desirable physicochemical properties (McClements, 2004). Proteins can adsorb on the surfaces of freshly formed oil droplets during homogenization, reducing the interfacial tension and forming a membrane around the droplets in order to protect them from aggregation by generating repulsive interactions (Guzey & McClements, 2006; McClements, 2005).

Whey proteins have been widely used in food products due to their high nutritional value and excellent technological properties, such as the emulsifying properties (Morr & Ha, 1993). Due to its amphiphilic character, whey protein isolate (WPI) can provide protection to the oil droplets through a combination of electrostatic and steric interactions, stabilizing the emulsions against flocculation and/or coalescence (Sun & Gunasekaran, 2009; Taherian, Britten, Sabik, & Fustier, 2011).

Flaxseed proteins have received attention for their health benefits (Rabetafika, Remoortel, Danthine, Paquot, & Blecker, 2011), but also show interesting technological properties, such as greater capacity to absorb water and oil and improved emulsifying and stabilizing activity, if compared with soybean protein isolate (Dev & Quensel, 1986). Flaxseed proteins consist of two major fractions, one salt-soluble with high molecular weight (11-12S) and another water-soluble with low molecular weight (1.6-2S) (Chung Chung, Lei, & Li-Chan, 2005; Madhusudhan & Singh, 1985a,b; Marcone, Kakuda, & Yada, 1998; Youle & Huang, 1981). Hydrophilic properties of flaxseed proteins are influenced by the presence of polysaccharide gums (Dev & Quensel, 1988; Oomah &

Mazza, 1993), which can also interfere with the settling and isolation of the protein (Oomah & Mazza, 1993; Smith, Johnsen, & Beckel, 1946). Emulsifying properties of flaxseed proteins have been evaluated in pure and mixed systems (Karaca, Low, & Nickerson, 2011; Krause, Schultz, & Dudek, 2002; Martínez-Flores et al., 2006; Wanasundara & Shahidi, 1997; Wang, Li, Wang, Adhikari, & Shi, 2010; Wang, Li, Wang, & Özkan, 2010; Wang, Wang, Li, Adhikari, & Shi, 2011). Wang et al. (2011) found that the gum Arabic addition (up to 2% w/w) improved the stability of oil-in-water emulsions stabilized by flaxseed protein concentrate (FPC), by increasing the emulsion viscosity. In a similar way, Wang et al. (2010a) observed higher stability of soybean oil-in-water emulsions with increasing FPC concentration. However, in our knowledge, there are no published works related to whey protein isolate – flaxseed protein isolate emulsions.

Therefore, the objective of this work was to evaluate the potential use of flaxseed protein isolate as an emulsifier agent and its interaction with WPI. Systems containing whey protein, flaxseed protein or mixed whey protein – flaxseed protein were prepared under high pressure homogenization (20, 40 or 60 MPa) with one or two passes through the homogenizer. Interfacial tension and emulsions properties such as creaming stability, droplet size, microscopy, rheology and protein load were analyzed, in order to characterize and find a better stability condition for these systems.

4.2. MATERIAL AND METHODS

4.2.1. Material

The whey protein isolate (WPI) was obtained from New Zealand Milk Products (ALACEN 895, New Zealand) and the flaxseed protein isolate (FPI) was extracted from partially defatted flaxseed meal (Cisbra, Panambi, RS, Brazil), according to methodology described by Silva, O'Callagahan, O'Brien, and Netto (2013). Flaxseed oil was purchased from Cisbra (Panambi, RS, Brazil), showing the following fatty acids composition: 6.2% C16:0, 5.3% C18:0, 20.1% C18:1, 13.7% C18:2 and 52.3% C18:3 (provided by Cisbra). The protein concentration, determined by the Kjeldahl procedure (AOAC, 1997), lipids (Bligh & Dyer, 1959), moisture (AOAC, 1997), ashes (AOAC, 1997) and carbohydrates content (% w/w, wet basis) of the WPI were 87.66 ± 0.91% (N x 6.38), 0.36 ± 0.02%, 4.54 ± 0.11%, 1.36 ± 0.07% and 6.08% (by difference), respectively, and of the FPI were 68.53 ± 0.33% (N x 6.25), 3.07 ± 0.11%, 8.81 ± 0.02%, 1.23 ± 0.03% and 16.20 ± 0.29% (Total dietary fiber – AOAC, 2005), respectively. All other reagents were of analytical grade.

4.2.2. Characterization of the WPI and the FPI

4.2.2.1. Zeta potential

The pH dependence of the zeta potential of WPI (0.5% w/v), FPI (0.5% w/v) and WPI-FPI (0.5%-0.5% w/v) dispersed in deionized water was measured using a Zetasizer Nano-ZS (Malvern Instruments Ltd., Worcestershire, UK) equipment. Titration curves from pH 7.0 to 2.0 by adding 0.25 M NaOH or HCl were performed, in triplicate, at 25 °C.

4.2.2.2. Fourier transform infrared spectroscopy (FTIR)

A spectrophotometer Model Spectrum One (Perkin Elmer, Ohio, USA) with Fourier transform and provided with a Universal Attenuated Total Reflectance (UATR) accessory was used to characterize the flaxseed protein isolate (FPI). Automatic signals were collected in 16 scans and the measurement range was 4000-650 cm^{-1}, at resolution of 4 cm^{-1}

(Vicentini, Dupuy, Leitzelman, Cereda, & Sobral, 2005). The software Spectrum One B (version 5.31) was used to analyze the results.

4.2.3. Preparation of the WPI and the FPI stock solutions

The WPI (10% w/v) and the FPI (2% w/v) stock solutions were prepared by dissolution of the powders in deionized water with magnetic stirring for 90 and 120 min, respectively, at room temperature (25 °C). The pH of the solutions was then adjusted to 7.0 ± 0.3 using 10.0 M NaOH. The solutions were kept overnight at 10 °C to allow complete protein dissolution.

4.2.4. Preparation of the emulsions

Oil-in-water (O/W) emulsions were prepared at 25 °C by homogenizing the oil in the aqueous phase using two sequential homogenization methods. The first method involved mixing the solutions in an Ultra Turrax model T18 homogenizer (IKA, Germany) for 4 min at 14,000 rpm. The second method involved subjecting the previously prepared macroemulsion to a high-pressure homogenization process using a Panda 2K NS1001L double stage homogenizer (Niro Soavi, Italy). The pressure in the first stage was 20, 40 or 60 MPa and in the second stage was fixed at 5 MPa. Samples were subjected to one or two passes through the homogenizer. Three types of emulsions were evaluated, containing only WPI or FPI and a mixture of WPI-FPI, according to described in Table 4.1. Small FPI concentrations were chosen because a high viscosity was observed in the FPI emulsions containing 0.7% (w/v). Such high viscosity was attributed to the presence of flaxseed gum (soluble fiber) that was not removed during the protein extraction process. Sodium azide

(0.02% w/v) was added to the emulsions for microbial growth prevention and the pH was adjusted to 7.0 ± 0.1 using 0.1 M NaOH and/or HCl.

Table 4.1. Composition of the O/W emulsions evaluated.

Emulsion	Flaxseed oil (% v/v)	WPI (% w/v)	FPI (% w/v)
WPI	30	3	-
FPI	30	-	0.14, 0.35 or 0.7
WPI-FPI	30	3	0.14 or 0.7

4.2.5. Characterization of the O/W emulsions

4.2.5.1. Interfacial tension

The interfacial tension between water and oil phase using the same composition of the emulsions (% w/v) was measured using a tensiometer Tracker-S (Teclis, Longessaigne, France), by the pendant (W/O) and rising (O/W) drop method. The measurements were performed at 25 ± 1 °C with the formation of an oil droplet in the aqueous phase (3% WPI and 0.14% FPI solutions) or a droplet of the aqueous phase in the oil phase (0.35 and 0.7% FPI solutions and 3% WPI – 0.14 or 0.7% FPI solutions). Drop volume was 3 μL for FPI (0.35 and 0.7%) or mixed WPI-FPI (3% – 0.7%) systems and 4 μL for WPI (3%), FPI (0.14%) or mixed WPI-FPI (3% – 0.14%) systems.

4.2.5.2. Creaming stability

Immediately after preparation, 25 mL of each emulsion were poured into a cylindrical glass tube (internal diameter = 17 mm, height = 105 mm), sealed with a plastic cap and stored at 25 °C. The WPI emulsions were stored for a period of 11 days and the

FPI and WPI-FPI emulsions were stored up to reach kinetic equilibrium (11 and 14 days, respectively). The emulsion stability was measured by the change in height of the bottom serum phase (H) along storage time. The creaming index (CI) was determined according to Eq. (4.1) (Keowmaneechai & McClements, 2002).

$$CI\ (\%) = (H/H_0) \times 100 \tag{4.1}$$

where H_0 represents the initial height of the emulsion. To facilitate visualization of the phase separation, Sudam III (reddish dye) was added to the flaxseed oil. The analyses were carried out in duplicate.

4.2.5.3. Optical and fluorescence microscopy

The microstructure of the emulsions was evaluated by optical microscopy (WPI emulsions) after 1 day and by fluorescence microscopy (FPI and WPI-FPI emulsions) after 14 days of storage (steady state conditions). The emulsions were poured onto microscope slides, covered with glass cover slips and observed using a Carl Zeiss Model Axio Scope.A1 optical microscope (Zeiss, Germany), with a 100 x objective lens, and an Olympus BX51 epifluorescence microscope (Olympus, Japan), with a digital camera DP72, and objective lenses of 10 x for the FPI emulsions and of 80 x for the WPI-FPI emulsions. For the fluorescence microscopy, Rhodamine B was added to the protein solutions in order to label the molecules and images were collected using filter excitation/emission of 480-590/590 nm.

4.2.5.4. Particle size distribution

A Mastersizer 2000 (Malvern Instruments Ltd., Worcestershire, UK) was used to determine the particle size distribution of the emulsions. Samples were dispersed in distilled water (~0.03-0.06% v/v) prior to measurements. The size of the oil droplets was expressed as the volume-surface mean diameter (d_{32}) and the dispersion index (span) was also reported (Jafari, He, & Bhandari, 2007), according to Eqs. (4.2) and (4.3), respectively. The WPI and WPI-FPI emulsions were analyzed 1 and 14 days after their preparation, respectively, and each sample was measured in triplicate.

$$d_{32} = \sum n_i d_i^3 \Big/ \sum n_i d_i^2 \tag{4.2}$$

$$Span = \left(d_{90} - d_{10}\right)/d_{50} \tag{4.3}$$

where n_i is the number of droplets with diameter d_i, and d_{10}, d_{50} and d_{90} are diameters at 10, 50 and 90% of cumulative volume, respectively.

4.2.5.5. Rheological measurements

The rheological measurements were carried out using a Physica MCR301 modular compact rheometer (Anton Paar, Austria). A stainless steel plate geometry (75 mm) and a 0.6 mm gap was used to analyze the WPI-FPI emulsions. For the top cream and bottom serum phases of the FPI emulsions, a stainless steel plate geometry (50 and 75 mm) and a 0.5 and 0.4 mm gap were used, respectively. The emulsions were evaluated after 14 days of storage and the measurements were made in triplicate at 25 °C. Flow curves were obtained using an *up-down-up* steps program with the shear rate varying between 0 and 300 s^{-1}, in order to evaluate the thixotropy. The shear time-dependence (thixotropic behavior) was estimated using the area between the curves S_1 and S_2 (first and last shear cycle, respectively) (hysteresis) (Perrechil, Santana, Fasolin, Silva, & Cunha, 2010; Sato & Cunha, 2007; Steffe, 1996). The third flow curve data were fitted to the models for Newtonian (Eq. (4.4)) and shear-thinning fluids (Power law model) (Eq. (4.5)).

$$\sigma = \eta . \dot{\gamma} \tag{4.4}$$

$$\sigma = k . \left(\dot{\gamma} \right)^{n} \tag{4.5}$$

where σ is the shear stress (Pa), $\dot{\gamma}$ is the shear rate (s^{-1}), k is the consistency index ($Pa.s^{n}$) and n is the flow behavior index (dimensionless).

4.2.5.6. Protein load

The protein load (PL) is the total protein (mg) adsorbed on the oil (g) of the top cream phase. It was determined according to adapted methodology from Girard, Turgeon, and Paquin (2002). The FPI emulsions were centrifuged (15,317 x g, 45 min, 20 °C) using a temperature-controlled centrifuge model Allegra 25 – R (Beckman Coulter, Fullerton, USA). The bottom serum phase was collected, weighed and the mass of the top cream phase was determined by difference. The protein content of separated phases was determined by Kjeldahl method (AOAC, 1997) and the protein load was calculated according to Eq. (4.6).

$$\mathrm{PL} = \frac{(\mathrm{PCP}) \times (\mathrm{MCP})}{(\mathrm{OP}) \times (\mathrm{EM})} \tag{4.6}$$

where PCP and MCP correspond to the protein concentration (%) and the total mass (g) of cream phase after centrifugation, respectively, OP the oil concentration in the initial emulsion (30% v/v) and EM the emulsion mass (g).

The surface protein concentration (SPC) (mg/m^2) of the WPI-FPI emulsions was calculated as the ratio of the protein content (mg/g of emulsion) in the top cream phase (PCP) to the surface area (m^2/g of sample) of the oil droplets, determined from the particle size distribution analysis (section 4.2.5.4), according to Eq. (4.7).

$$\text{SPC}\left(\text{mg}/\text{m}^2\right) = \frac{\text{PCP}}{\text{Surface area}} \tag{4.7}$$

All the emulsions were analyzed 1 day after their preparation.

4.2.6. Statistical analysis

The results were evaluated by analysis of variance (ANOVA), and significant differences ($p<0.05$) between the treatments were evaluated by the Tukey's procedure. The statistical analyses were carried out using the software STATISTICA 6.0 (Statisoft Inc., Tulsa, USA).

4.3. RESULTS AND DISCUSSION

4.3.1. Characterization of the biopolymers

Zeta potential of the biopolymers could help to predict the destabilization mechanisms of the emulsions (flocculation and coalescence), since interfaces electrically charged exert positive influence on the emulsions stability (Bouyer, Mekhloufi, Rosilio, Grossiord, & Agnely, 2012; Gharsallaoui et al., 2010).

The pH dependence of the zeta potential of the aqueous solutions of whey protein (WPI), flaxseed protein isolate (FPI) and whey protein-flaxseed protein isolate (WPI-FPI) was determined (Fig. 4.1). Aqueous solution of WPI (0.5% w/v) showed a zeta potential which changed from a negative (-24.2 mV) to a positive value (+21.7 mV) when pH was lowered from 7.0 to 2.0. The isoelectric point (pI) of whey protein isolate was around pH 4.8, close to the reported in the literature for the main fractions of whey protein (α-La, pI 4.8-5.1 and β-Lg, pI 5.2) (Bryant & McClements, 1998).

For aqueous solution of FPI (0.5% w/v), the zeta potential varied from a negative value (-47.8 mV) to a slightly positive value (+6.7 mV) when the pH was lowered from 7.0 to 2.0, and the pI of the protein was near pH 4.2, which is in agreement with the reported in literature (Wang et al., 2010a). The wide pH range in which the zeta potential was close to zero (4.2 to 2.7) could be a consequence of the presence of gum (16.20 ± 0.29% of total dietary fiber).

The zeta potential of the aqueous solution containing whey protein and flaxseed protein isolate (WPI-FPI) (0.5%-0.5% w/v) showed a pH-dependence similar to the aqueous solution of FPI, but the charge density was near zero at pH around pI of the WPI. Since at pH 7.0 the aqueous solutions of WPI, FPI and WPI-FPI showed a zeta potential value between -25 mV and -45 mV, this pH condition was considered adequate to prepare the emulsions in order to keep an enhanced stability.

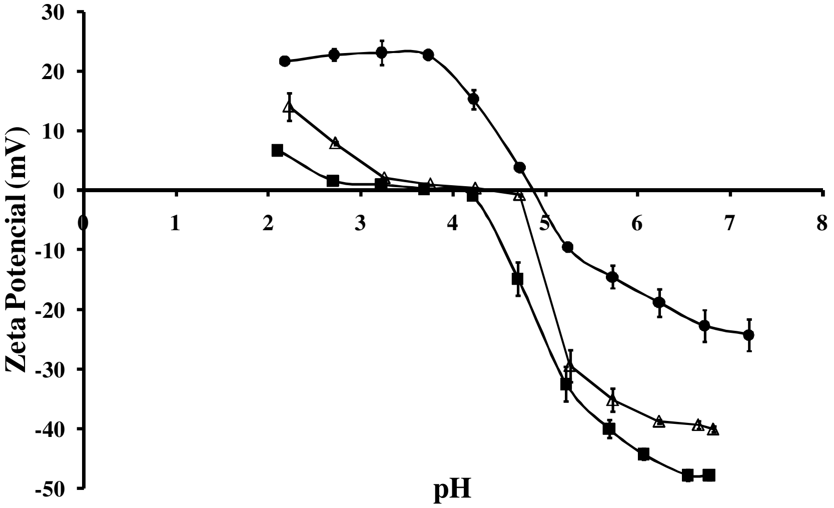

Fig. 4.1. pH-dependence of zeta potential for aqueous solutions of (●) WPI, (■) FPI and (△) WPI-FPI.

The frequency of light and the corresponding absorbed energy in the infrared region by a sample allows identifying its constituent molecules. Fig. 4.2 shows the FTIR spectrum for flaxseed protein isolate (FPI). One peak was obtained at a wavelength near 3280 cm^{-1}, whereas the region 3600-2500 cm^{-1} is associated with O-H stretching absorption due to inter- and intramolecular hydrogen bonds (Gnanasambandam & Proctor, 2000). A second smaller peak, superimposed upon the broader O-H band, was found at 2934 cm^{-1}, similar to the observed by Gnanasambandam and Proctor (2000) for pectin samples. Bands around 2950 cm^{-1} (3000-2800 cm^{-1}) refer to C-H absorption, including C-H, $C\text{-}H_2$ and $C\text{-}H_3$ stretching and bending vibrations (Gnanasambandam & Proctor, 2000).

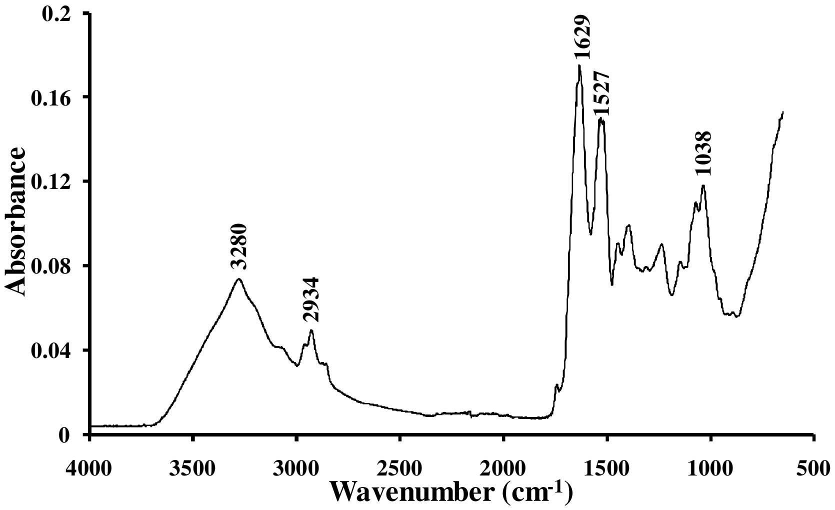

Fig. 4.2. FTIR spectrum of flaxseed protein isolate (FPI).

The peak at 1629 cm^{-1} corresponds to amide I band (~1620-1700 cm^{-1}), which arises predominantly from the C=O stretching vibration of the amide C=O group, and its vibrational frequency can be used to predict protein secondary structure (Yu, McKinnon, Soita, Christensen, & Christensen, 2005). For α-helix, the amide I lies in the range between 1648-1658 cm^{-1} and for β-sheet, the peak can be found within the range of 1620-1640 cm^{-1} (Yu et al., 2005). Thus, it may be suggested that there is a predominance of β-sheet structure in the FPI. Indeed Yu et al. (2005) found that the brown flaxseed contained relatively higher content of β-sheet (46.3%) as compared to α-helix (36.9%). The peak found at 1527 cm^{-1} belongs to the amide II band (~1500-1560 cm^{-1}), corresponding mainly to N-H bending vibration (60%) coupled to C-N stretching (40%). This peak can be also used to evaluate protein conformation, but is less useful because it arises from complex vibrations involving multiple functional groups (Yu et al., 2005).

Carbohydrates are composed of sugars containing C-C, O-H and C-O bonds (Yu et al., 2005). Depending on the linkage and type of sugar, the carbohydrates band can be placed between 1180-950 cm^{-1} (Yu et al., 2005), region in which was observed the peak 1038 cm^{-1}. Thus, this peak could be associated with the non-removed flaxseed gum present in the FPI (16.20 ± 0.29% of total dietary fiber).

4.3.2. Characterization of the emulsions

The interfacial tension between aqueous and oil phases was measured and the results are shown in Fig. 4.3. The initial interfacial tension was around 9.8 mN/m for WPI system and decreased from 10.9 to 9 mN/m in the FPI systems with the increase of FPI concentration from 0.14 to 0.7% (w/v). Nonetheless, for both systems, the interfacial tension decreased with time, reaching values around 1.5-2.5 mN/m under steady state. The initial interfacial tension at water–flaxseed oil interface was slightly lower (8.1-8.7 mN/m) for the mixed systems. However, the systems containing only FPI (0.35 or 0.7% w/v) took less time (2700-3300 s) to reach interfacial tension equilibrium (~1.4 mN/m) than the systems with WPI-FPI (4800-7300 s). Therefore, the drop formation and protein adsorption at the interface occurred more readily in mixed systems (lowest initial interfacial tension), which could be indicating a higher surface activity of these systems. The longest time to rearrange and reach equilibrium could be associated with the increased complexity of the mixed system. Oilseed proteins (canola and flaxseed) can be slightly more effective in reduction of the interfacial tension when compared with WPI (Karaca et al., 2011), which is in agreement with our results.

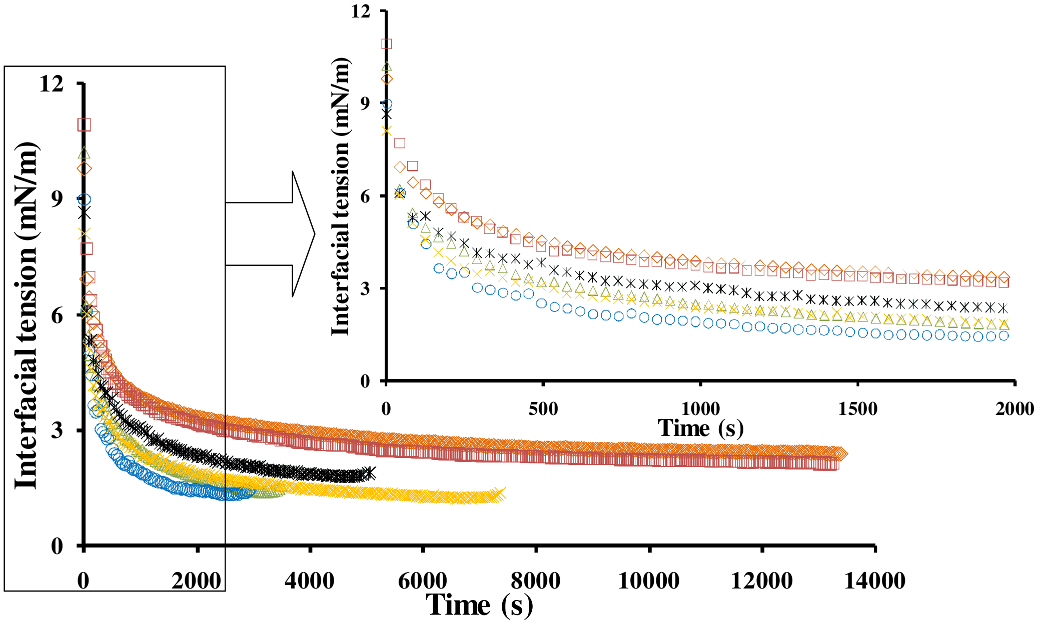

Fig. 4.3. Interfacial tension (mN/m) between flaxseed oil and protein in the WPI (3% w/v) (◇), FPI (0.14 (□), 0.35 (△) or 0.7% (w/v) (○)) and WPI-FPI (3% (w/v) - 0.14% (w/v) (✳) or 3% (w/v) - 0.7% (w/v) (×)) systems.

4.3.2.1. WPI emulsions

Emulsions stabilized by WPI showed no phase separation during 11 days of storage. Increasing homogenization pressure and the number of passes, a reduction in droplet size was observed, as can be seen in Fig. 4.4, in a similar way to that observed in a previous study (Kuhn & Cunha, 2012).

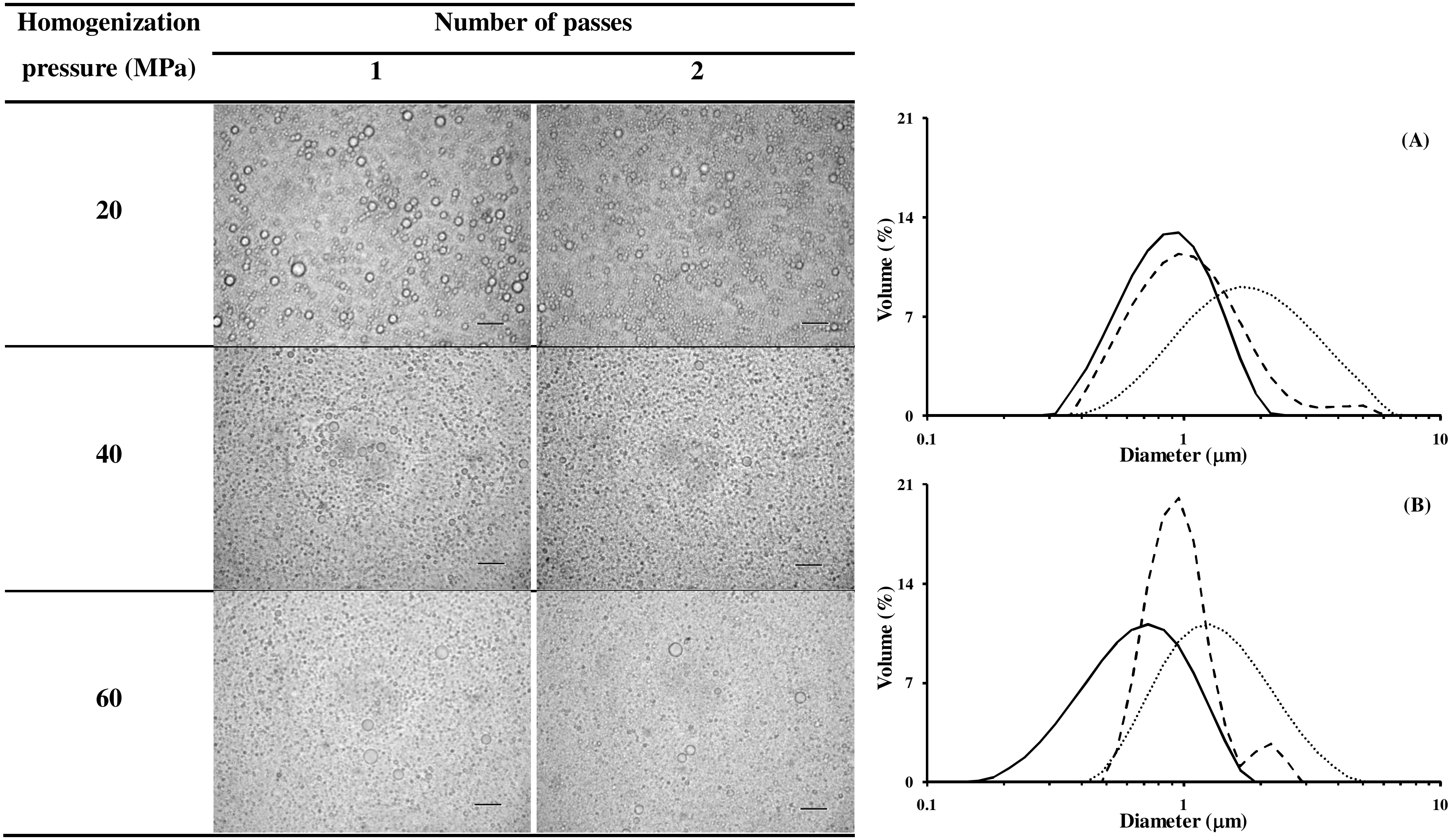

Fig. 4.4. Microstructure and particle size distribution of the O/W emulsions containing 3% (w/v) WPI and 30% (v/v) flaxseed oil, homogenized at (·····) 20, (– –) 40 and (——) 60 MPa, with (A) one or (B) two passes through the homogenizer. Scale bar = 10 µm.

In general, higher homogenization conditions (pressure and number of passes) led to a decrease in the mean droplet diameter and the distribution width (span) (Table 4.2). However, the span values (dispersion index) increased ($p<0.05$) in the extreme energy condition (60 MPa, two passes), which could be a consequence of increase in volume of smaller droplets. In this condition, a significant increase ($p<0.05$) in apparent viscosity of the emulsions (η_{100}) was also observed (Kuhn & Cunha, 2012).

Table 4.2. Mean droplet diameter (d_{32}) and span of the WPI emulsions (3% w/v).

Homogenization pressure (MPa)	**Number of passes**			
	1		**2**	
	d_{32} (μm)	**Span**	**d_{32} (μm)**	**Span**
20	1.60 ± 0.01^{aA}	1.62 ± 0.02^{aA}	1.30 ± 0.08^{aB}	1.33 ± 0.01^{aB}
40	0.88 ± 0.01^{bA}	1.32 ± 0.03^{bA}	0.87 ± 0.00^{bA}	0.77 ± 0.02^{cB}
60	0.74 ± 0.00^{cA}	1.05 ± 0.00^{cB}	0.54 ± 0.01^{cB}	1.23 ± 0.01^{bA}

Different letters indicate significant differences ($p<0.05$). Small letters: differences in the same column. Capital letters: differences in the same line.

The temperature of the O/W emulsions stabilized by WPI (3% w/v) was measured at the exit of the homogenizer after each pressure and pass. The maximum temperatures, 38 and 40 °C, were observed at pressure of 60 MPa, after one and two passes through the homogenizer, respectively. However, these values were below the denaturation temperature (T_d) of the whey proteins (β-Lg, T_d = 78 °C and α-La, T_d = 62 °C) (Bryant & McClements, 1998), indicating that no thermal denaturation would have occured.

From these results, the pressures of 40 and 60 MPa, with one and two passes through the homogenizer, were chosen to prepare the O/W emulsions in the following steps, since the emulsions homogenized at 20 MPa showed much higher droplet size.

4.3.2.2. FPI emulsions

All the emulsions stabilized by FPI (0.14, 0.35 or 0.7% w/v) showed kinetic instability, forming a bottom serum phase and a top cream phase. The creaming index (CI) of these emulsions with the storage time is presented in Fig. 4.5. Emulsions stabilized with lower FPI concentration (0.14% w/v) were the least stable, exhibiting the highest equilibrium creaming index, about 40% after 24 h, regardless of pressure and the number of passes through the homogenizer. An increase in homogenization pressure and/or the number of passes exerted little influence on the CI of the emulsions containing 0.35% (w/v) FPI (similar CI at equilibrium). However, the separation kinetics of the emulsions was different. Emulsions homogenized at 40 and 60 MPa, with one pass through homogenizer, destabilized only after 1 and 6 days of storage, respectively. At higher FPI concentration (0.7% w/v), a decrease in the CI was observed with increasing homogenization pressure and/or the number of passes. Moreover, there was a clear increase in viscosity of the emulsions, leading to a greater stability (CI ~ 1.5%), mainly when homogenized at 60 MPa and two passes through homogenizer. Regardless of the method of protein isolate production (isoelectric precipitation or salt extraction), Karaca et al. (2011) also found a phase separation in the emulsions containing higher flax protein isolate concentration (1% w/w) and lower flaxseed oil content (20% w/w) than it was evaluated in our work.

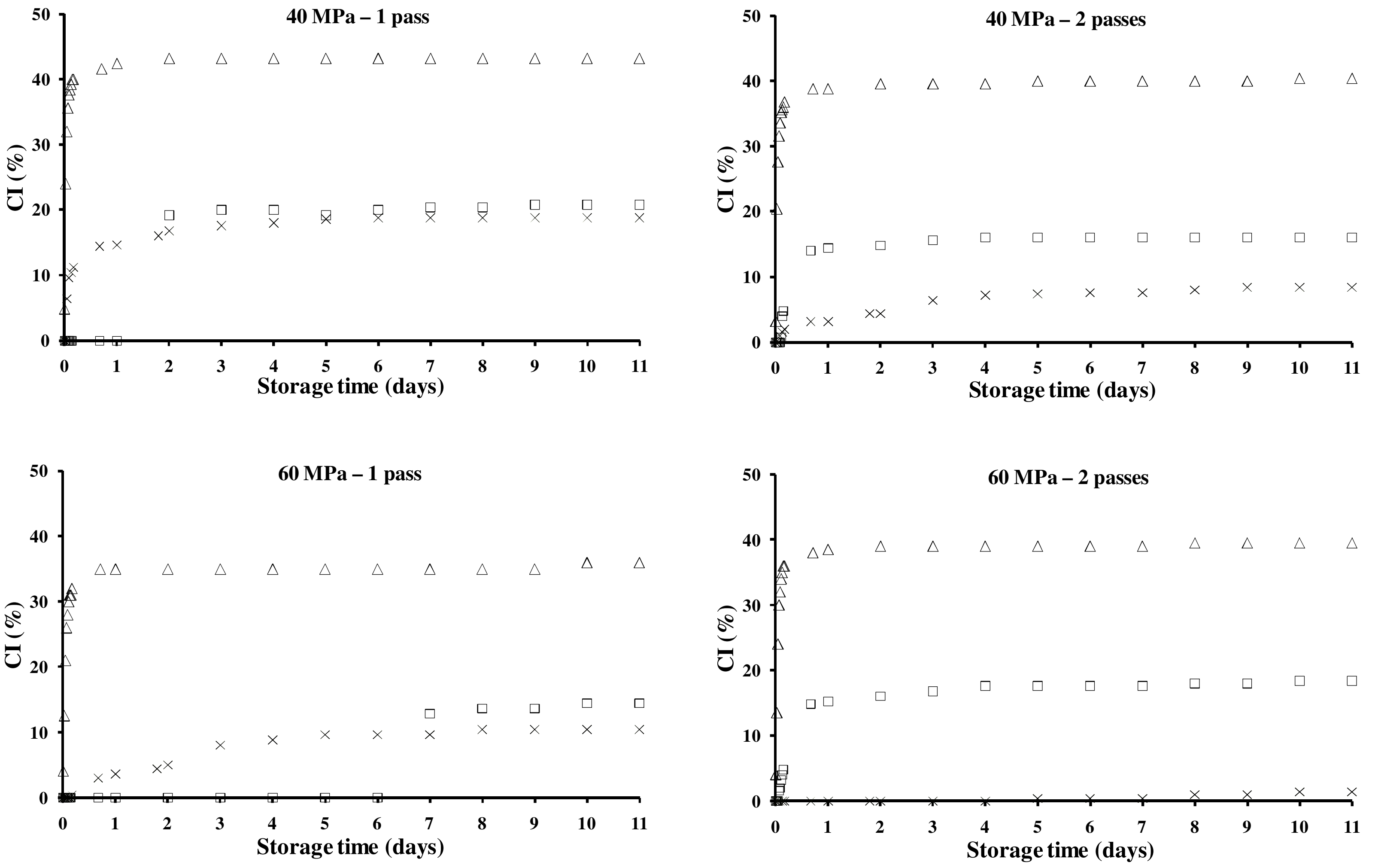

Fig. 4.5. Effect of flaxseed protein isolate (FPI) concentration on the creaming index (CI) of the O/W emulsions homogenized at 40 or 60 MPa, with one or two passes through the homogenizer. FPI concentration: (Δ) 0.14, (□) 0.35 or (X) 0.7% (w/v).

The structure of the emulsions stabilized by different FPI concentrations was assessed by fluorescence microscopy and the images are presented in Fig. 4.6, under white (top) and fluorescent light (bottom). An emulsion in destabilization process was observed at lowest FPI concentration (0.14% w/v). While that, at 0.35% (w/v) FPI, an emulsion with an onset of gelation was visualized, and at highest FPI concentration (0.7% w/v), there was complete gelation. Moreover, at higher FPI concentrations (0.35 or 0.7% w/v), an excess protein was observed on the microscopy of the cream phase of the emulsions. It was evidenced by the lighter regions in images under fluorescent light, since Rhodamine B dye was used to stain the protein molecules. Homogenization pressure and the number of passes through the homogenizer did not exert influence on the droplet size of the emulsions.

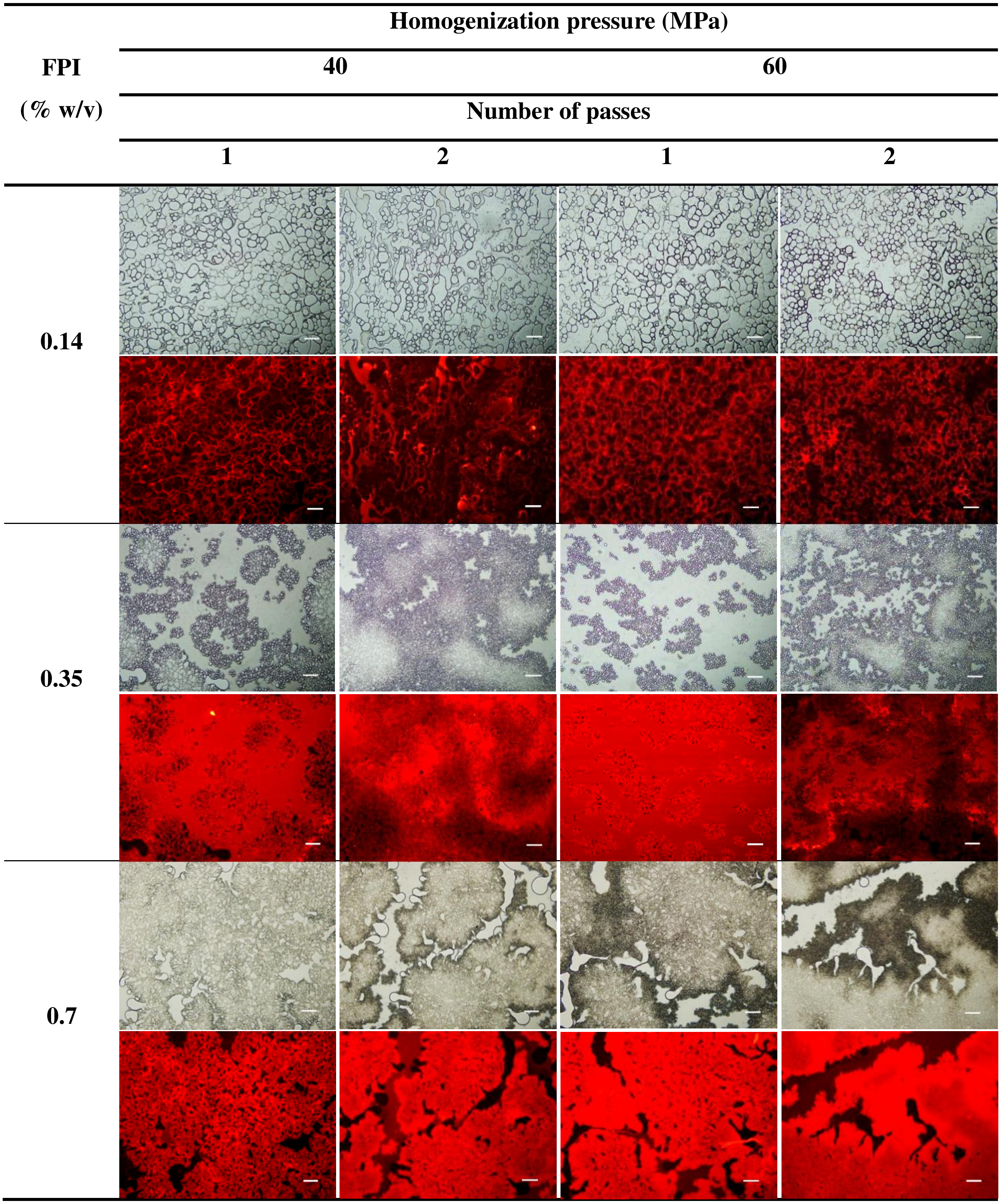
Homogenization pressure (MPa)
FPI
(% w/v)
40
60
Number of passes
1
2
1
2
0.14
0.35
0.7

Fig. 4.6. Microstructures of the top cream phase of the O/W emulsions containing 0.14, 0.35 or 0.7% (w/v) FPI and 30% (v/v) flaxseed oil. Scale bar = 100 μm.

The flow curves of the top phase of the emulsions were fitted to the power law model ($R^2 > 0.996$) and the bottom phase to the Newtonian model ($R^2 > 0.973$). The rheological parameters are presented in Table 4.3. The apparent viscosity at a low shear rate (3 s^{-1}) was analyzed in order to evaluate the viscosity under conditions similar to storage (stability). In general, an increase in the number of passes and/or the FPI concentration led to a significant increase ($p<0.05$) in the flow behavior index (n), as well as a decrease in the consistency index (k) and in the apparent viscosity of the top phase of the emulsions. The viscosity of the bottom phase of the emulsions usually was not significantly influenced by pressure and number of passes through the homogenizer. At lower FPI concentration (0.14% w/v), this phase showed a viscosity similar to water, but the increase of protein concentration led to a higher viscosity ($p<0.05$).

Table 4.3. Rheological parameters obtained from the Newtonian and the power law model and the apparent viscosity at 3 s^{-1} (η_3) for the O/W emulsions stabilized by FPI (0.14, 0.35 or 0.7% w/v).

FPI (% w/v)	**Phase**		**Homogenization pressure (MPa)**			
			40		**60**	
			Number of passes			
			1	**2**	**1**	**2**
0.14	**Top**	**n**	0.61 ± 0.02^{bC}	0.66 ± 0.01^{aC}	0.57 ± 0.01^{bC}	0.69 ± 0.01^{aC}
		k ($Pa.s^n$)	0.327 ± 0.045^{bA}	0.242 ± 0.017^{bA}	0.563 ± 0.058^{aA}	0.245 ± 0.028^{bA}
		η_3 (mPa.s)	162.67 ± 16.62^{bA}	180.67 ± 6.43^{bA}	292.00 ± 12.53^{aA}	278.00 ± 6.00^{aA}
	Bottom	**η (mPa.s)**	1.03 ± 0.02^{aC}	1.00 ± 0.02^{aC}	1.07 ± 0.06^{aC}	1.10 ± 0.06^{aC}
0.35	**Top**	**n**	0.65 ± 0.01^{cB}	0.71 ± 0.00^{bB}	0.70 ± 0.00^{bB}	0.77 ± 0.00^{aB}
		k ($Pa.s^n$)	0.221 ± 0.012^{aB}	0.146 ± 0.006^{bB}	0.237 ± 0.005^{aB}	0.141 ± 0.071^{bB}
		η_3 (mPa.s)	166.67 ± 13.61^{aA}	182.00 ± 6.00^{aA}	105.20 ± 5.91^{bB}	120.33 ± 2.08^{bB}
	Bottom	**η (mPa.s)**	1.46 ± 0.08^{aB}	1.42 ± 0.00^{abB}	1.39 ± 0.03^{abB}	1.30 ± 0.02^{bB}
0.7	**Top**	**n**	0.69 ± 0.00^{cA}	0.79 ± 0.00^{aA}	0.72 ± 0.01^{bA}	0.80 ± 0.00^{aA}
		k ($Pa.s^n$)	0.275 ± 0.016^{aAB}	0.127 ± 0.010^{cB}	0.224 ± 0.020^{bB}	0.119 ± 0.007^{cB}
		η_3 (mPa.s)	108.67 ± 3.21^{aB}	58.93 ± 2.65^{cB}	89.40 ± 5.14^{bB}	54.53 ± 1.76^{cC}
	Bottom	**η (mPa.s)**	2.29 ± 0.04^{aA}	2.25 ± 0.08^{aA}	2.28 ± 0.04^{aA}	2.06 ± 0.04^{bA}

Different letters indicate significant differences ($p<0.05$). Small letters: differences in the same line. Capital letters: differences between concentrations in the same process condition.

Fig. 4.7 shows the shear time-dependent behavior of the top phase of the emulsions. The reduction in viscosity with the shear time (reduction in shear stress value at a same shear rate), which is indicated by hysteresis between the curves S_1 and S_2, is an indication that the top cream phase of the emulsions showed thixotropic behavior.

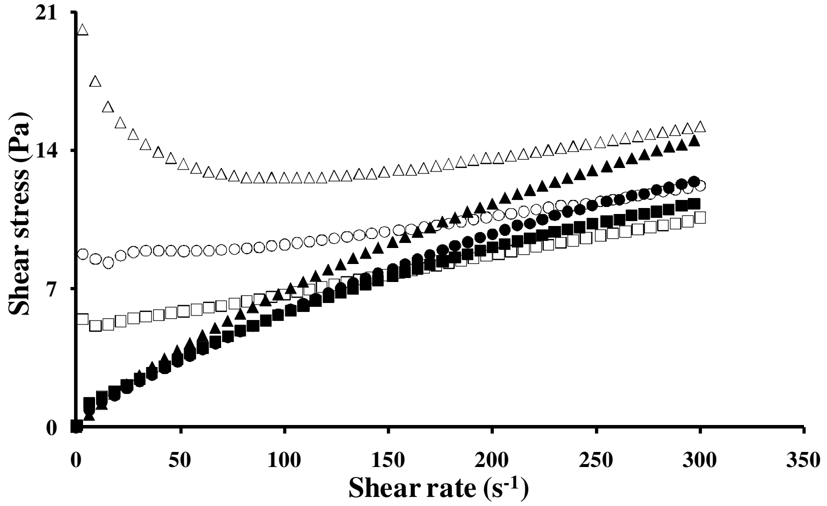

Fig. 4.7. Time-dependence of the top cream phase of the O/W emulsions containing 0.14, 0.35 or 0.7% (w/v) FPI and 30% (v/v) flaxseed oil. S_1 (open symbols): data without prior shearing and S_2 (closed symbols): data at steady state. FPI concentration: (□, ■) 0.14, (○, ●) 0.35 or (△, ▲) 0.7% (w/v).

In general, hysteresis between the curves decreased significantly ($p<0.05$) with the increase of the number of passes through the homogenizer (Table 4.4). However, the homogenization pressure did not exert a clear influence on shear time dependence. The emulsions with a higher FPI concentration (0.7% w/v) showed the highest values of thixotropy.

Table 4.4. Area between the curves corresponding to the first (S_1) and last cycle (S_2) of shear (thixotropy, Pa/s) of the emulsions stabilized by FPI (0.14, 0.35 or 0.7% w/v).

FPI (% w/v)	Homogenization pressure (MPa)			
	40		60	
	Number of passes			
	1	2	1	2
0.14	452.67 ± 11.44^{aC}	344.51 ± 12.48^{bC}	416.23 ± 16.40^{aC}	280.84 ± 14.32^{cC}
0.35	1126.93 ± 80.54^{aB}	664.78 ± 4.81^{cB}	1068.76 ± 22.04^{aB}	844.96 ± 13.02^{bB}
0.7	1387.64 ± 63.05^{aA}	1618.67 ± 17.48^{aA}	1459.97 ± 123.12^{aA}	1134.59 ± 71.37^{bA}

Different letters indicate significant differences ($p<0.05$). Small letters: differences in the same line. Capital letters: differences in the same column.

The protein load (PL) of each emulsion was calculated based on the protein concentration of the top cream phase of the emulsions stabilized by FPI (Table 4.5). For the emulsions stabilized by 0.14% (w/v) FPI, an increase in homogenization pressure or the number of passes through the homogenizer led to an increase in the amount of protein adsorbed on the surface oil droplets (top phase). Meanwhile, in the emulsions containing higher FPI concentrations (0.35 or 0.7% w/v) the interface seemed to be saturated, mainly with 0.7% (w/v), since a clear influence of the homogenization conditions on the protein load was not observed. The highest FPI concentration (0.7% w/v) led to greater amount of protein adsorbed on the oil droplets. This indicates that proteins adsorption at the oil-water interface is proportional to their concentration in the aqueous phase (Raikos, 2010; Taherian et al., 2011; Ye, 2008).

After centrifugation, three phases were observed in the emulsions containing 0.14% (w/v) FPI: serum, cream and free oil phases. This behavior could be associated with the lack of protein to cover the oil droplets, since in the emulsions stabilized by 0.35% (w/v)

FPI the amount of free oil was quite smaller and in the emulsions with 0.7% (w/v) FPI, this oil phase was not observed. Such results confirm that a higher amount of FPI would be necessary to stabilize the emulsions.

Table 4.5. Protein concentration of the top (TP) and bottom (BP) phases and protein load (PL) of the O/W emulsions containing different FPI concentrations (0.14, 0.35 or 0.7% w/v).

FPI (% w/v)	Homogenization pressure (MPa)	Number of passes	Phase after centrifugation	Protein (%)	PL$^{(*1)}$
0.14	40	1	**TP**	0.31 ± 0.00	3.14 ± 0.03
			BP	0.22 ± 0.00	
		2	**TP**	0.38 ± 0.03	3.60 ± 0.27
			BP	0.12 ± 0.02	
	60	1	**TP**	0.40 ± 0.01	4.13 ± 0.07
			BP	0.10 ± 0.02	
		2	**TP**	0.49 ± 0.00	4.52 ± 0.00
			BP	0.04 ± 0.00	
0.35	40	1	**TP**	0.62 ± 0.12	6.65 ± 1.24
			BP	0.13 ± 0.00	
		2	**TP**	0.57 ± 0.04	5.71 ± 0.41
			BP	0.10 ± 0.02	
	60	1	**TP**	0.62 ± 0.04	6.78 ± 0.44
			BP	0.14 ± 0.03	
		2	**TP**	0.65 ± 0.02	6.84 ± 0.19
			BP	0.00 ± 0.00	
0.7	40	1	**TP**	1.34 ± 0.07	15.48 ± 0.81
			BP	0.08 ± 0.00	

	2	**TP**	1.25 ± 0.04	14.70 ± 0.45
		BP	0.11 ± 0.03	
60	**1**	**TP**	1.22 ± 0.03	14.56 ± 0.32
		BP	0.10 ± 0.02	
	2	**TP**	1.24 ± 0.10	15.52 ± 1.28
		BP	0.10 ± 0.02	

(*1) In the top phase (TP).

4.3.2.3. WPI-FPI emulsions

The emulsions stabilized by WPI (3% w/v) and FPI (0.14 or 0.7% w/v), homogenized at high pressure (40 or 60 MPa), with one or two passes through the homogenizer, showed phase separation during storage. However, they separated in a different way depending on the FPI concentration. The systems with the lowest FPI concentration (0.14% w/v) showed a separation in two cream phases, with the formation of a “top cream concentrated phase” and a “bottom cream phase”. On the other hand, the emulsions containing 0.7% (w/v) FPI, exhibited a more pronounced phase separation, with a “top cream phase” and a “bottom serum phase”, as can be seen in Fig. 4.8. In the latter, the bottom aqueous phase observed could be explained by the excess protein that could not bind to the oil droplets, remaining free in aqueous solution. Moreover, the flaxseed gum present in the FPI (section 4.2.1), can bind to the water more easily, favoring phase separation.

In general, the emulsions (0.14 or 0.7% (w/v) FPI) started to destabilize at 1 day and remained almost constant after 4 days of storage. The corresponding values of the separated bottom phase of the WPI-FPI emulsions after 14 days of storage are presented in Fig. 4.8. An increase of pressure and the number of passes through the homogenizer decreased even more the stability of the emulsions containing 0.7% (w/v) FPI (increased the bottom serum phase), but led to less unstable emulsions with 0.14% (w/v) FPI (decreased the top cream concentrated phase). Such results suggest that WPI-FPI stable emulsions (with no phase separation) could be obtained if more drastic homogenization conditions (pressure and number of passes) were used, in combination with low content of FPI in mixed systems.

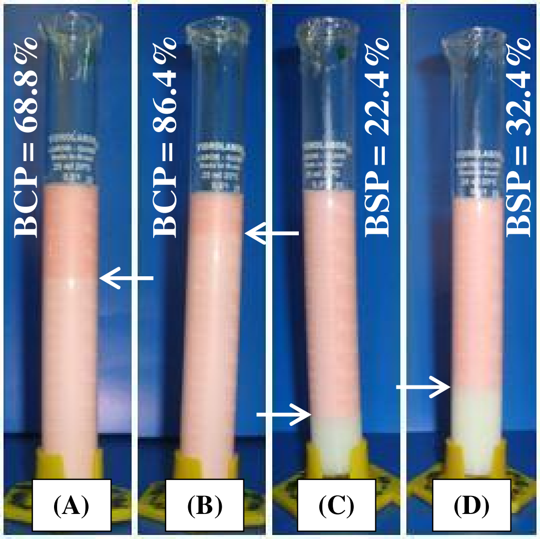

Fig. 4.8. Visual appearance and separation percentage (BCP = bottom cream phase and BSP = bottom serum phase) of the O/W emulsions containing 3% (w/v) WPI, (A, B) 0.14 or (C, D) 0.7% (w/v) FPI and 30% (v/v) flaxseed oil, homogenized at 40 MPa, with (A, C) one or (B, D) two passes through the homogenizer.

The particle size distribution of the top cream concentrated phase of the emulsions containing 0.14% (w/v) FPI was influenced only by increase of the number of passes, which led to a reduction in size and polydispersity of the droplets (Fig. 4.9A). Generally, in the top cream phase of the emulsions containing 0.7% (w/v) FPI (Fig. 4.9B), the increase of pressure and the number of passes decreased the polidispersity of the droplets. However, a bimodal distribution was observed, with an increased population of smaller droplets, in the extreme process condition (60 MPa, two passes), which could be explained by the increased viscosity that makes difficult the coalescence of the droplets. Homogenization pressure and the number of passes did not exert influence on the particle size distribution of the bottom cream phase of the emulsions containing lower FPI concentration (0.14% w/v) (Fig. 4.9A), but led to an increase in volume of smaller droplets of the bottom serum phase of the emulsions containing higher FPI concentration (0.7% w/v) (Fig. 4.9B).

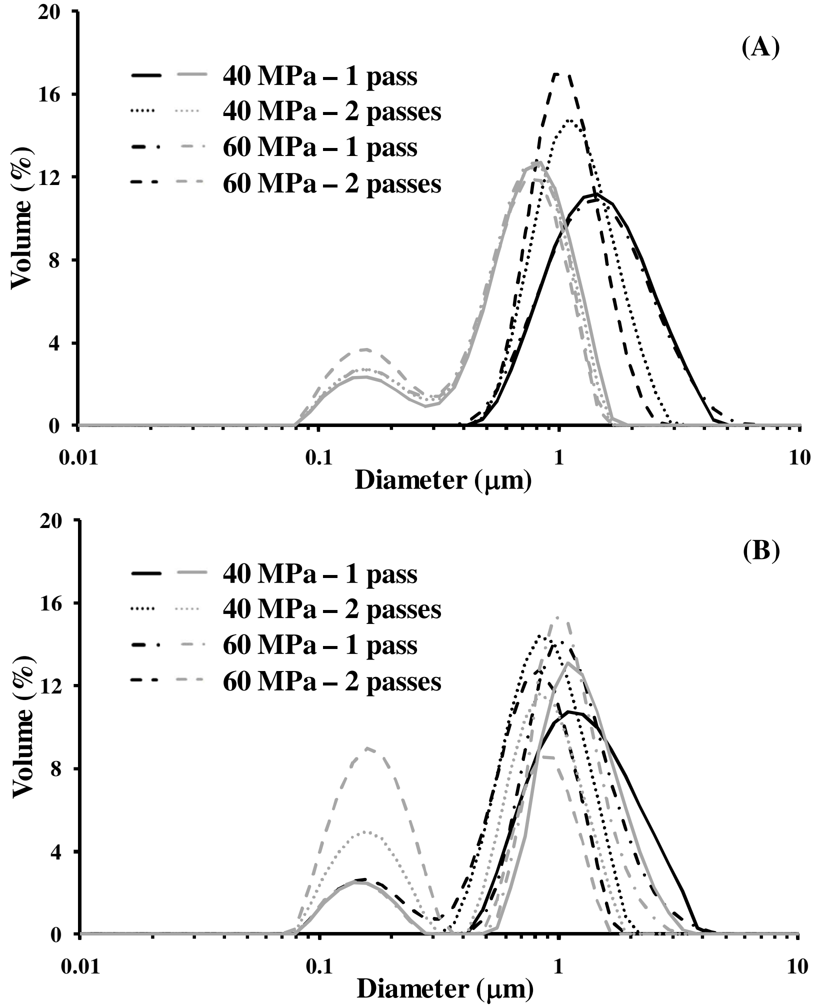

Fig. 4.9. Particle size distribution of the O/W emulsions containing 3% (w/v) WPI, (A) 0.14 or (B) 0.7% (w/v) FPI and 30% (v/v) flaxseed oil, homogenized at 40 or 60 MPa, with one or two passes through the homogenizer. Phase of the emulsion: Top (black color) and bottom (gray color) phase.

An increase in the number of passes through the homogenizer was primarily responsible for the significant reduction ($p<0.05$) in the d_{32} values (Table 4.6) of the top and bottom phases of the emulsions (0.14 or 0.7% (w/v) FPI). In addition, increasing FPI concentration also led to a significant decrease ($p<0.05$) in the mean droplet diameter, especially in the top cream phase of the emulsions. In general, the span values (dispersion index) of the bottom serum phase with 0.7% (w/v) FPI were greater ($p<0.05$), and the highest value was noticed in the extreme homogenization condition (60 MPa, two passes), similar to the observed for the WPI emulsions. This result is in agreement with the large increase in volume of smaller droplets observed in Fig. 4.9B.

Table 4.6. Mean droplet diameter (d_{32}) and span of the O/W emulsions stabilized by WPI (3% w/v) and FPI (0.14 or 0.7% w/v).

% FPI (w/v)	**Phase**		**Homogenization pressure (MPa)**			
			40		**60**	
			Number of passes			
			1	**2**	**1**	**2**
0.14	**Top**	**d_{32} (μm)**	1.41 ± 0.02^{aA}	1.15 ± 0.03^{bA}	1.37 ± 0.01^{aA}	1.07 ± 0.02^{cA}
		Span	1.26 ± 0.04^{aB}	0.99 ± 0.05^{bA}	1.35 ± 0.01^{aA}	0.88 ± 0.08^{bB}
	Bottom	**d_{32} (μm)**	0.50 ± 0.00^{aB}	0.46 ± 0.00^{bA}	0.45 ± 0.02^{bB}	0.40 ± 0.01^{cA}
		Span	1.36 ± 0.00^{bA}	1.37 ± 0.00^{bB}	1.36 ± 0.03^{bB}	1.41 ± 0.00^{aB}
0.7	**Top**	**d_{32} (μm)**	1.22 ± 0.01^{aB}	0.87 ± 0.00^{cB}	1.11 ± 0.02^{bB}	0.49 ± 0.00^{dB}
		Span	1.35 ± 0.02^{aA}	0.96 ± 0.00^{cA}	1.16 ± 0.10^{bB}	1.39 ± 0.00^{aA}
	Bottom	**d_{32} (μm)**	0.62 ± 0.02^{aA}	0.37 ± 0.03^{bB}	0.56 ± 0.04^{aA}	0.25 ± 0.01^{cB}
		Span	1.70 ± 0.30^{bA}	1.54 ± 0.04^{bA}	1.43 ± 0.03^{bA}	4.13 ± 0.20^{aA}

Different letters indicate significant differences ($p<0.05$). Small letters: differences in the same line. Capital letters: differences between concentrations in the same process condition.

The microscopic images of the top and bottom phases of the mixed emulsions (Fig. 4.10) suggest an excess protein (lighter regions under fluorescence) in both emulsions (0.14 or 0.7% (w/v) FPI). Furthermore, a decrease in droplet size with increasing FPI concentration and the number of passes through the homogenizer was observed in the top phase, in agreement to the observed in Table 4.6. But, it was not possible to observe homogenization pressure effect on the structure of the emulsions stabilized by WPI and FPI. According to the bottom cream phase microstructures (0.14% w/v FPI) (under white light), oil droplets were observed in this phase, which was expected since the phase separation of these emulsions was less drastic. However, in the emulsions containing 0.7% (w/v) FPI, practically no oil droplet was visualized in the bottom serum phase (not shown).

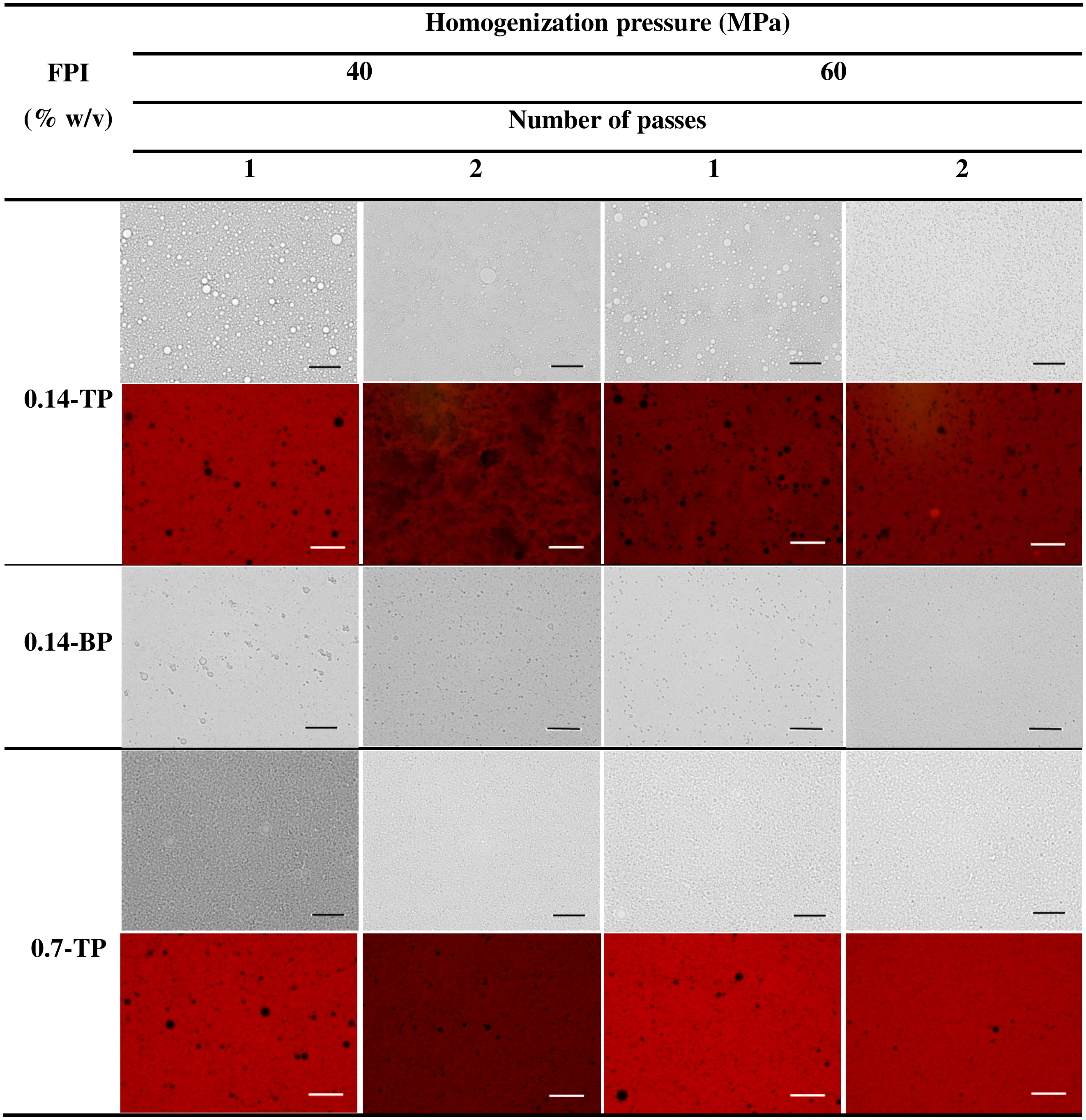
Homogenization pressure (MPa)
FPI
(% w/v)
40
60
Number of passes
1
2
1
2
0.14-TP
0.14-BP
0.7-TP

Fig. 4.10. Microstructures of the top (TP) and bottom (BP) phases of the O/W emulsions containing 3% (w/v) WPI, 0.14 or 0.7% (w/v) FPI and 30% (v/v) flaxseed oil. Scale bar = 25 µm.

The flow curves of the WPI-FPI emulsions were well-fitted ($R^2 > 0.996$) to the Newtonian and power law models (Eqs. (4.4) and (4.5), respectively). Table 4.7 shows these results as well as the apparent viscosity values at 3 s^{-1} (η_3). Separated phases of the emulsions containing 0.14% (w/v) FPI (top cream concentrated and bottom cream) showed shear thinning behavior. On the other hand, the emulsions containing 0.7% (w/v) FPI showed Newtonian and shear thinning behavior for the bottom serum and top cream phases, respectively. The increase of homogenization pressure and the number of passes led to an increase in the apparent viscosity and in the consistency index (*k*), but also led to an increase in the pseudoplasticity (lower *n*) of the top cream phases of the emulsions containing both FPI concentration (0.14 or 0.7% w/v), opposite result to that observed in the absence of WPI with increasing number of passes (Table 4.3). The bottom serum phase of the emulsions with higher FPI concentration practically was not influenced by the process conditions.

The increase of FPI concentration modified the flow behavior of the bottom phase of the emulsions from shear thinning to Newtonian. In addition, a decrease in viscosity of this phase was observed, which could be a consequence of excess oil droplets interacting and forming an emulsion packed in the top cream phase. It was also observed that at lower FPI concentration (0.14% w/v), the increase of the number of passes through the homogenizer hindered the phase separation, decreasing height of the top cream concentrated phase. Such result could be associated to the higher viscosity (Table 4.7) and lower droplets size (Table 4.6) in the bottom cream phase. According to Stokes Law, the decrease in average size of fat droplets and the increase of the continuous phase viscosity reduce the creaming velocity, enhancing the stability of the emulsions (Desrumaux &

Marcand, 2002). The highest viscosity was observed in the top cream phase of the emulsion containing 0.7% (w/v) FPI, homogenized at 60 MPa with two passes, confirming what was discussed on the particle size distribution of this condition (Fig. 4.9B).

Table 4.7. Rheological parameters obtained from the Newtonian and the power law model and the apparent viscosity at 3 s^{-1} (η_3) for the O/W emulsions stabilized by WPI (3% w/v) and FPI (0.14 or 0.7% w/v).

% FPI (w/v)	**Phase**		**Homogenization pressure (MPa)**			
			40		**60**	
			Number of passes			
			1	**2**	**1**	**2**
0.14	**Top**	**n**	0.81 ± 0.02^{aA}	IS	0.76 ± 0.02^{bA}	IS
		k (Pa.s^n)	0.027 ± 0.003^{bB}		0.141 ± 0.023^{aB}	
		η_3 (mPa.s)	37.60 ± 3.12^{bB}		144.00 ± 4.00^{aB}	
	Bottom	**n**	0.80 ± 0.04^{ab}	0.76 ± 0.03^{b}	0.85 ± 0.01^{a}	0.80 ± 0.01^{ab}
		k (Pa.s^n)	0.009 ± 0.002^{b}	0.016 ± 0.003^{a}	0.008 ± 0.001^{b}	0.014 ± 0.001^{a}
		η_3 (mPa.s)	16.05 ± 1.65^{bc}	27.60 ± 6.90^{a}	10.65 ± 0.25^{c}	24.75 ± 0.65^{ab}
0.7	**Top**	**n**	0.64 ± 0.00^{aB}	0.59 ± 0.01^{b}	0.59 ± 0.01^{bB}	0.56 ± 0.01^{c}
		k (Pa.s^n)	0.152 ± 0.007^{cA}	0.337 ± 0.014^{b}	0.315 ± 0.008^{bA}	0.684 ± 0.071^{a}
		η_3 (mPa.s)	209.33 ± 12.10^{cA}	412.00 ± 8.72^{b}	368.33 ± 9.02^{bA}	686.33 ± 30.92^{a}
	Bottom	**η (mPa.s)**	2.83 ± 0.01^{a}	2.83 ± 0.03^{a}	2.78 ± 0.01^{b}	2.77 ± 0.01^{b}

IS = insufficient sample for analysis.

Different letters indicate significant differences ($p<0.05$). Small letters: differences in the same line. Capital letters: differences between concentrations in the same process condition.

The surface protein concentration (SPC) of the WPI-FPI emulsions was determined and the results are presented in Table 4.8. The second pass through the homogenizer resulted in a reduction in the amount of protein adsorbed at the surface of the oil droplets and the increase of homogenization pressure led to a similar behavior for the emulsions containing 0.7% (w/v) FPI. At higher FPI concentration, a significant increase ($p<0.05$) on the surface protein of the emulsions homogenized at 40 MPa was observed, but at 60 MPa with two passes through the homogenizer, there was a significant reduction of the SPC, due to the much higher surface area (lower mean droplet diameter, Table 4.6). A decrease in surface concentration with increasing homogenization pressure (i.e., increasing oil surface area) may be attributed to increased spreading and rearrangement of adsorbed protein molecules at the interface (Srinivasan, Singh, & Munro, 1996).

Table 4.8. Surface protein concentration (SPC) (mg/m^2) of the O/W emulsions stabilized by WPI (3% w/v) and FPI (0.14 or 0.7% w/v).

% FPI (w/v)	Homogenization pressure (MPa)	Number of passes	Protein (%) (*1)	Surface area (m^2/g) (*1)	SPC (mg/m^2)
0.14	40	1	2.06 ± 0.06	4.25 ± 0.06	4.85 ± 0.13^{aB}
		2	2.23 ± 0.09	5.22 ± 0.12	4.28 ± 0.18^{bB}
	60	1	2.25 ± 0.15	4.39 ± 0.04	5.12 ± 0.34^{aA}
		2	2.59 ± 0.08	5.62 ± 0.09	4.61 ± 0.14^{abA}
0.7	40	1	2.96 ± 0.06	4.90 ± 0.03	6.05 ± 0.12^{aA}
		2	3.16 ± 0.02	6.89 ± 0.02	4.59 ± 0.04^{cA}
	60	1	2.91 ± 0.02	5.41 ± 0.09	5.38 ± 0.04^{bA}
		2	3.55 ± 0.04	12.23 ± 0.06	2.91 ± 0.03^{dB}

(*1) Corresponding to the top phase.

Different letters indicate significant differences ($p<0.05$). Small letters: differences in the same concentration. Capital letters: differences between concentrations in the same process condition.

4.4. CONCLUSIONS

WPI-stabilized emulsions showed good stability, while FPI- and WPI-FPI-stabilized emulsions showed phase separation and were affected by the FPI concentration and homogenization conditions (pressure and number of passes). A higher FPI content (0.7% w/v) led to a greater stability of the FPI systems as a consequence of the increased viscosity, while the mixed systems were more unstable at this concentration. The increase in pressure and the number of passes increased stability of the FPI (0.7% w/v) and WPI-FPI (0.14% w/v) emulsions, but increased the phase separation of the WPI-FPI (0.7% w/v) emulsions. Higher number of passes through the homogenizer led to a decrease in the consistency index and in the pseudoplasticity of the top phase of the emulsions stabilized by FPI, which exhibited shear thinning and thixotropic behavior. Opposite effect was observed for the WPI-FPI emulsions (top cream phase) in more drastic homogenization conditions. Mixed emulsions showed a rheological behavior dependent on the FPI concentration. Systems containing 0.14% (w/v) FPI showed only shear thinning behavior, while the emulsions with 0.7% (w/v) FPI showed Newtonian and shear thinning behavior for the bottom serum and top cream phases, respectively. Mean droplet diameter of the WPI-stabilized emulsions decreased with increasing homogenization pressure and the number of passes, while for the top cream phase of the WPI-FPI emulsions, a higher FPI concentration and number of passes were primarily responsible for its reduction. Thus, our results suggest that even though FPI was not a good emulsifier, its combination with WPI (3% w/v) improved the kinetic stability of the emulsions, using a low FPI concentration (0.14% w/v) and more drastic homogenization conditions. Therefore, a higher homogenization pressure (60 MPa) and two passes through the homogenizer should be used in order to obtain a better stability of the emulsions composed by whey and flaxseed proteins.

4.5. ACKNOWLEDGEMENTS

The authors would like to acknowledge the financial support of CNPq (140287/2009-4), CAPES and FAPESP (2011/06083-0 and EMU 09/54137-1), the donation of whey protein isolate by Professor Valdemiro Carlos Sgarbieri (DEPAN/UNICAMP) and to the Professors Gonçalo Amarante Guimarães Pereira (LGE/Institute of Biology/UNICAMP) and Paulo José do Amaral Sobral (FZEA/USP) by the Fluorescence Microscopy and FTIR analysis, respectively.

4.6. REFERENCES

AOAC. (1997). *Official methods of analysis of AOAC international.* (16th ed.). Gaithersburg, USA: Association of Official Analytical Chemists.

AOAC Method 985.29. (2005). Total dietary fiber in foods. Enzymatic-gravimetric method. In *Official Methods of Analysis of AOAC International*, (18th ed.). Gaithersburg, USA: Association of Official Analytical Chemists.

Bligh, E. G., & Dyer, W. J. (1959). A rapid method of total lipid extraction and purification. *Canadian Journal of Biochemistry*, 37(8), 911-917.

Bouyer, E., Mekhloufi, G., Rosilio, V., Grossiord, J.-L., & Agnely, F. (2012). Proteins, polysaccharides, and their complexes used as stabilizers for emulsions: Alternatives to synthetic surfactants in the pharmaceutical field? *International Journal of Pharmaceutics*, 436(1-2), 359-378.

Bryant, C. M., & McClements, D. J. (1998). Molecular basis of protein functionality with special consideration of cold-set gels derived from heat-denatured whey. *Trends in Food Science & Technology*, 9(4), 143-151.

Chung, M. W. Y., Lei, B., & Li-Chan, E. C. Y. (2005). Isolation and structural characterization of the major protein fraction from NorMan flaxseed (*Linum usitatissimum L.*). *Food Chemistry*, 90(1-2), 271–279.

Desrumaux, A., & Marcand, J. (2002). Formation of sunflower oil emulsions stabilized by whey proteins with high-pressure homogenization (up to 350 MPa): effect of pressure on emulsion characteristics. *International Journal of Food Science and Technology*, 37(3), 263-269.

Dev, D. K., & Quensel, E. (1986). Functional and microstructural characteristics of linseed (*Linum usitatissimum* L.) flour and a protein isolate. *LWT - Food Science and Technology*, 19(4), 331-337.

Dev, D. K., & Quensel, E. (1988). Preparation and functional properties of linseed protein products containing different levels of mucilage. *Journal of Food Science*, 53(6), 1834-1837.

Gharsallaoui, A., Saurel, R., Chambin, O., Cases, E., Voilley, A., & Cayot, P. (2010). Utilisation of pectin coating to enhance spray-dry stability of pea protein-stabilised oil-in-water emulsions. *Food Chemistry*, 122(2), 447-454.

Girard, M., Turgeon, S. L., & Paquin, P. (2002). Emulsifying properties of whey protein-carboxymethylcellulose complexes. *Journal of Food Science*, 67(1), 113-119.

Gnanasambandam, R., & Proctor, A. (2000). Determination of pectin degree of esterification by diffuse reflectance Fourier transform infrared spectroscopy. *Food Chemistry*, 68(3), 327-332.

Guzey, D., & McClements, D. J. (2006). Formation, stability and properties of multilayer emulsions for application in the food industry. *Advances in Colloid and Interface Science*, 128-130, 227-248.

Jafari, S. M., He, Y., & Bhandari, B. (2007). Effectiveness of encapsulating biopolymers to produce sub-micron emulsions by high energy emulsification techniques. *Food Research International*, 40(7), 862-873.

Karaca, A. C., Low, N., & Nickerson, M. (2011). Emulsifying properties of canola and flaxseed protein isolates produced by isoelectric precipitation and salt extraction. *Food Research International*, 44(9), 2991-2998.

Keowmaneechai, E., & McClements, D. J. (2002). Influence of EDTA and citrate on physicochemical properties of whey protein-stabilized oil-in-water emulsions containing $CaCl_2$. *Journal of Agricultural and Food Chemistry*, 50 (24), 7145-7153.

Krause, J.-P., Schultz, M., & Dudek, S. (2002). Effect of extraction conditions on composition, surface activity and rheological properties of protein isolates from flaxseed (*Linum usitativissimum* L). *Journal of the Science of Food and Agriculture*, 82(9), 970-976.

Kuhn, K. R., & Cunha, R. L. (2012). Flaxseed oil – Whey protein isolate emulsions: Effect of high pressure homogenization. *Journal of Food Engineering*, 111(2), 449-457.

Madhusudhan, K. T., & Singh, N. (1985a). Isolation and characterization of a small molecular weight protein of linseed meal. *Phytochemistry*, 24(11), 2507-2509.

Madhusudhan, K. T., & Singh, N. (1985b). Isolation and characterization of the major fraction (12 S) of linseed proteins. *Journal of Agricultural and Food Chemistry*, 33(4), 673-677.

Marcone, M. F., Kakuda, Y., & Yada, R. Y. (1998). Salt-soluble seed globulins of various dicotyledonous and monocotyledonous plants - I. Isolation/purification and characterization. *Food Chemistry*, 62(1), 27-47.

Martínez-Flores, H. E., Barrera, E. S., Garnica-Romo, M. G., Penagos, C. J. C., Saavedra, J. P., & Macazaga-Alvarez, R. (2006). Functional characteristics of protein flaxseed concentrate obtained applying a response surface methodology. *Journal of Food Science*, 71(8), C495-C498.

McClements, D. J. (2004). Protein-stabilized emulsions. *Current Opinion in Colloid & Interface Science*, 9(5), 305-313.

McClements, D. J. (2005). *Food emulsions: Principles, practice, and techniques*. (2nd ed.). Boca Raton: CRC Press.

Morr, C. V., & Ha, E. Y. W. (1993). Whey protein concentrates and isolates: Processing and functional properties. *Critical Reviews in Food Science and Nutrition*, 33(6), 431-476.

Oomah, B. D., & Mazza, G. (1993). Flaxseed proteins – a review. *Food Chemistry*, 48(2), 109-114.

Perrechil, F. A., Santana, R. C., Fasolin, L. H., Silva, C. A. S., & Cunha, R. L. (2010). Rheological and structural evaluations of commercial italian salad dressings. *Ciência e Tecnologia de Alimentos*, 30(2), 477-482.

Rabetafika, H. N., Remoortel, V. V., Danthine, S., Paquot, M., & Blecker, C. (2011). Flaxseed proteins: food uses and health benefits. *International Journal of Food Science and Technology*, 46(2), 221-228.

Raikos, V. (2010). Effect of heat treatment on milk protein functionality at emulsion interfaces. A review. *Food Hydrocolloids*, 24(4), 259-265.

Sato, A. C. K, & Cunha, R. L. (2007). Influence of temperature on the rheological behavior of jaboticaba pulp. *Ciência e Tecnologia de Alimentos*, 27(4), 890-896.

Silva, F. G. D., O'Callagahan, Y., O'Brien, N. M., & Netto, F. M. (2013). Antioxidant capacity of flaxseed products: The effect of in vitro digestion. *Plant Foods for Human Nutrition*, 68(1), 24-30.

Smith, A. K., Johnsen, V. L., & Beckel, A. C. (1946). Linseed proteins: Alkali dispersion and acid precipitation. *Industrial and Engineering Chemistry*, 38(3), 353-356.

Srinivasan, M., Singh, H., & Munro, P. A. (1996) Sodium caseinate-stabilized emulsions: Factors affecting coverage and composition of surface proteins. *Journal of Agricultural and Food Chemistry*, 44(12), 3807-3811.

Steffe, J. F. (1996). *Rheological methods in food process engineering*. (2nd ed.). East Lansing: Freeman Press.

Sun, C., & Gunasekaran, S. (2009). Effects of protein concentration and oil-phase volume fraction on the stability and rheology of menhaden oil-in-water emulsions stabilized by whey protein isolate with xanthan gum. *Food Hydrocolloids*, 23(1), 165-174.

Taherian, A. R., Britten, M., Sabik, H., & Fustier, P. (2011). Ability of whey protein isolate and/or fish gelatin to inhibit physical separation and lipid oxidation in fish oil-in-water beverage emulsion. *Food Hydrocolloids*, 25(5), 868-878.

Vicentini, N. M., Dupuy, N., Leitzelman, M., Cereda, M. P., & Sobral, P. J. A. (2005). Prediction of cassava starch edible film properties by chemometric analysis of infrared spectra. *Spectroscopy Letters*, 38(6), 749-767.

Wanasundara, P. K. J. P. D., & Shahidi, F. (1997). Functional properties of acylated flax protein isolates. *Journal of Agricultural and Food Chemistry*, 45(7), 2431-2441.

Wang, B., Li, D., Wang, L.-J., Adhikari, B., & Shi, J. (2010a). Ability of flaxseed and soybean protein concentrates to stabilize oil-in-water emulsions. *Journal of Food Engineering*, 100(3), 417-426.

Wang, B., Li, D., Wang, L.-J., & Özkan, N. (2010b). Effect of concentrated flaxseed protein on the stability and rheological properties of soybean oil-in-water emulsions. *Journal of Food Engineering*, 96(4), 555-561.

Wang, B., Wang, L.-J., Li, D., Adhikari, B., & Shi, J. (2011). Effect of gum Arabic on stability of oil-in-water emulsion stabilized by flaxseed and soybean protein. *Carbohydrate Polymers*, 86(1), 343-351.

Waraho, T., McClements, D. J., & Decker, E. A. (2011). Mechanisms of lipid oxidation in food dispersions. *Trends in Food Science and Technology*, 22(1), 3-13.

Ye, A. (2008). Interfacial composition and stability of emulsions made with mixtures of commercial sodium caseinate and whey protein concentrate. *Food Chemistry*, 110(4), 946-952.

Youle, R. J., & Huang, A. H. C. (1981). Occurrence of low molecular weight and high cysteine containing albumin storage proteins in oilseeds of diverse species. *American Journal of Botany*, 68(1), 44-48.

Yu, P., McKinnon, J. J., Soita, H. W., Christensen, C. R., & Christensen, D. A. (2005). Use of synchrotron-based FTIR microspectroscopy to determine protein secondary structures of raw and heat-treated brown and golden flaxseeds: A novel approach. *Canadian Journal of Animals Sc*ience, 85(4), 437-448.

CHAPTER 5

Production of whey protein isolate – gellan microbeads for encapsulation and release of bioactive compounds from flaxseed

Kuhn, K. R.; Silva, F. G. D.; Netto, F. M.; Cunha, R. L.

To be submitted to Food Hydrocolloids

CHAPTER 5. Production of whey protein isolate – gellan microbeads for encapsulation and release of bioactive compounds from flaxseed

Kátia Regina Kuhn[a], Fernanda Guimarães Drummond e Silva[b], Flavia Maria Netto[b], Rosiane Lopes da Cunha[a,]*

[a]Department of Food Engineering, Faculty of Food Engineering, University of Campinas (UNICAMP), 13083-862 – Campinas, SP, Brazil

[b]Department of Food and Nutrition, Faculty of Food Engineering, University of Campinas (UNICAMP), 13083-862 – Campinas, SP, Brazil

*Corresponding author: Tel.: +55 19 3521 4047; fax: +55 19 3521 4027

E-mail address: rosiane@fea.unicamp.br

ABSTRACT

Production of whey protein isolate (WPI) – gellan gum microbeads from extrusion of the O/W emulsions into a $CaCl_2$ solution was evaluated to encapsulate oil and protein hydrolysate (FPH) from flaxseed. In addition, microgels resistance and the controlled release of oil and FPH were investigated. Microscopic images showed that gellan prevailed at the external surface of the particles and that there were few free oil droplets in microbeads containing high gellan concentration, indicating that FPH and oil were encapsulated. Microbeads produced at higher gellan concentrations showed a more regular and spherical morphology, but a significant decrease in their size and an increase in their polydispersity were observed with the FPH addition, which can be consequence of the formation of a more dense biopolymers network. The microbeads suspensions were stable at different salt concentrations with regard to their shape, not releasing the encapsulated oil.

And the FPH presence decreased the viscosity and shear thinning behavior of microbeads suspensions, which could be attributed to their smaller size. WPI-gellan microbeads were resistant to simulated gastric conditions, but did not resist to intestinal conditions, making these microgels able to protect bioactive compounds during their passage through the stomach for releasing them in the small intestine.

Keywords: Extrusion; Flaxseed protein hydrolysate; Flaxseed oil; Rheology; *In vitro* digestion.

5.1. INTRODUCTION

Encapsulation can be used for protection of actives compounds against evaporation, chemical reactions or migration in food, reduction of flavor loss during the product shelf-life and extend its perception and mouthfeel, prevention of undesirable interactions with other components in food products and masking unpleasant feelings (Klaypradit & Huang, 2008; Nedovic, Kalusevic, Manojlovic, Levic, & Bugarski, 2011). In addition, encapsulation allows controlling the release and preservating the stability of bioactive compounds during processing and storage, in order to ensure their bioavailability and efficacy (Klaypradit & Huang, 2008; Nedovic et al., 2011). It has been employed to protect active components such as probiotics (Cook, Tzortzis, Charalampopoulos, & Khutoryanskiy, 2012; Doherty et al., 2011), vitamins (Beaulieu, Savoie, Paquin, & Subirade, 2002; Chen & Subirade, 2006), oils (Tonon, Pedro, Grosso, & Hubinger, 2012) and peptides (Chandy, Mooradian, & Rao, 1998).

The application, economic features and health safety are the main criteria that govern the choice of encapsulation material and process (Chan, 2011). In the food sector, materials used for encapsulation must be food-grade and biodegradable, providing maximal protection to the encapsulated material during processing and storage and not reacting with it (Nedovic et al., 2011).

The extrusion method followed by an ionotropic gelation is extensively used to produce microbeads (Albertini et al., 2010; Corbo, Bevilacqua, & Sinigaglia, 2011; Perrechil, Vilela, Guerreiro, & Cunha, 2012; Smrdel, Bogataj, Zega, Planinšek, & Mrhar, 2008), which can encapsulate bioactive compounds. It consists in forming droplets by the use of a syringe or an atomizer nozzle into a gelling solution (ionic), where microgels are formed, hardened and then collected (Perrechil et al., 2012). One advantage of these microgels is that they can be used in hydrated media without breaking (Burey, Bhandari, Howes, & Gidley, 2008).

Polysaccharides are most widely used as wall materials (Nedovic et al., 2011) due to their good biocompatibility, biodegradability, low toxicity, abundance in nature and low cost (Kaihara, Suzuki, & Fujimoto, 2011; Karewicz, Łęgowik, & Nowakowska, 2011; Perrechil et al., 2012). However, proteins are also a good coating material for the encapsulation of bioactive compounds, due to their unique functional properties such as the ability to form gels and stabilize emulsions (Chen, Remondetto, & Subirade, 2006). Moreover, they have high nutritional value, good sensory properties and are widely available, inexpensive, natural and GRAS (generally recognized as safe) materials, as the milk proteins (Livney, 2010). Protein-polysaccharide mixtures have been also evaluated as wall materials (Chen & Subirade, 2005, 2006; Perrechil et al., 2012; Tang et al., 2013).

Flaxseed (*Linum usitatissimum* L.) has been emerging as one of the key sources of bioactive ingredients in the functional food area (Zhang, Xu, Wang, Yang, & Lu, 2009). It is an oilseed, rich in lipids, dietary fiber (both soluble and insoluble), proteins and lignans (Marambe, Shand, & Wanasundara, 2008). Its major product is oil, which is the richest known plant source of the omega 3 (ω-3) fatty acid (α-linolenic acid, ALA) (Marambe et al., 2008), increasingly recognized for their role in reducing the risk of diseases and maintaining human health (Liu, Low, & Nickerson, 2010; Shahidi & Miraliakbari, 2005). Flaxseed proteins are gaining prominence with respect to their health benefits (Rabetafika, Remoortel, Danthine, Paquot, & Blecker, 2011), since studies have reported that their hydrolysates have biological activities such as antihypertensive, antioxidant and anti-inflammatory properties (Marambe et al., 2008; Udenigwe, Lin, Hou, & Aluko, 2009; Udenigwe, Lu, Han, Hou, & Aluko, 2009).

For obtaining health benefits it is necessary to ensure the stability of the compounds in the gastrointestinal (GI) system and to facilitate controlled release at the appropriate GI target (Champagne & Fustier, 2007). In view of this, the protection of bioactive compounds from flaxseed, through encapsulation, could be an alternative in the attempt to avoid their functionality and bioavailability loss before their release. Thus, the aim of this work was to produce microbeads of whey protein isolate and gellan gum from extrusion of O/W emulsions containing these biopolymers into a calcium chloride ($CaCl_2$) solution in order to encapsulate oil and protein hydrolysate from flaxseed and then evaluate the release of these compounds by simulation of *in vitro* digestion process. For this, microgels were characterized according to their morphology, particle size, zeta potential, stability and rheological behavior of particles suspensions and resistance to gastrointestinal conditions.

5.2. MATERIAL AND METHODS

5.2.1. Material

The whey protein isolate (WPI) was obtained from New Zealand Milk Products (ALACEN 895, New Zealand), the gellan gum was donated by Kelco Biopolymers (San Diego, California, USA) and the flaxseed protein hydrolysate (FPH) was obtained from the protein extracted from partially defatted flaxseed meal (Cisbra, Panambi, RS, Brazil), according to methodology from Silva, O'Callagahan, O'Brien, and Netto (2013). The hydrolysis condition chosen was that resulted in a FPH with the highest antioxidant capacity (pH 8.5 and enzyme:substrate ratio 1:90, w/w). The protein concentration (% w/w, wet basis), determined by the Kjeldahl analysis (AOAC, 1997), of the WPI, gellan and FPH was 87.66 ± 0.91% (N x 6.38), 0.40 ± 0.00% (N x 6.25) and 70.38 ± 0.91% (N x 6.25), respectively. Flaxseed oil was purchased from Cisbra (Panambi, RS, Brazil), showing the following fatty acids composition: 6.2% C16:0, 5.3% C18:0, 20.1% C18:1, 13.7% C18:2 and 52.3% C18:3 (provided by Cisbra). The enzymes Alcalase 2.4 L, pepsin from porcine gastric mucosa (P7000) and pancreatin from porcine pancreas (P1625), bile extract porcine (B8631) and FITC were purchased from Sigma Chemical Co. (St. Louis, Missouri, USA). Reagents dimethyl sulfoxide (DMSO), pyridine and dibutyltin dilaurate were purchased from Merck KGaA (Darmstadt, Germany). All other reagents were of analytical grade.

5.2.2. Preparation of stock solutions

The WPI (10% w/v) and the FPH (2.5% w/v) stock solutions were prepared by dispersing the powder in deionized water using magnetic stirring during 90 and 120 min, respectively, at room temperature (25 °C). Then, the solutions were kept overnight at 10 °C to allow complete protein dissolution. The gellan (1% w/v) stock solution was prepared by dissolving the powder in deionized water during 120 min (25 °C), followed by heat treatment at 90 °C for 30 min under magnetic stirring and subsequent cooling to room temperature in an ice bath. Stock solutions were prepared at natural pH (WPI solution ≅ 6.5, FPH solution ≅ 8.4–8.8 and gellan solution ≅ 5.2).

5.2.3. Preparation of the O/W emulsions

Primary oil-in-water (O/W) emulsions were prepared at 25 °C by homogenizing the oil with the aqueous phase using two sequential homogenization methods. The first involved mixing the solutions in an Ultra Turrax model T18 homogenizer (IKA, Germany) for 4 min at 14,000 rpm, and the second method involved a homogenization at 60 MPa / 5 MPa, with two passes through the homogenizer, using a Panda 2K NS1001L double stage homogenizer (Niro Soavi, Italy). The WPI and flaxseed oil content were fixed at 3% (w/v) and 30% (v/v), respectively, and the FPH concentration varied between 0 and 1% (w/v). Secondary O/W emulsions were prepared by mixing the primary emulsion into gellan solutions using magnetic stirring for 1 h at 25 °C. The final composition of secondary emulsions was 15% (v/v) flaxseed oil, 1.5% (w/v) WPI, 0 – 0.5% (w/v) FPH and 0.1 – 0.5% (w/v) gellan.

5.2.4. Gelation of the emulsions

Preliminary trials were conducted in order to determine the appropriate $CaCl_2$ concentration (0.56, 0.74, 0.93 or 1.11% w/v) for gelation of the emulsions (15% (v/v) flaxseed oil, 1.5% (w/v) WPI and 0.1 – 0.5% (w/v) gellan). For this, a syringe (5 mL) coupled to a needle (0.8 mm diameter) was used to drip samples (20 drops) in $CaCl_2$ solutions (50 mL) under magnetic stirring at room temperature (25 °C). The height between the needle outlet and the $CaCl_2$ solution was fixed at 10 cm (Chan, Lee, Ravindra, & Poncelet, 2009). The particles were held in $CaCl_2$ solutions for 30 min under orbital stirring (100 rpm) (Model TE-420, Tecnal, Brazil). After that, the gelled particles were separated using a sieve and visually observed.

5.2.5. Production of microbeads

Secondary emulsions were extruded through an atomizer nozzle (1 mm diameter) into a 0.56% (w/v) $CaCl_2$ solution (concentration determined in section 5.2.4) at room temperature (25 °C) (Fig. 5.1). The collecting distance between the atomizer nozzle and the $CaCl_2$ solution (H) was of 30 cm and the feed flow rate and the compressed air pressure were fixed at 0.268 L/h and 1.0 bar, respectively. In order to obtain smaller particles diameter, the higher difference between the air pressure and the feed rate was used (Herrero, Martín Del Valle, & Galán, 2006; Perrechil, Sato, & Cunha, 2011; Rizk & Lefebvre, 1980), avoiding that the salt solution was splashed out of the container. The best relation gellan/FPH to produce microbeads was investigated from the particles preparation using different concentrations of gellan (0.1, 0.3 or 0.5% w/v) and FPH (0, 0.25 or 0.5% w/v). Microbeads produced were maintained in the salt solution under magnetic stirring for 30 min (Chan et al., 2009; Perrechil et al., 2011), filtered using a sieve with opening of 0.037 mm and then stored at room temperature for 1 day, for their evaluation and characterization (sections 5.2.6 and 5.2.7).

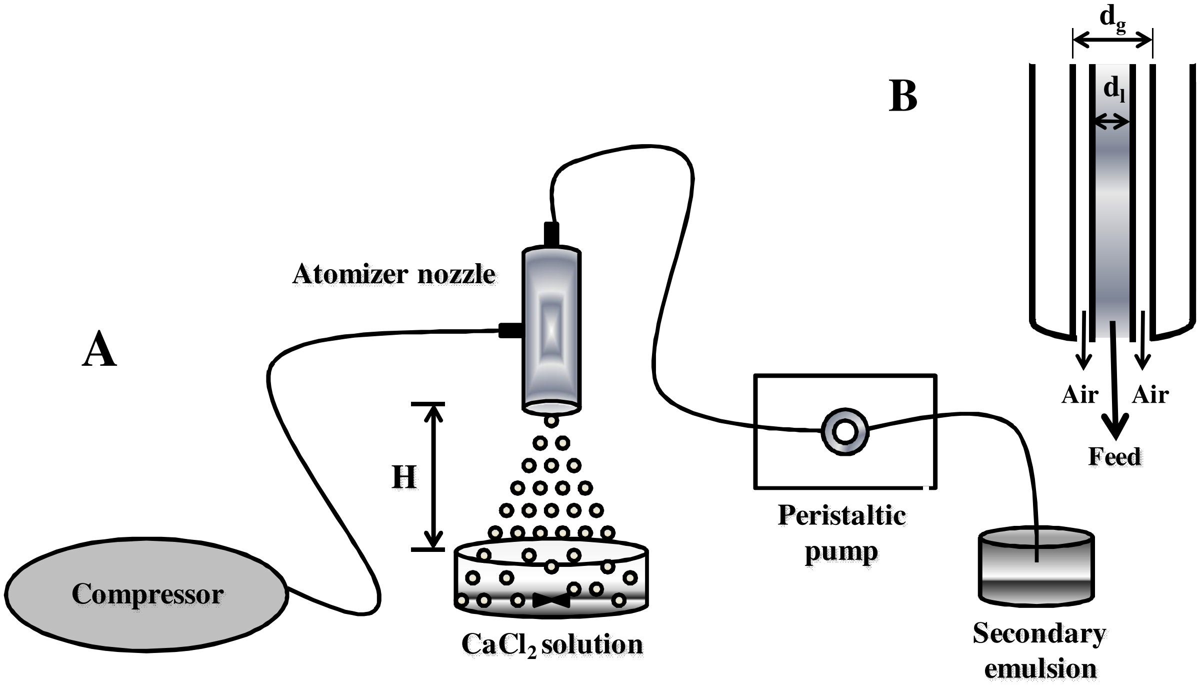
A
B
Atomizer nozzle
Compressor
H
$CaCl_2$ solution
Peristaltic pump
Secondary emulsion
d_g
d_l
Air
Air
Feed

Fig. 5.1. A) Schematic representation of the production of microbeads by extrusion and B) atomizer nozzle. H = distance between the atomizer nozzle and the salt solution, d_l = diameter of the feed nozzle exit (1 mm) and d_g = diameter of air nozzle exit (3.08 mm).

5.2.6. Evaluation of microbeads

5.2.6.1. Stability

Microbeads stability in different media (water and $CaCl_2$ aqueous solutions (0.56, 1.11 or 2.22% w/v)) was monitored by particle size distribution (section 5.2.7.2) during 60 min, and samples were collected every 10 min. Suspensions were prepared by dispersing microbeads containing 0.3% (w/v) gellan in distilled water, directly in the measurement unit of the laser diffraction equipment (Mastersizer 2000, Malvern Instruments Ltd., UK). At the same time, the microstructure of microbeads suspensions in these different media was evaluated by optical microscopy (section 5.2.7.3).

5.2.6.2. Rheological properties of microbeads suspensions

The rheological properties of the suspensions (10, 30, 50, 70 or 90% w/v) of microbeads (0 or 0.25% (w/v) FPH and 0.3% (w/v) gellan) in 0.56% (w/v) $CaCl_2$ solution were evaluated using a Physica MCR301 modular compact rheometer (Anton Paar, Austria). A stainless steel plate geometry (50 mm) and a 0.6 mm gap was used for the measurements. Flow curves were obtained using an *up-down-up* steps program with the shear rate varying between 0 and 300 s^{-1}. All measurements were performed in triplicate at 25 °C. The model for shear-thinning fluids (Power law model) (Eq. (5.1)) was used to fit the flow curves.

$$\sigma = k \, . \left(\dot{\gamma} \right)^n \tag{5.1}$$

where σ is the shear stress (Pa), $\dot{\gamma}$ is the shear rate (s^{-1}), k is the consistency index ($Pa.s^n$) and n is the flow behavior index (dimensionless).

5.2.6.3. Simulation of *in vitro* digestion process

Microbeads were incubated in different media simulating buccal (salivary), gastric and intestinal digestion. In the simulation of oral digestion step, microgels were mixed in phosphate buffer (0.005 M, pH 6.9, 1 M NaCl + 0.004 M $CaCl_2$) at a ratio of 1 g of sample to 4 mL of buffer (Hoebler et al., 2002). Then, gastric and intestinal digestions were simulated, following the methodology of Garrett, Failla, and Sarama (1999). Porcine pepsin (40 mg/mL in 0.1 M HCl) was added to simulate the gastric juice, at a ratio of 0.5 g of pepsin per 100 g of sample (Miller, Schricker, Rasmussen, & Van Campen, 1981), the pH was adjusted to 2 by adding 6 M HCl and then the mixture was incubated for 1 h at 37 °C under orbital stirring (100 rpm). After, in intestinal digestion, the pH of the resulting mixture was raised to 5.3 using 0.9 M sodium bicarbonate solution followed by the addition of a mixture of pancreatin and bile extract (2 mg/mL pancreatin + 12 mg/mL bile extract in 0.1 M sodium bicarbonate), in order to obtain final concentrations of 0.4 mg/mL pancreatin and 2.4 mg/mL bile extract. The pH of the system was adjusted to 7 with 0.1 M NaOH prior to its incubation at 37 °C for 2 h under orbital stirring (100 rpm) (Model TE-420, Tecnal, Brazil). The zeta potential, particle size distribution and morphology (sections 5.2.7.1, 5.2.7.2 and 5.2.7.3, respectively) of the particles were evaluated before, during (samples were collected every 15 min) and after the gastric and intestinal digestion steps.

5.2.7. Characterization of microbeads

5.2.7.1. Zeta potential

To determine the electrical charge on the surface of microbeads, aliquots of their suspensions in different media were diluted in Milli-Q water and a Zetasizer Nano-ZS (Malvern Instruments Ltd., UK) equipment was used. Measurements were performed at 25 °C in triplicate.

5.2.7.2. Particle size distribution

A Mastersizer 2000 (Malvern Instruments Ltd., UK) was used to determine the particle size distribution of microbeads in distilled water as dispersion medium (~0.06% v/v). The size of particles was determined as the volume-surface mean diameter (d_{32}) and the dispersion index (span) was also reported (Jafari, He, & Bhandari, 2007), according to Eqs. (5.2) and (5.3), respectively. The particle size and span were reported as the average and corresponding standard deviation of three replicates.

$$d_{32} = \sum n_i d_i^3 \Big/ \sum n_i d_i^2 \tag{5.2}$$

$$Span = \left(d_{90} - d_{10}\right) / d_{50} \tag{5.3}$$

where n_i is the number of microbeads with diameter d_i, and d_{10}, d_{50} and d_{90} are diameters at 10, 50 and 90% of cumulative volume, respectively.

5.2.7.3. Optical microscopy

The morphology of microbeads was evaluated by optical microscopy. Microgels were poured onto microscope slides, carefully covered with glass cover slips and observed using a Carl Zeiss Model Axio Scope.A1 optical microscope (Zeiss, Germany), with a 10 x objective lens.

5.2.7.4. Confocal scanning laser microscopy (CSLM)

Fluorescein-5-isothiocyanate (FITC) was used to label the gellan gum according to methodology described by Heilig, Göggerle, and Hinrichs (2009). 20 mL DMSO and 80 μL pyridine were mixed with 1 g gellan gum and stirred for 30 min at room temperature. Then, 0.1 g FITC and 40 μL dibutyltin dilaurate were added, the mixture was incubated for 3 h in a water bath (95 °C) and after cooled down to room temperature. The resulting sample was crushed, washed with ethanol (99.5%) and dried in a vacuum oven (65 °C). To prepare the polysaccharide solution, FITC-labeled gellan was dissolved and heat treated as described in section 5.2.2. The proteins (WPI and FPH) were stained with a fluorescent dye Rhodamine B, which was directly added to solutions.

Emulsions and microbeads were prepared with protein and polysaccharide labeled solutions, according to sections 5.2.3 and 5.2.5, respectively. Samples were evaluated using a Zeiss LSM 780-NLO confocal on an Axio Observer Z.1 microscope (Carl Zeiss AG, Germany) with a 40 x objective. Images were collected using 488 and 543 nm laser lines for excitation of FITC and Rhodamine B fluorophores, respectively, with pinholes set to 1 airy unit for each channel, 1024×1024 image format.

5.2.8. Statistical analysis

The results were evaluated by analysis of variance (ANOVA), and significant differences ($p<0.05$) between the treatments were evaluated by the Tukey's procedure. The statistical analyses were carried out using the software STATISTICA 6.0 (Statisoft Inc., Tulsa, USA).

5.3. RESULTS AND DISCUSSION

5.3.1. Gelation of the O/W emulsions

Gelation of the emulsions was performed at different concentrations of gellan gum (0.1, 0.3 or 0.5% w/v) and $CaCl_2$ (0.56, 0.74, 0.93 or 1.11% w/v). Gelled particles on a macroscopic scale (Fig. 5.2) were observed and the adequate $CaCl_2$ concentration for gel formation was determined. At lower gellan concentration (0.1% w/v), emulsions did not form gelled particles, but gelled wires. However, at higher gellan concentrations (0.3 or 0.5% w/v), gelled particles were observed, which became more regular and spherical with increasing gellan concentration, regardless of salt concentration. Thus, as the salt concentration studied had no apparent effect on gelation of the emulsions for these gellan concentrations, the lowest $CaCl_2$ concentration (0.56% w/v) was chosen to be used in the production of microgels by extrusion. Despite the size and the appearance of whey protein beads are influenced by $CaCl_2$ concentration (Hébrard et al., 2006), such influence was not visually observed at the range of salt concentration evaluated.

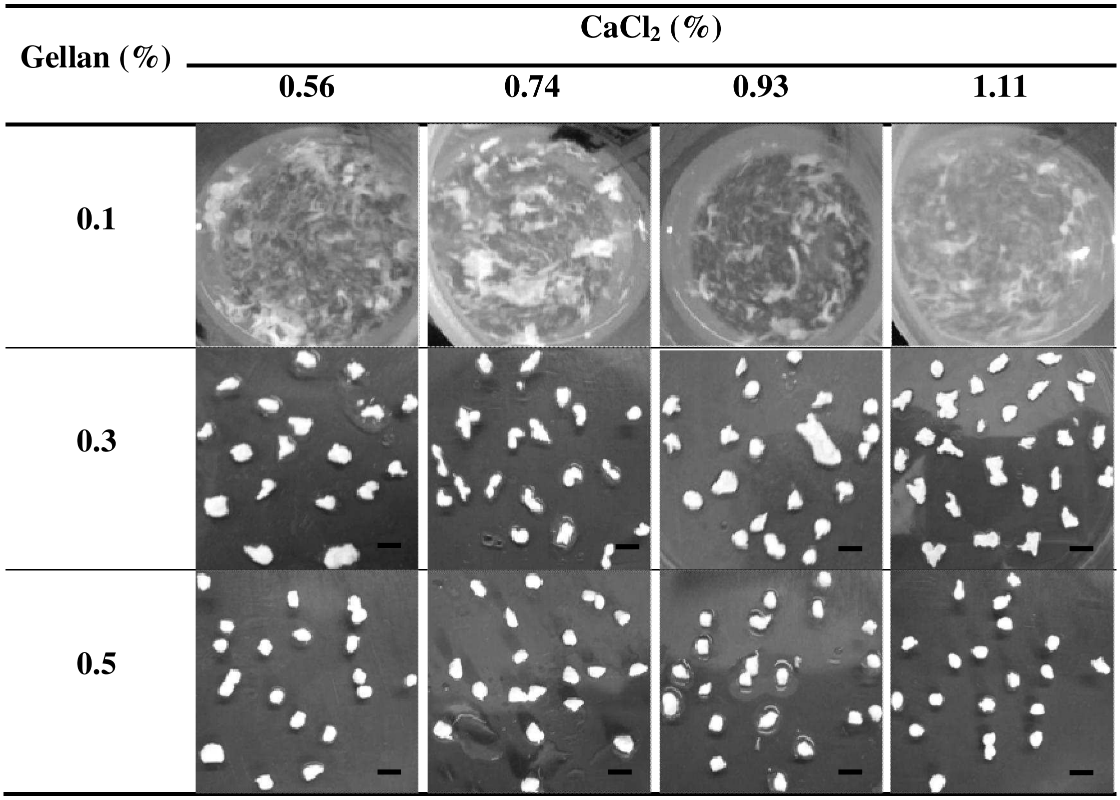

Fig. 5.2. Visual appearance of the particles composed by 15% (v/v) flaxseed oil, 1.5% (w/v) WPI and 0.1, 0.3 or 0.5% (w/v) gellan, gelled in 0.56, 0.74, 0.93 or 1.11% (w/v) $CaCl_2$. Scale bar = 0.5 cm.

5.3.2. Microbeads

5.3.2.1. Choosing the ratio gellan/FPH

Different concentrations of gellan (0.1, 0.3 or 0.5% w/v) and FPH (0, 0.25 or 0.5% w/v) were evaluated aiming to determine the appropriate ratio gellan/FPH for producing stable and smaller microgels. Fig. 5.3 shows that microgels containing 0.1% (w/v) gellan exhibited a bimodal distribution, which was more accentuated in the absence of FPH (Fig. 5.3A) or at lower concentration (0.25% w/v) (Fig. 5.3B). Increasing gellan concentration to

0.3% (w/v), the particle distribution was similar to that of lower gellan concentration. However, microbeads composed by 0.3% (w/v) gellan and 0.5% (w/v) FPH (Fig. 5.3C) or with greater gellan concentration (0.5% w/v) showed higher polydispersity, which could be attributed to the increased solution viscosity at higher polysaccharide concentration or total concentration of polymers (Chen & Subirade, 2006). Such observations were confirmed by the increase in the mean diameter (d_{32}) and span values (dispersion index) of microbeads (Fig. 5.3) with the increase of gellan concentration. However the effect of flaxseed hydrolysate depended on the gellan concentration. Microbeads produced with 0.1% (w/v) gellan showed a significant increase ($p<0.05$) of the size at highest FPH concentration (0.5% w/v), while a significant decrease was observed for microbeads containing 0.3 or 0.5% (w/v) gellan. Opposite result was found for the span values. Such size reduction and polydispersity increase of microbeads could be related to an electrostatic interaction between biopolymers, since WPI and FPH have amphiphilic character (they have negative and positive charges), and/or to the bridges formed between the negatively charged groups of gellan and the $CaCl_2$. Both events could contribute to a more dense biopolymers network and consequently with a reduced size.

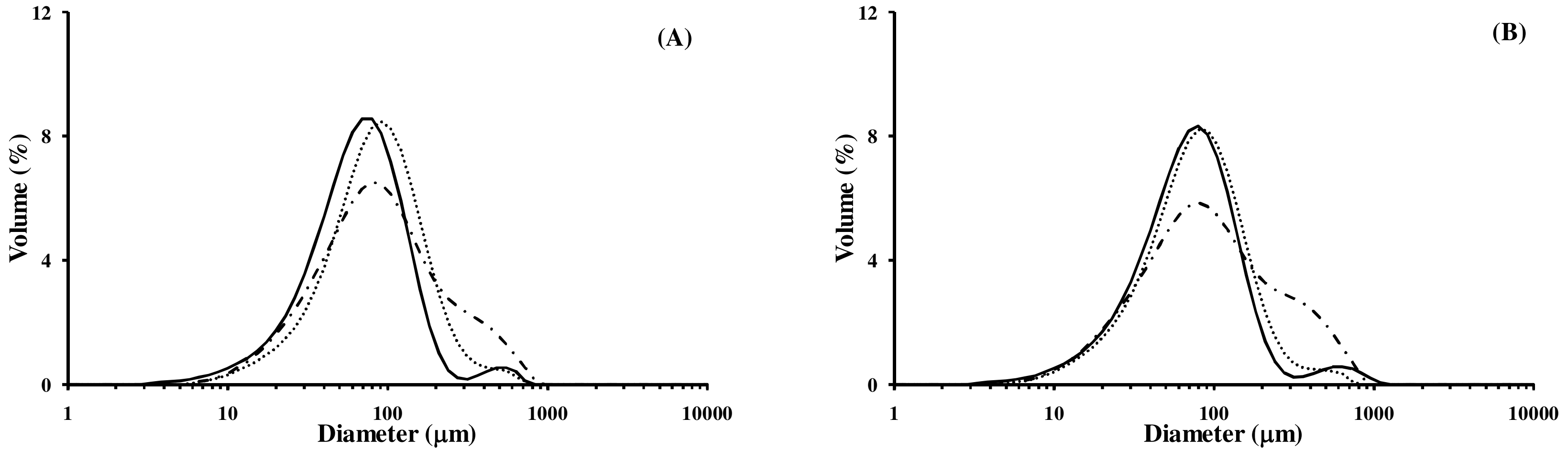

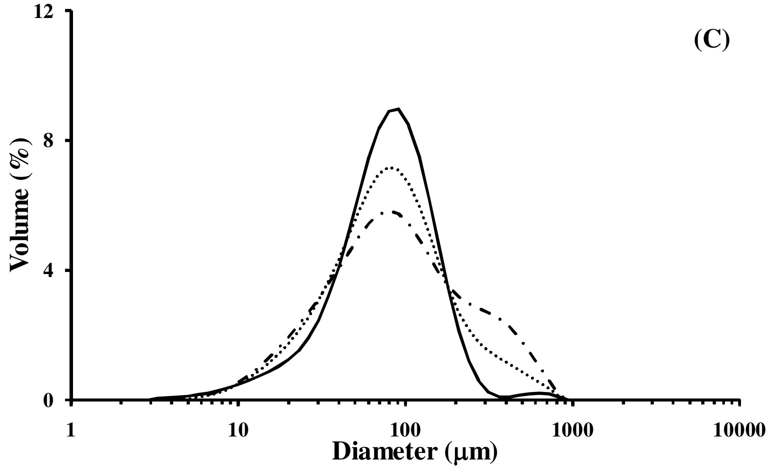

Gellan (%)		FPH (%)		
		0	0.25	0.5
0.1	d$_{32}$ (µm)	42.50 ± 0.49^{cB}	43.24 ± 1.39^{bB}	47.42 ± 0.33^{bA}
	Span	1.81 ± 0.04^{bA}	1.84 ± 0.02^{bA}	1.69 ± 0.02^{cB}
0.3	d$_{32}$ (µm)	56.41 ± 0.43^{aA}	50.72 ± 0.26^{aB}	49.38 ± 0.41^{aC}
	Span	1.80 ± 0.04^{bB}	1.93 ± 0.04^{bB}	2.57 ± 0.09^{bA}
0.5	d$_{32}$ (µm)	54.51 ± 0.30^{bA}	50.48 ± 0.71^{aB}	50.20 ± 0.80^{aB}
	Span	3.21 ± 0.10^{aB}	3.58 ± 0.12^{aA}	3.55 ± 0.05^{aA}

Different letters indicate significant differences ($p<0.05$). Small letters: differences in the same column. Capital letters: differences in the same line.

Fig. 5.3. Particle size distribution, mean particle diameter (d$_{32}$) and span of microbeads containing 15% (v/v) flaxseed oil, 1.5% (w/v) WPI, (A) 0, (B) 0.25 or (C) 0.5% (w/v) FPH and (▬▬) 0.1, (·····) 0.3 or (▬ ·) 0.5% (w/v) gellan.

The influence of gellan and FPH concentration on the microstructure of microbeads can be observed in Fig. 5.4. According to the pictures, the increase of gellan concentration from 0.1 to 0.3% (w/v) led to more regular and spherical microgels, while microbeads with 0.5% (w/v) gellan were similar to those with 0.3% (w/v) gellan. Tang et al. (2013) also observed more spherical alginate-whey protein microspheres produced at higher polymers concentration. The hydrolysate concentration affected the morphology of microgels in a lesser extension. However, microbeads without the FPH addition or with lower gellan concentration seemed to have a greater number of free oil droplets (indicated in Figure), indicating that the presence of the hydrolysate and high gellan concentration (0.3 or 0.5% w/v) may have assisted in the flaxseed oil encapsulation. Regarding this, the combined effect of amphiphilic interface and the higher viscosity of the continuous phase in these conditions must be taken into account.

Thus, despite the smaller size of microgels with 0.1% (w/v) gellan, it was chosen 0.3% (w/v) gellan for the production of microbeads in the following steps, since at this concentration microgels were more uniform and presented less free oil droplets in solution. The hydrolysate concentration chosen was 0 or 0.25% (w/v) in order to better evaluate its influence on the microgels produced with 0.3% (w/v) gellan and on the flaxseed oil encapsulation.

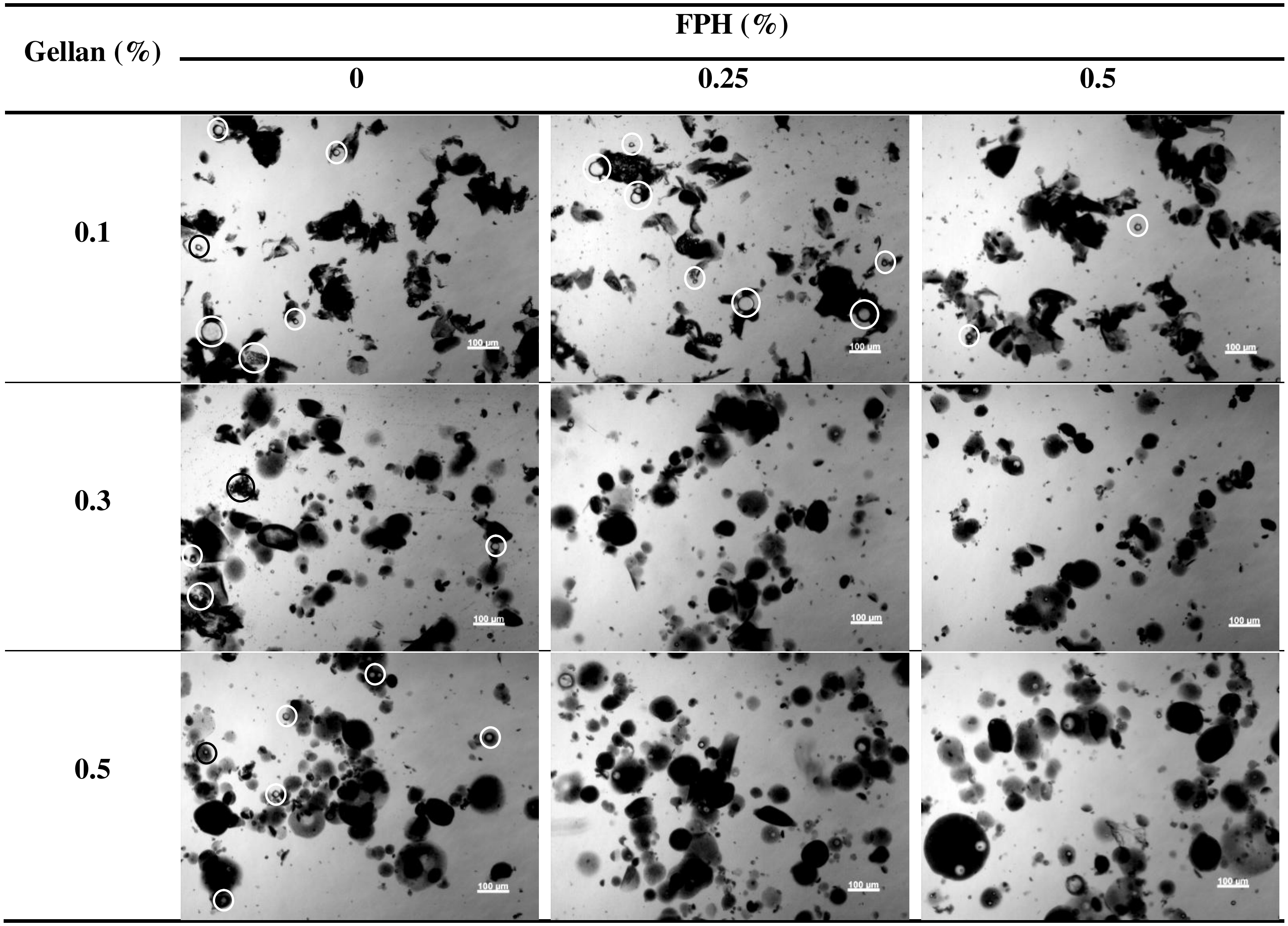
FPH (%)
Gellan (%)
0
0.25
0.5
0.1
0.3
0.5
100 µm

Fig. 5.4. Microstructure of microbeads composed by 15% (v/v) flaxseed oil, 1.5% (w/v) WPI, 0 – 0.5% (w/v) FPH and 0.1 – 0.5% (w/v) gellan. Scale bar = 100 µm.

5.3.2.2. Evaluation of stability

Microbeads stability with the time was evaluated in different media (water and $CaCl_2$ solutions (0.56, 1.11 or 2.22% w/v)) in order to determine their resistance to release the encapsulated oil during the storage. The mean diameter (d_{32}) of microbeads decreased from 65.25 ± 0.21 μm to 50.16 ± 0.03 μm in distilled water over time (from 0 to 60 min) (Fig. 5.5), which could be indicating a disaggregation of some particles agglomerates. In $CaCl_2$ solutions, the mean diameter decreased mainly in the first 10 min (from ~67 μm to ~60 μm) and then became almost stable, with no difference between the $CaCl_2$ concentrations. Such size reduction with the salts addition could be explained by the type of interaction performed by divalent cations, which form bridges between the negatively charged groups on biopolymers, allowing the release of free water (Chandrasekaran, Puigjaner, Joyce, & Arnott, 1988; Kuhn, Cavallieri, & Cunha, 2010; Vilela, Cavallieri, & Cunha, 2011), thus leading to shrinkage of the particles.

The particle size distribution of microbeads in these different media (results not shown) was monomodal and similar. The results showed size slightly larger at time zero when dispersed in water, whereas in $CaCl_2$ the size distribution did not change with time.

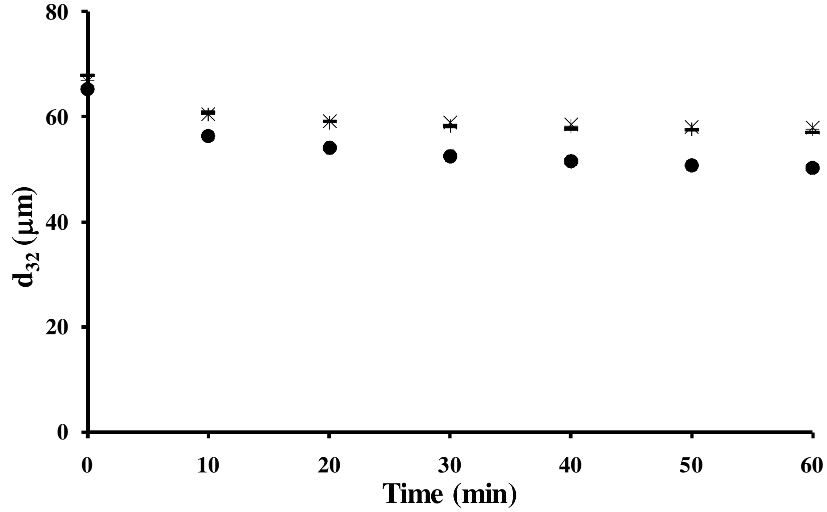

Fig. 5.5. Mean particle diameter (d_{32}) of microbeads containing 15% (v/v) flaxseed oil, 1.5% (w/v) WPI and 0.3% (w/v) gellan, dispersed in (•) distilled water and in $CaCl_2$ solutions: (X) 0.56, (—) 1.11 and (+) 2.22% (w/v).

The morphology of microbeads before and after dispersion in distilled water or in $CaCl_2$ solutions was observed (Fig. 5.6). The oil droplets were not released from microbeads during 1 h in any medium, which may be an indication of good stability of these microgels during the storage period. In general, it was not observed difference between the microstructures of microbeads dispersed in distilled water or in $CaCl_2$ solutions, nor with respect to time of dispersion. Then, according to these results, a low salt concentration (0.56% (w/v) $CaCl_2$) was chosen as dispersion medium of microgels in the rheological measurements.

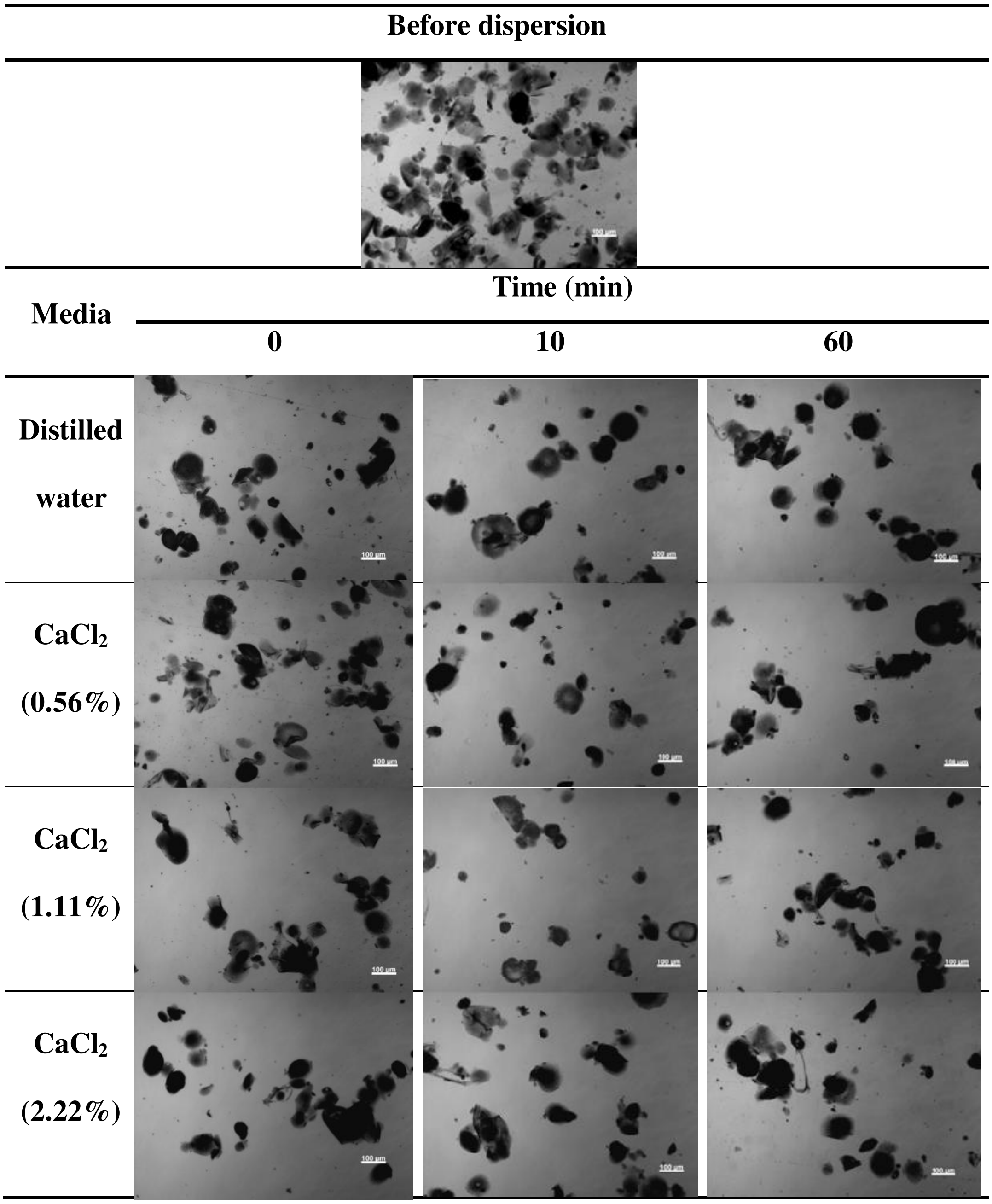
Before dispersion
100 µm
Media
Time (min)
0
10
60
Distilled water
CaCl₂ (0.56%)
CaCl₂ (1.11%)
CaCl₂ (2.22%)
100 µm

Fig. 5.6. Microstructure of microbeads composed by 15% (v/v) flaxseed oil, 1.5% (w/v) WPI and 0.3% (w/v) gellan in different media. Scale bar = 100 µm.

5.3.2.3. Rheological properties

The microbeads suspensions in $CaCl_2$ solution (0.56% w/v) showed a shear thinning behavior, regardless of the concentration of suspensions (Fig. 5.7). Apparent viscosity was greater in the microbeads suspensions without hydrolysate addition (Fig. 5.7A) than of microbeads with 0.25% (w/v) FPH (Fig. 5.7B), which was more noticeable at larger concentrations (above 50% w/v), indicating higher resistance to shear.

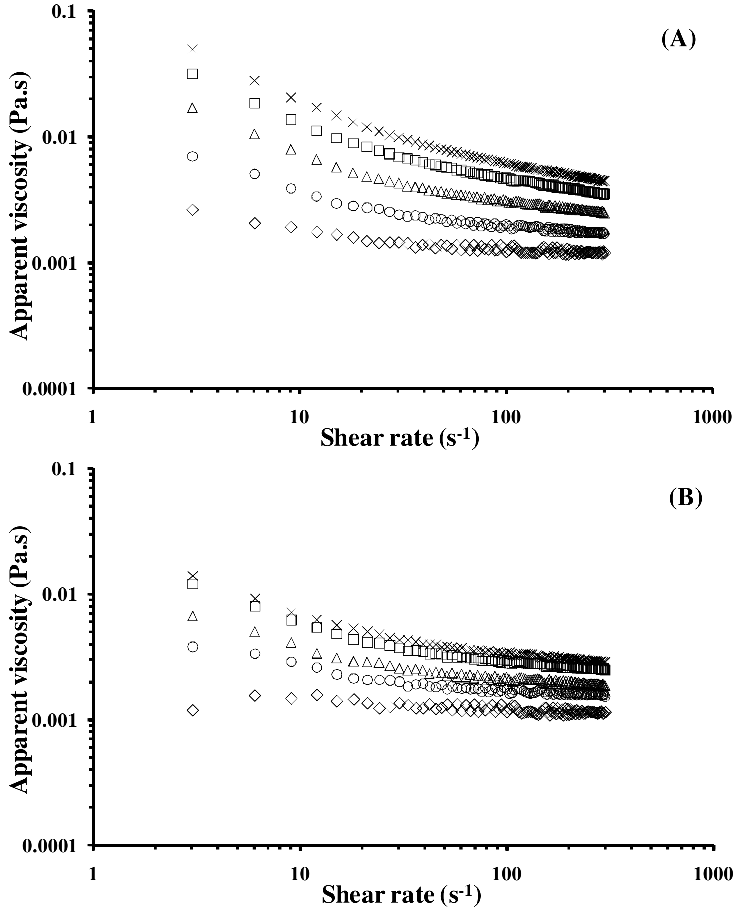

Fig. 5.7. Apparent viscosity of microbeads suspensions composed by 15% (v/v) flaxseed oil, 1.5% (w/v) WPI, (A) 0 or (B) 0.25% (w/v) FPH and 0.3% (w/v) gellan in $CaCl_2$ solution (0.56% w/v). Volume fraction of microbeads: (◇) 10, (○) 30, (△) 50, (□) 70 and (×) 90% (w/v).

Thus, the flow curves were fitted to power law model (R^2 > 0.996) and the flow behavior index (*n*), the consistency index (*k*), as well as the apparent viscosity at 50 s^{-1} (η_{50}) are shown in Table 5.1. Apparent viscosity was evaluated at this shear rate in order to simulate a shear rate typical of chewing (Steffe, 1996). Suspensions with a lower concentration of microbeads (10% w/v) showed a behavior close to Newtonian (n = 0.94 and n = 0.95 for microbeads without and with FPH addition, respectively), but with increasing concentration of microbeads, suspensions became more pseudoplastic (n value decreased). The rheological behavior of suspensions at low volume fraction is determined by the continuous phase since there is no interaction between the suspended particles (Sato & Cunha, 2012). However, at higher solids concentration there is an increase of interactions of weak intensity, which are broken with increasing shear rate, leading to reaggregation and shear shinning behavior (Vilela, 2012). An increase of the consistency index (k) was also observed with increasing concentration of suspensions, mainly for microbeads without FPH addition, which also showed a flow behavior index (n) lower ($p<0.05$) than microgels with hydrolysate. This result may suggest that microgels without FPH addition are more susceptible to alignment and elongations resulting from the shear rate application, which would explain the intensification of shear thinning behavior (decrease in n values) (Vilela, 2012).

The apparent viscosity (η_{50}) showed a significant increase ($p<0.05$) with the increase of concentration of microbeads in suspension. However, the viscosity values were very low (the maximum was 0.0078 Pa.s), which could be indicating that the addition of microbeads would exert little influence on the rheological behavior of food products (Perrechil, 2012). Microbeads with 0.25% (w/v) FPH showed lower viscosity (and k values) than microgels without hydrolysate. This behavior became more evident as the concentration of microbeads in suspension was increased and could be explained by lower particles size (Fig. 5.3).

Table 5.1. Rheological parameters obtained from the power law model and the apparent viscosity at 50 s^{-1} (η_{50}) for the microbeads suspensions composed by 15% (v/v) flaxseed oil, 1.5% (w/v) WPI, 0 or 0.25% (w/v) FPH and 0.3% (w/v) gellan in $CaCl_2$ solution (0.56% w/v).

Suspension		**FPH (%)**	
(% w/v)		**0**	**0.25**
10	***n***	0.94 ± 0.00^{aB}	0.95 ± 0.01^{aA}
30		0.87 ± 0.01^{bB}	0.91 ± 0.00^{bA}
50		0.80 ± 0.00^{cB}	0.89 ± 0.01^{cA}
70		0.72 ± 0.00^{dB}	0.86 ± 0.00^{dA}
90		0.67 ± 0.01^{eB}	0.84 ± 0.01^{eA}
10	***k* (Pa.s^n)**	0.002 ± 0.000^{eA}	0.002 ± 0.000^{eB}
30		0.004 ± 0.000^{dA}	0.002 ± 0.000^{dB}
50		0.008 ± 0.000^{cA}	0.004 ± 0.000^{cB}
70		0.017 ± 0.001^{bA}	0.006 ± 0.000^{bB}
90		0.028 ± 0.001^{aA}	0.007 ± 0.000^{aB}
10	**η_{50} (mPa.s)**	1.4 ± 0.00^{eA}	1.2 ± 0.06^{eB}
30		2.2 ± 0.00^{dA}	1.8 ± 0.00^{dB}
50		3.5 ± 0.10^{cA}	2.3 ± 0.06^{cB}
70		5.7 ± 0.15^{bA}	3.3 ± 0.06^{bB}
90		7.8 ± 0.15^{aA}	3.8 ± 0.00^{aB}

Different letters indicate significant differences ($p<0.05$). Small letters: differences in the same column. Capital letters: differences in the same line.

5.3.2.4. Confocal microscopy

The microstructure of microbeads with 0 or 0.25% (w/v) FPH and 0.1 or 0.3% (w/v) gellan was characterized by CSLM (Fig. 5.8). As observed in optical microscopy (section

5.3.2.1), microgels composed by 0.3% (w/v) gellan showed a more regular shape. In these micrographs, proteins (WPI and FPH) are represented in red and the green areas indicate the presence of gellan gum. Thus, it can be verified that there was a predominance of polysaccharide at the external surface of microbeads, regardless of gellan concentration and FPH addition, which confirms that the hydrolysate was encapsulated.

Due to the amphiphilic character of proteins and the polar character of gellan, it is believed that the WPI and the FPH were to the oil/water interface, whereas the gellan migrated to the external surface, coating the particles.

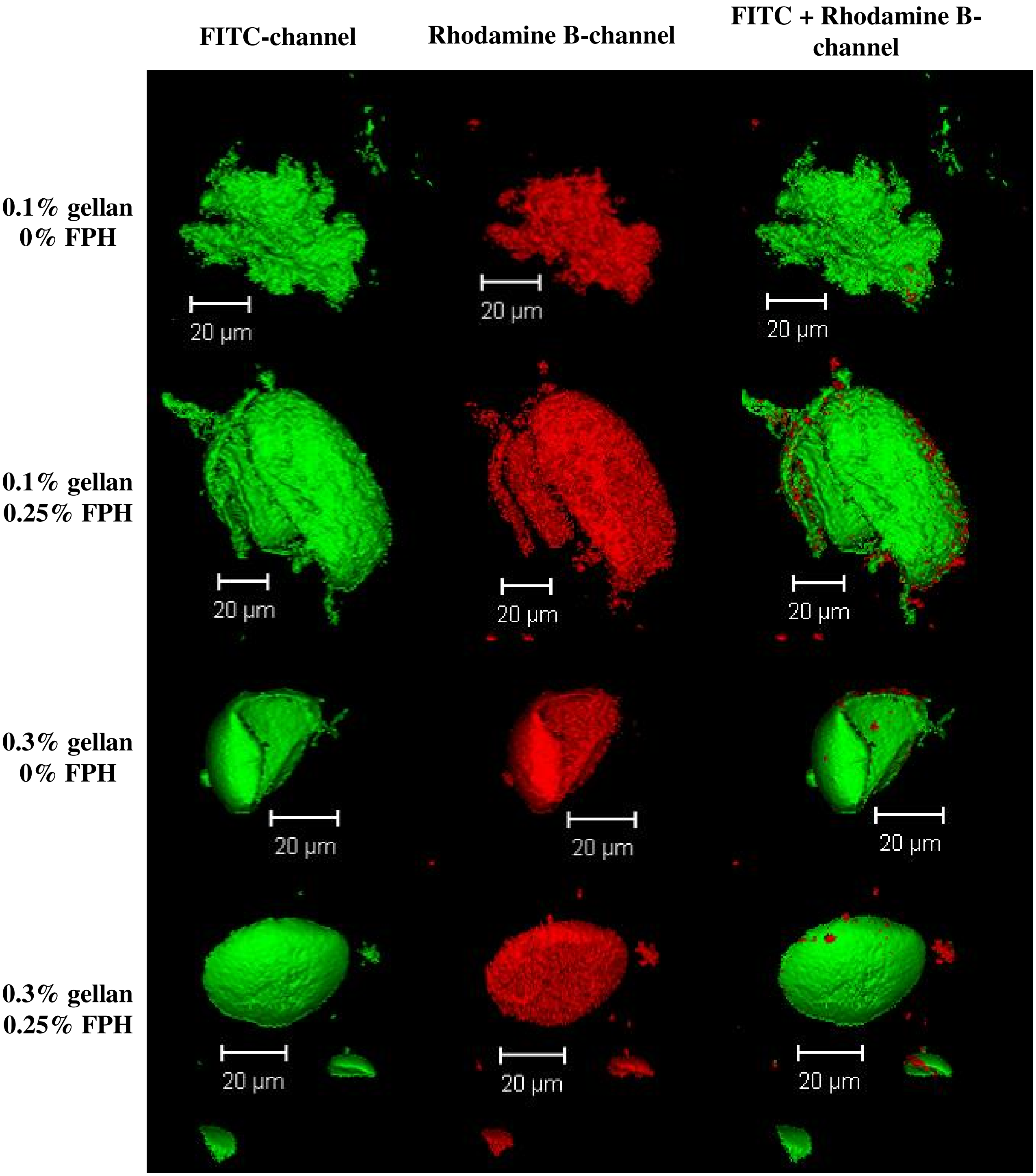
FITC-channel
Rhodamine B-channel
FITC + Rhodamine B-channel
0.1% gellan 0% FPH
0.1% gellan 0.25% FPH
0.3% gellan 0% FPH
0.3% gellan 0.25% FPH
20 µm

Fig. 5.8. CSLM micrographs of microbeads composed by 15% (v/v) flaxseed oil, 1.5% (w/v) WPI, 0 or 0.25% (w/v) FPH and 0.1% or 0.3% (w/v) gellan. Scale bar = 20 µm.

5.3.2.5. *In vitro* digestion

The evaluation of the resistance of microbeads and release of encapsulated compounds was performed by simulating *in vitro* human digestive process. Fig. 5.9 shows the zeta potential of microgels before digestion and in gastric and intestinal media during and after these steps. A control of digestive media, without sample addition, was also carried out to compare with these results.

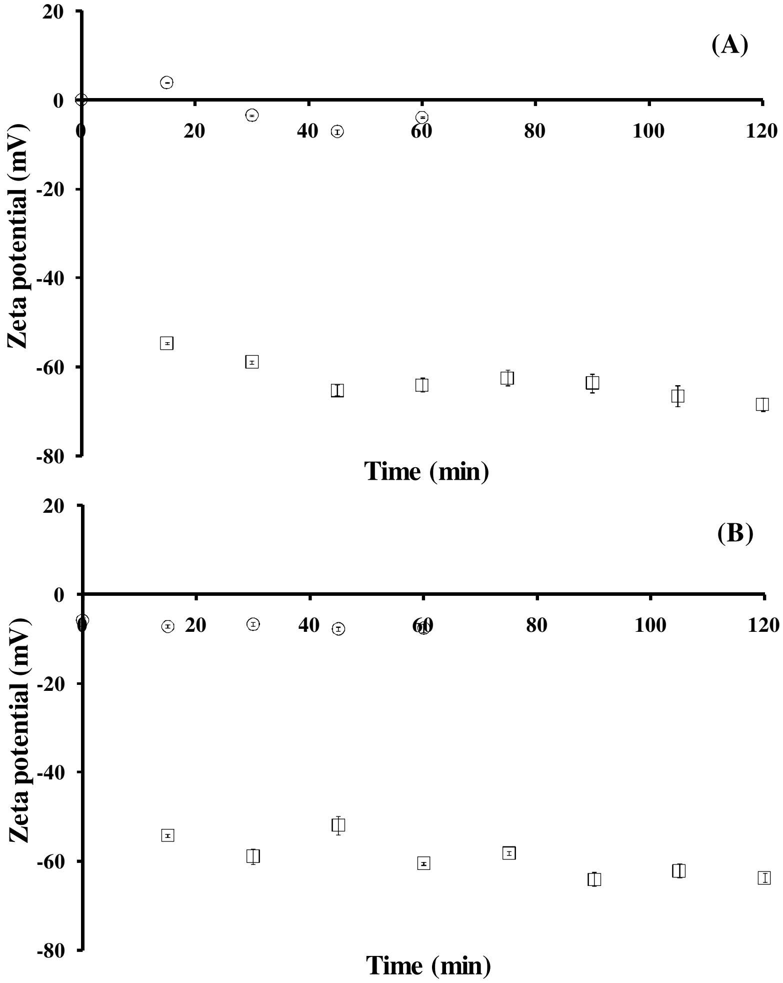

Before digestion
Zeta potential (mV)
0% FPH
-20.6 ± 0.58

Before digestion
Zeta potential (mV)
0.25% FPH
-19.8 ± 0.59

Fig. 5.9. Zeta potential (mV) of microbeads composed by 15% (v/v) flaxseed oil, 1.5% (w/v) WPI, (A) 0 or (B) 0.25% (w/v) FPH and 0.3% (w/v) gellan, before digestion and of microbeads in (○) gastric and (□) intestinal media during digestion.

After gastric step (1 h), the zeta potential of microgels without and with FPH addition in gastric medium reached values around -3.88 ± 0.20 mV and -7.54 ± 0.95 mV, respectively. On the other hand, microbeads in intestinal medium showed a reduction in zeta potential and reached values around -65 mV after 2 h of digestion. The zeta potential determined for the gastric and intestinal media, without sample addition, was around 0 and from -40 to -50 mV, respectively. Thus, it could be said that there was interaction between microgels and gastric and enteric media, since a change in zeta potential values was observed.

The effect of the digestive process conditions on the morphology of microbeads was also evaluated (Fig. 5.10). The gastric digestion step did not alter the morphology of microgels, which was similar to the result obtained by Vilela (2012) for microbeads of gellan (1% w/w) produced with gelation induced by $CaCl_2$ (1.1% w/v) or KCl (2.28% w/v). But, it was also observed that the FPH presence seems to have reduced the amount of free oil droplets, suggesting that the hydrolysate can be assisting in stabilizing the emulsions. At the beginning of gastric digestion (time zero), there were many nonencapsulated oil droplets (indicated in Figure) in microgels without hydrolysate, whereas it was not observed in microbeads with 0.25% (w/v) FPH. However, during the intestinal digestion (15 min) free oil droplets were observed in both systems.

	FPH (%)	
	0	**0.25**
Before digestion	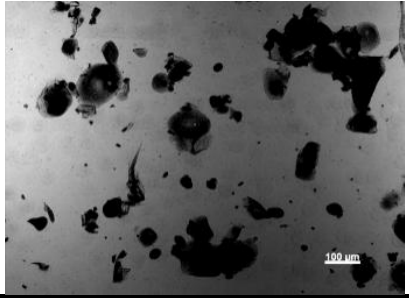	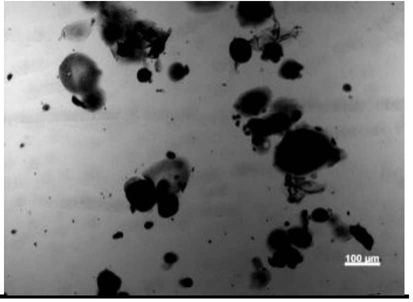

Step	**Time (min)**	**FPH (%)**	
		0	**0.25**
Gastric	**0**	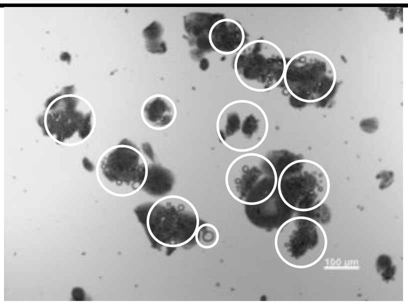	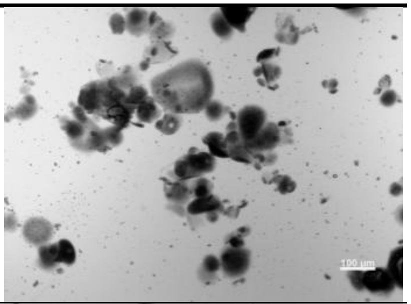
	60	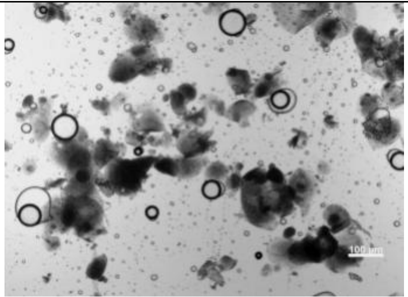	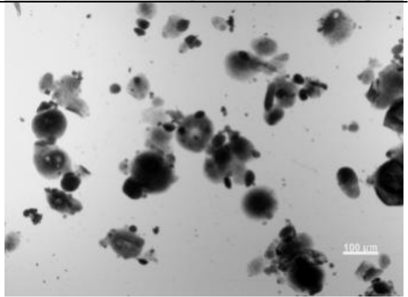

Step	Time (min)	FPH (%)	
		0	0.25
Intestinal	15	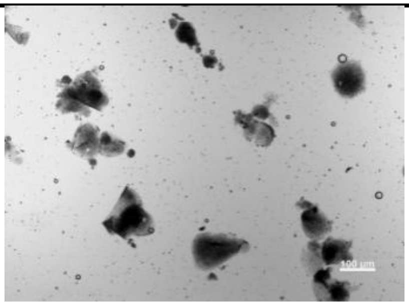	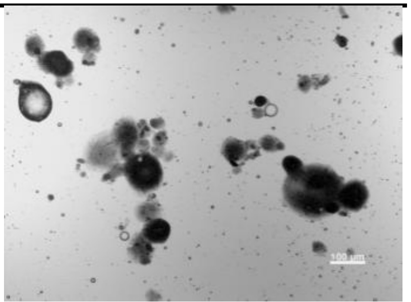
	60	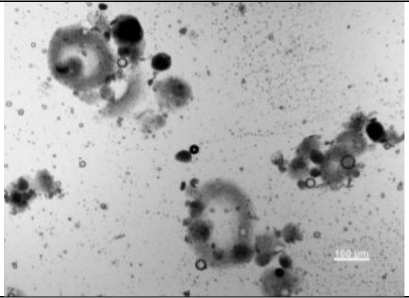	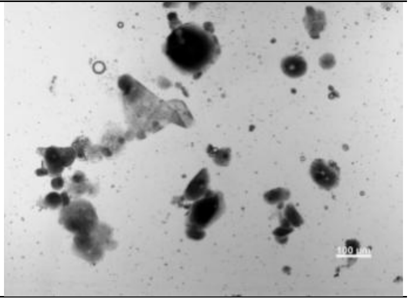
	120	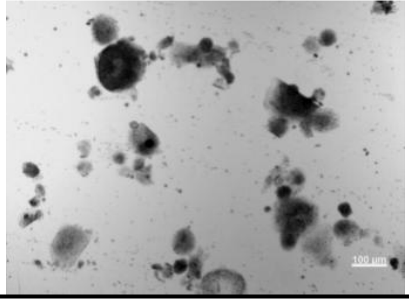	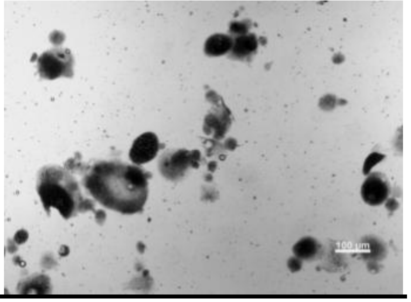

Fig. 5.10. Microstructure of microbeads composed by 15% (v/v) flaxseed oil, 1.5% (w/v) WPI, 0 or 0.25% (w/v) FPH and 0.3% (w/v) gellan, before and during the gastric and intestinal steps. Scale bar = 100 µm.

The mean diameter (d_{32}) and the span values of microbeads were almost constant over time (up to 60 min) during the gastric digestion (Fig. 5.11), and the dispersion index was greater for microgels with 0.25% (w/v) FPH. In the simulation of intestinal digestion, a drastic reduction in the size was observed at 15 min, indicating that microgels were disintegrated, and suggesting that mainly the mean diameter of oil droplets was measured, maybe due to presence of large amount of free oil in the medium (Fig. 5.10). Over time, diameter values have slightly increased, and this increase was more significant in microgels without hydrolysate, which also showed an increase in the span values. On the other hand, through the microscopy, it can be observed that some particles remained almost unchanged after the intestinal step. This observation was corroborated by the particle size distribution (Fig. 5.11), which showed that despite the size of microgels has been substantially reduced in intestinal digestion, a population with large particle size could still be observed (Fig. 5.11B). Vilela (2012) also observed no change in size of some particles after the intestinal digestion, which was confirmed by the bimodal volumetric particles distribution.

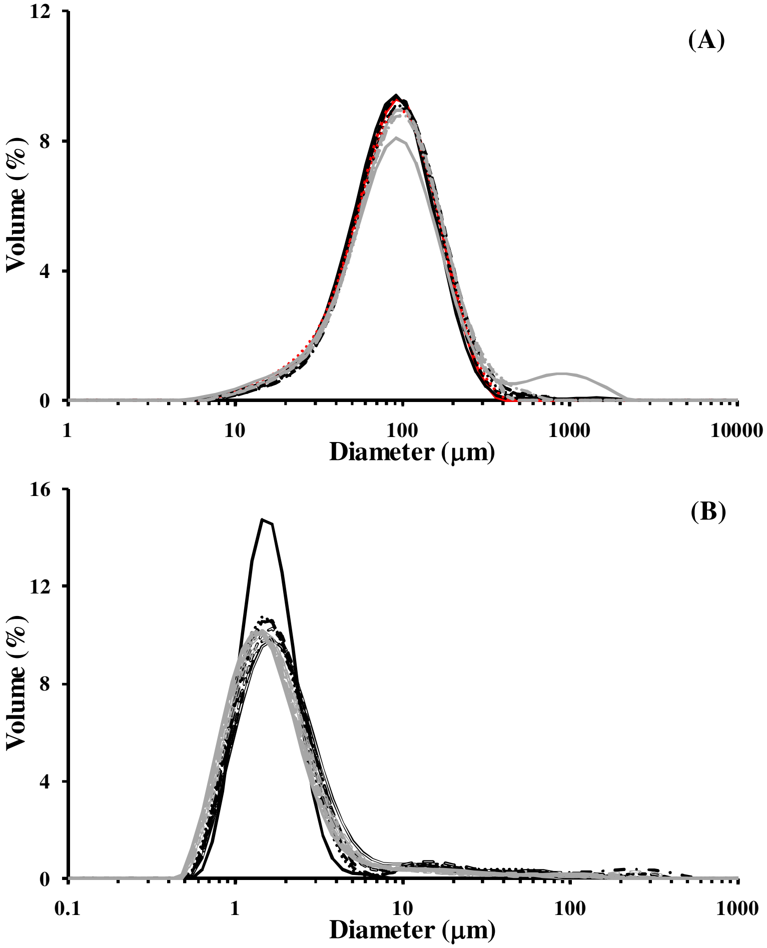

Step	Time (min)	FPH (%)			
		0		0.25	
		d_{32} (μm)	Span	d_{32} (μm)	Span
Before digestion	-	61.18 ± 0.62^{A}	1.64 ± 0.01^{B}	60.19 ± 0.84^{A}	1.72 ± 0.03^{A}
Gastric	**0**	58.20 ± 2.28^{bA}	1.68 ± 0.02^{abB}	56.22 ± 3.08^{bA}	1.97 ± 0.11^{aA}
	15	63.95 ± 0.30^{aA}	1.68 ± 0.02^{abB}	63.25 ± 2.17^{aA}	1.80 ± 0.04^{bA}
	30	64.01 ± 1.05^{aA}	1.63 ± 0.03^{bA}	62.26 ± 0.90^{aA}	1.69 ± 0.06^{bA}
	45	65.02 ± 0.60^{aA}	1.68 ± 0.01^{aB}	63.17 ± 0.44^{aB}	1.75 ± 0.02^{bA}
	60	65.80 ± 0.56^{aA}	1.70 ± 0.01^{aB}	62.54 ± 1.38^{aB}	1.74 ± 0.02^{bA}
Intestinal	**15**	1.36 ± 0.02^{dA}	1.00 ± 0.02^{fB}	1.33 ± 0.00^{bB}	2.20 ± 0.28^{aA}
	30	1.41 ± 0.01^{dA}	1.54 ± 0.02^{eB}	1.37 ± 0.10^{abA}	1.89 ± 0.19^{abA}
	45	1.48 ± 0.01^{cA}	1.82 ± 0.05^{dA}	1.33 ± 0.00^{bB}	1.90 ± 0.09^{abA}
	60	1.50 ± 0.02^{bcA}	1.83 ± 0.12^{dA}	1.35 ± 0.01^{abB}	1.93 ± 0.03^{abA}
	75	1.55 ± 0.02^{abA}	2.54 ± 0.04^{aA}	1.37 ± 0.00^{abB}	1.84 ± 0.08^{bB}
	90	1.56 ± 0.03^{aA}	2.05 ± 0.10^{cA}	1.38 ± 0.01^{abB}	1.77 ± 0.03^{bB}
	105	1.55 ± 0.00^{abA}	2.06 ± 0.09^{cA}	1.41 ± 0.03^{abB}	1.81 ± 0.08^{bB}
	120	1.57 ± 0.03^{aA}	2.32 ± 0.13^{bA}	1.43 ± 0.02^{aB}	1.87 ± 0.09^{abB}

Different letters indicate significant differences ($p<0.05$). Small letters: differences in the same column and condition. Capital letters: differences in the same line.

Fig. 5.11. Particle size distribution, mean particle diameter (d_{32}) and span of microbeads composed by 15% (v/v) flaxseed oil, 1.5% (w/v) WPI, (black color) 0 or (gray color) 0.25% (w/v) FPH and 0.3% (w/v) gellan, before and during the (A) gastric and (B) intestinal steps. Before digestion: (—) 0 or (·····) 0.25% (w/v) FPH. Time of gastric step: (—) 0, (·····) 15, (- - -) 30, (— —) 45 and (— ·) 60 min and of intestinal step: (—) 15, (·····) 30, (- - -) 45, (— —) 60, (— ·) 75, (═) 90, (═ ═ ·) 105 and (═ ═) 120 min.

These results indicate that microbeads of WPI and gellan show resistance against the conditions found in the human stomach (gastric digestion), but they are partially disintegrated in intestinal digestion step. Pepsin is known to preferentially attack peptide bonds involving hydrophobic aromatic amino acids (Beaulieu et al., 2002). In its native structure, the major protein of whey, β-lactoglobulin (β-Lg), is known to be resistant to peptic digestibility (Beaulieu et al., 2002; Morr & Ha, 1993; Reddy, Kella, & Kinsella, 1988), since its amino acid hydrophobic lateral chains are located on the inside (Beaulieu et al., 2002; Bertrand & Turgeon, 2007). Furthermore, the gellan gum is not easily degraded by the action of enzymes (Nag, Han, & Singh, 2011) and is resistant to acidic environments (Nag et al., 2011; Sun & Griffiths, 2000), which could explain the resistance to gastric medium of WPI–gellan microbeads. The degradation by pancreatin (intestinal digestion) would be attributed to the combined effect of the proteases, mainly trypsin, chymotrypsin, and elastase, which catalyze the hydrolysis of the peptide bonds, but with different specificities (Beaulieu et al., 2002). If not at high concentration, bile salts can decrease the interfacial tension, facilitating the emulsification of oil droplets, and leading to an increase in the available surface area for pancreatic lipase activity (Bauer, Jakob, & Mosenthin, 2005; Malaki Nik, Wright, & Corredig, 2011).

Beaulieu et al. (2002) observed that whey protein beads produced using an emulsification/cold gelation method, exhibited resistance to the hydrolytic action of pepsin (after 30 min), but they were totally degraded in pancreatic medium (within 6 h). According to the authors, after gastric incubation, the beads showed a very slight degradation, suggesting that they are gastroresistant and therefore, they can be used as matrix to protect fat-soluble bioactive molecules that are sensible to stomach pH (i.e., retinol) (Beaulieu et al., 2002). Pure alginate and pure whey protein microspheres did not allow satisfactory protection of bioactive compounds in gastric fluids, but the mixture of alginate and WPI produced microspheres capable of delaying riboflavin release in the stomach and allow complete release in small intestine (Chen & Subirade, 2006).

5.4. CONCLUSIONS

The results showed that it was possible to produce WPI – gellan microbeads to encapsulate bioactive compounds from flaxseed using a simple process. Amphiphilic character of proteins and polar of gellan led to the migration of the WPI and the FPH to the oil/water interface and of gellan to the external surface, coating microgels. At higher gellan concentrations, the hydrolysate addition led to a significant size reduction and to a polydispersity increase of microbeads, maybe due to an electrostatic interaction between biopolymers and/or the bridges between gellan and $CaCl_2$. A smaller number of free oil droplets was observed in these conditions and could be related to the amphiphilic interface and to a higher viscosity of the continuous phase. Microgels were resistant to gastric conditions, since that showed no change in size distribution and morphology, but they were disintegrated under intestinal conditions, releasing the encapsulated flaxseed oil, although some microbeads remained almost intact during the evaluated time. Thus, microbeads of WPI and gellan gum produced from extrusion of the O/W emulsions into a $CaCl_2$ solution could be used as a vehicle for the encapsulation and protection of oil and protein hydrolysate from flaxseed during the digestion process and for their release in the small intestine.

5.5. ACKNOWLEDGEMENTS

The authors are grateful to CNPq (140287/2009-4), CAPES and FAPESP (EMU 09/54137-1) for their financial support and to Professor Valdemiro Carlos Sgarbieri (DEPAN/UNICAMP) for the donation of whey protein isolate. The authors also thank the access to equipment and assistance provided by the National Institute of Science and Technology on Photonics Applied to Cell Biology (INFABIC) at the University of Campinas; INFABIC is co-funded by FAPESP (08/57906-3) and CNPq (573913/2008-0).

5.6. REFERENCES

Albertini, B., Vitali, B., Passerini, N., Cruciani, F., Di Sabatino, M., Rodriguez, L., et al. (2010). Development of microparticulate systems for intestinal delivery of *Lactobacillus acidophilus* and *Bifidobacterium lactis*. *European Journal of Pharmaceutical Sciences*, 40(4), 359-366.

AOAC. (1997). *Official methods of analysis of AOAC international.* (16th ed.). Gaithersburg, USA: Association of Official Analytical Chemists.

Bauer, E., Jakob, S., & Mosenthin, R. (2005). Principles of physiology of lipid digestion. *Asian-Australasian Journal of Animal Sciences*, 18(2), 282-295.

Beaulieu, L., Savoie, L., Paquin, P., & Subirade, M. (2002). Elaboration and characterization of whey protein beads by an emulsification/cold gelation process: Application for the protection of retinol. *Biomacromolecules*, 3(2), 239-248.

Bertrand, M.-E., & Turgeon, S. L. (2007). Improved gelling properties of whey protein isolate by addition of xanthan gum. *Food Hydrocolloids*, 21(2), 159-166.

Burey, P., Bhandari, B. R., Howes, T., & Gidley, M. J. (2008). Hydrocolloid gel particles: Formation, characterization, and application. *Critical Reviews in Food Science and Nutrition*, 48(5), 361-377.

Champagne, C. P., & Fustier, P. (2007). Microencapsulation for the improved delivery of bioactive compounds into foods. *Current Opinion in Biotechnology*, 18(2), 184-190.

Chan, E.-S. (2011). Preparation of Ca-alginate beads containing high oil content: Influence of process variables on encapsulation efficiency and bead properties. *Carbohydrate Polymers*, 84(4), 1267-1275.

Chan, E.-S., Lee, B.-B., Ravindra, P., & Poncelet, D. (2009). Prediction models for shape and size of ca-alginate macrobeads produced through extrusion-dripping method. *Journal of Colloid and Interface Science*, 338(1), 63-72.

Chandrasekaran, R., Puigjaner, L. C., Joyce, K. L., & Arnott, S. (1988). Cation interactions in gellan: an X-ray study of the potassium salt. *Carbohydrate Research*, 181, 23-40.

Chandy, T., Mooradian, D. L., & Rao, G. H. R. (1998). Chitosan/polyethylene glycol–alginate microcapsules for oral delivery of hirudin. *Journal of Applied Polymer Science*, 70(11), 2143-2153.

Chen, L., Remondetto, G. E., & Subirade, M. (2006). Food protein-based materials as nutraceutical delivery systems. *Trends in Food Science & Technology*, 17(5), 272-283.

Chen, L., & Subirade, M. (2005). Chitosan/β-lactoglobulin core–shell nanoparticles as nutraceutical carriers. *Biomaterials*, 26(30), 6041-6053.

Chen, L., & Subirade, M. (2006). Alginate–whey protein granular microspheres as oral delivery vehicles for bioactive compounds. *Biomaterials*, 27(26), 4646-4654.

Cook, M. T., Tzortzis, G., Charalampopoulos, D., & Khutoryanskiy, V. V. (2012). Microencapsulation of probiotics for gastrointestinal deliver. *Journal of Controlled Release*, 162(1), 56-67.

Corbo, M. R., Bevilacqua, A., & Sinigaglia, M. (2011). Shelf life of alginate beads containing lactobacilli and bifidobacteria: characterisation of microspheres containing *Lactobacillus delbrueckii* subsp. *bulgaricus*. *International Journal of Food Science and Technology*, 46(10), 2212-2217.

Doherty, S. B., Gee, V. L., Ross, R. P., Stanton, C., Fitzgerald, G. F., & Brodkorb, A. (2011). Development and characterisation of whey protein micro-beads as potential matrices for probiotic protection. *Food Hydrocolloids*, 25(6), 1604-1617.

Garrett, D. A., Failla, M. L., & Sarama, R. J. (1999). Development of an in vitro digestion method to assess carotenoid bioavailability from meals. *Journal of Agricultural and Food Chemistry*, 47(10), 4301-4309.

Hébrard, G., Blanquet, S., Beyssac, E., Remondetto, G., Subirade, M., & Alric, M. (2006). Use of whey protein beads as a new carrier system for recombinant yeasts in human digestive tract. *Journal of Biotechnology*, 127(1), 151-160.

Heilig, A., Göggerle, A., & Hinrichs, J. (2009). Multiphase visualisation of fat containing β-lactoglobulin–κ-carrageenan gels by confocal scanning laser microscopy, using a novel dye, V03-01136, for fat staining. *LWT – Food Science and Technology*, 42(2), 646-653.

Herrero, E. P., Martín Del Valle, E. M., & Galán, M. A. (2006). Development of a new technology for the production of microcapsules based in atomization processes. *Chemical Engineering Journal*, 117(2), 137-142.

Hoebler, C., Lecannu, G., Belleville, C., Devaux, M.-F., Popineau, Y., & Barry, J.-L. (2002). Development of an *in vitro* system simulating bucco-gastric digestion to assess the physical and chemical changes of food. *International Journal of Food Sciences and Nutrition*, 53(5), 389-402.

Jafari, S. M., He, Y., & Bhandari, B. (2007). Effectiveness of encapsulating biopolymers to produce sub-micron emulsions by high energy emulsification techniques. *Food Research International*, 40(7), 862-873.

Kaihara, S., Suzuki, Y., & Fujimoto, K. (2011). In *situ* synthesis of polysaccharide nanoparticles via polyion complex of carboxymethyl cellulose and chitosan. *Colloids and Surfaces B: Biointerfaces*, 85(2), 343-348.

Karewicz, A., Łęgowik, J., & Nowakowska, M. (2011). New bilayer-coated microbead system for controlled release of 5-aminosalicylic acid. *Polymer Bulletin*, 66(3), 433-443.

Klaypradit, W., & Huang, Y.-W. (2008). Fish oil encapsulation with chitosan using ultrasonic atomizer. *LWT - Food Science and Technology*, 41(6), 1133-1139.

Kuhn, K. R., Cavallieri, A. L. F., & Cunha, R. L. (2010). Cold-set whey protein gels induced by calcium or sodium salt addition. *International Journal of Food Science and Technology*, 45(2), 348-357.

Liu, S., Low, N. H., & Nickerson, M. T. (2010). Entrapment of flaxseed oil within gelatin-gum arabic capsules. *Journal of the American Oil Chemists' Society*, 87(7), 809-815.

Livney, Y. D. (2010). Milk proteins as vehicles for bioactives. *Current Opinion in Colloid & Interface Science*, 15(1-2), 73-83.

Malaki Nik, A., Wright, A. J., & Corredig, M. (2011). Impact of interfacial composition on emulsion digestion and rate of lipid hydrolysis using different *in vitro* digestion models. *Colloids and Surfaces B: Biointerfaces*, 83(2), 321-330.

Marambe, P. W. M. L. H. K., Shand, P. J., & Wanasundara, J. P. D. (2008). An in-vitro investigation of selected biological activities of hydrolysed flaxseed (*Linum usitatissimum* L.) proteins. *Journal of the American Oil Chemists' Society*, 85(12), 1155-1164.

Miller, D. D., Schricker, B. R., Rasmussen, R. R., & Van Campen, D. (1981). An in vitro method for estimation of iron availability from meals. *The American Journal of Clinical Nutrition*, 34(10), 2248-2256.

Morr, C. V., & Ha, E. Y. W. (1993). Whey protein concentrates and isolates: Processing and functional properties. *Critical Reviews in Food Science and Nutrition*, 33(6), 431-476.

Nag, A., Han, K.-S., & Singh, H. (2011). Microencapsulation of probiotic bacteria using pH-induced gelation of sodium caseinate and gellan gum. *International Dairy Journal*, 21(4), 247-253.

Nedovic, V., Kalusevic, A., Manojlovic, V., Levic, S., & Bugarski, B. (2011). An overview of encapsulation technologies for food applications. *Procedia Food Science*, 1, 1806-1815.

Perrechil, F. A. (2012). *Encapsulation of hydrophobic compounds in microgels*. 167 p. (PhD Thesis, University of Campinas, Campinas, Brazil).

Perrechil, F. A., Sato, A. C. K., & Cunha, R. L. (2011). κ-Carrageenan–sodium caseinate microgel production by atomization: Critical analysis of the experimental procedure. *Journal of Food Engineering*, 104(1), 123-133.

Perrechil, F. A., Vilela, J. A. P., Guerreiro, L. M. R., & Cunha, R. L. (2012). Development of Na-CN—κ-carrageenan microbeads for the encapsulation of lipophilic compounds. *Food Biophysics*, 7(3), 264-275.

Rabetafika, H. N., Remoortel, V. V., Danthine, S., Paquot, M., & Blecker, C. (2011). Flaxseed proteins: food uses and health benefits. *International Journal of Food Science and Technology*, 46(2), 221-228.

Reddy, I. M., Kella, N. K. D., & Kinsella, J. E. (1988). Structural and conformational basis of the resistance of β-Lactoglobulin to peptic and chymotryptic digestion. *Journal of Agricultural and Food Chemistry*, 36(4), 737-741.

Rizk, N. K., & Lefebvre, A. H. (1980). The influence of liquid film thickness on airblast atomization. *Journal of Engineering for Power*, 102(7), 706-710.

Sato, A. C. K., & Cunha, R. L. (2012). Influence of dispersing media and particle characteristics on rheological behavior of noncolloidal suspensions. *Journal of Dispersion Science and Technology*, 33(3), 437-446.

Shahidi, F., & Miraliakbari, H. (2005). Omega-3 fatty acids in health and disease: Part 2—Health effects of omega-3 fatty acids in autoimmune diseases, mental health, and gene expression. *Journal of Medicinal Food*, 8(2), 133-148.

Silva, F. G. D., O'Callagahan, Y., O'Brien, N. M., & Netto, F. M. (2013). Antioxidant capacity of flaxseed products: The effect of in vitro digestion. *Plant Foods for Human Nutrition*, 68(1), 24-30.

Smrdel, P., Bogataj, M., Zega, A., Planinšek, O., & Mrhar, A. (2008). Shape optimization and characterization of polysaccharide beads prepared by ionotropic gelation. *Journal of Microencapsulation*, 25(2), 90-105.

Steffe, J. F. (1996). *Rheological methods in food process engineering*. (2nd ed.). East Lansing: Freeman Press, (Chapter 1).

Sun, W., & Griffiths, M. W. (2000). Survival of bifidobacteria in yogurt and simulated gastric juice following immobilization in gellan–xanthan beads. *International Journal of Food Microbiology*, 61(1), 17-25.

Tang, Z., Huang, X., Baxi, S., Chambers, J. R., Sabour, P. M., & Wang, Q. (2013). Whey protein improves survival and release characteristics of bacteriophage Felix O1 encapsulated in alginate microspheres. *Food Research International*, 52(2), 460-466.

Tonon, R. V., Pedro, R. B., Grosso, C. R. F., & Hubinger, M. D. (2012). Microencapsulation of flaxseed oil by spray drying: Effect of oil load and type of wall material. *Drying Technology*, 30(13), 1491-1501.

Udenigwe, C. C, Lin, Y.-S., Hou, W.-C., & Aluko, R. E. (2009). Kinetics of the inhibition of renin and angiotensin I-converting enzyme by flaxseed protein hydrolysate fractions. *Journal of Functional Foods*, 1(2), 199-207.

Udenigwe, C. C, Lu, Y.-L., Han, C.-H., Hou, W.-C., & Aluko, R. E. (2009). Flaxseed protein-derived peptide fractions: Antioxidant properties and inhibition of lipopolysaccharide-induced nitric oxide production in murine macrophages. *Food Chemistry*, 116(1), 277-284.

Vilela, J. A. P. (2012). *Properties of gellan–chitosan microgels obtained from extrusion process*. 103 p. (Master Degree Thesis, University of Campinas, Campinas, Brazil). (In Portuguese).

Vilela, J. A. P., Cavallieri, A. L. F., & Cunha, R. L. (2011). The influence of gelation rate on the physical properties/structure of salt-induced gels of soy protein isolate–gellan gum. *Food Hydrocolloids*, 25(7), 1710-1718.

Zhang, W., Xu, S., Wang, Z., Yang, R., & Lu, R. (2009). Demucilaging and dehulling flaxseed with a wet process. *LWT - Food Science and Technology*, 42(6) 1193-1198.

CAPÍTULO 6

Conclusões Gerais

6. CONCLUSÕES GERAIS

Emulsões O/A estabilizadas por proteínas do soro e preparadas sob diferentes condições de homogeneização, pressão (200–1000 bar) e número de passagens pelo homogeneizador (1–7), foram estáveis à cremeação, sem sinais de separação de fases. O aumento da pressão de homogeneização de 200 para 800 bar e do número de passagens para até 3 vezes levou a menores tamanhos de gotas das emulsões, apesar da maior polidispersão. No entanto, maiores pressões e números de passagens levaram à coalescência das gotas e à formação de agregados protéicos de alta massa molecular, que foram resultantes da desnaturação das proteínas do soro pelo cisalhamento e conseqüente aumento de temperatura, o que levou a uma redução na sua capacidade emulsificante. Além disso, observou-se um aumento na viscosidade das emulsões e na formação de produtos primários da oxidação, sendo este último explicado pelo aumento de temperatura e diminuição no tamanho de gotas (aumento da área superficial) das emulsões em maior pressão. Portanto, visando uma maior estabilidade e uma menor oxidação lipídica do óleo de linhaça nas emulsões O/A, as melhores condições de processo seriam utilizar pressões de homogeneização intermediárias e menor número de passagens pelo homogeneizador.

A capacidade emulsificante do isolado protéico da linhaça (FPI) foi testada em sistemas puros e mistos com proteínas do soro (WPI), sendo obtidas emulsões instáveis com separação de fases, que foram influenciadas pela concentração de FPI e pelas condições de processo (pressão de homogeneização e número de passagens). Uma maior estabilidade foi obtida com o aumento da concentração de FPI e das condições de homogeneização nos sistemas puros, como conseqüência do aumento da viscosidade, enquanto que os sistemas mistos foram mais estáveis com menor concentração de FPI (0,14% m/v). Os resultados mostraram que o FPI não foi um bom emulsificante, porém a adição de WPI melhorou a estabilidade cinética das emulsões contendo menor concentração de FPI (0,14% m/v), e homogeneizadas em condições mais drásticas. Portanto, uma maior pressão de homogeneização (600 bar) com duas passagens pelo homogeneizador deveria ser utilizada visando maior estabilidade dos sistemas mistos.

A técnica de extrusão em uma solução gelificante foi eficaz na produção de microgéis de emulsões O/A com concentração fixa de proteínas do soro (WPI) e variada de gelana para a encapsulação de compostos bioativos da linhaça. O caráter anfifílico das proteínas e polar da gelana levou à migração de WPI e de hidrolisado protéico da linhaça (FPH) para a interface óleo/água e de gelana para a superfície externa, recobrindo as partículas, o que confirmou a encapsulação do hidrolisado. Em maiores concentrações de gelana, a adição de hidrolisado levou a uma redução no tamanho e a uma maior polidispersão dos microgéis, o que poderia ser resultado da formação de uma rede de biopolímeros mais densa. Além disso, através da microscopia observou-se uma menor quantidade de gotas de óleo livres nestas condições. Os microgéis mostraram resistência às condições gástricas, desde que não apresentaram mudança na distribuição de tamanho e na morfologia, mas foram desintegrados sob condições intestinais, liberando o óleo encapsulado, apesar de algumas partículas permanecerem praticamente intactas durante o tempo avaliado. Portanto, os microgéis de WPI e gelana poderiam ser utilizados como veículo para a encapsulação e proteção de óleo e FPH durante o processo digestivo e para sua liberação no intestino delgado.

7. SUGESTÕES PARA TRABALHOS FUTUROS

Visando dar continuidade ao estudo da produção de microgéis de proteínas do soro (WPI) e gelana para a encapsulação e liberação controlada de compostos bioativos da linhaça, algumas sugestões são apresentadas:

✓ A determinação da composição química (proteína, polissacarídeo e óleo) antes e após a separação de fases das emulsões puras de isolado protéico da linhaça (FPI) e mistas WPI-FPI poderia enriquecer a discussão e explicar alguns resultados;

✓ O estudo de emulsões de WPI e hidrolisado protéico da linhaça (FPH), sem e com a adição de gelana, antes da produção dos microgéis seria interessante para avaliar a interação entre os biopolímeros;

✓ Na simulação *in vitro* do processo digestivo seria importante avaliar também o comportamento dos microgéis em um meio sem a presença das enzimas (pepsina e pancreatina) e do extrato de bile e em um meio com a presença apenas do extrato de bile, para assim entender melhor o efeito das condições e das etapas do processo;

✓ A determinação da eficiência de encapsulação do óleo e do hidrolisado seria interessante para comprovar quantitativamente que os compostos foram encapsulados. Porém, é necessário encontrar uma forma de quantificar o hidrolisado sem que o WPI interfira.